

Cover Page



Universiteit Leiden



The handle <http://hdl.handle.net/1887/29450> holds various files of this Leiden University dissertation.

**Author:** Koens, Lianne

**Title:** Clinicopathologic and genetic aspects of primary cutaneous large B-cell lymphomas

**Issue Date:** 2014-10-29





# Clinicopathologic and genetic aspects of primary cutaneous large B-cell lymphomas

Publication of this thesis was financially supported by:

Janssen-Cilag, Roche Nederland BV, Dako Benelux, BD Biosciences, Takeda Nederland BV,  
Teva Nederland BV

Cover design and lay-out: Dinomar Daal (dmdaal@aanlegvoortalent.nl)

Printed by: Gildeprint Drukkerij

Clinicopathologic and genetic aspects of primary cutaneous large B-cell lymphomas  
Thesis, Universiteit Leiden, The Netherlands.

Copyright ©2014, Lianne Koens, The Netherlands.

ISBN 9789461087751

No part of this thesis may be reproduced, stored or transmitted without prior permission of  
the author.

# Clinicopathologic and genetic aspects of primary cutaneous large B-cell lymphomas

Proefschrift

ter verkrijging van

de graad van Doctor aan de Universiteit Leiden

op gezag van Rector Magnificus prof. mr. C.J.J.M. Stolker

volgens besluit van het College voor Promoties

te verdedigen op woensdag 29 oktober 2014

klokke 16.15 uur

door

Lianne Koens

geboren te Delft

in 1982

## **Promotiecommissie**

Promotor: Prof. dr. R. Willemze

Co-promotores: Dr. P.M. Jansen

Dr. C.P. Tensen

Overige leden: Prof. dr. P.M. Kluin (Rijksuniversiteit Groningen)

Prof. dr. H. Veelken

Prof. dr. V.T.H.B.M. Smit

*Voor mijn vader*





## Contents

	List of abbreviations	11
<b>Chapter 1</b>	General introduction	15
<b>Chapter 2</b>	IgM expression on paraffin sections distinguishes primary cutaneous large B-cell lymphoma, leg type from primary cutaneous follicle center lymphoma <i>The American Journal of Surgical Pathology 2010; 34(7):1043-1048</i>	37
<b>Chapter 3</b>	MicroRNA profiling of primary cutaneous large B-cell lymphomas <i>Public Library of Science ONE 2013; 8(12): e82471</i>	51
<b>Chapter 4</b>	Nuclear Factor- $\kappa$ B pathway-activating gene aberrancies in primary cutaneous large B-cell lymphoma, leg type <i>Abridged version published: Journal of Investigative Dermatology 2014; 134(1): 290-292</i>	77
<b>Chapter 5</b>	Genetic alterations in B-cell activation-related transcription factors in primary cutaneous large B-cell lymphoma, leg type <i>Submitted</i>	95
<b>Chapter 6</b>	Methotrexate-associated B-cell lymphoproliferative disorders presenting in the skin: a clinicopathologic and immunophenotypical study of 10 cases <i>The American Journal of Surgical Pathology 2014; 38(7): 999-1006</i>	113
<b>Chapter 7</b>	Summary and discussion	129
	Nederlandse samenvatting	143
	Curriculum vitae	151
	List of publications	153
	Nawoord	157



## List of abbreviations

ABC	activated B-cell
AID	activation-induced cytidine deaminase
B-LPD	B-cell lymphoproliferative disorder
BCL2	B-cell lymphoma 2
BCL6	B-cell lymphoma 6
BCR	B-cell receptor
Blimp1	B-lymphocyte-induced maturation protein
BTK	Bruton's tyrosine kinase
CARD11	caspase recruitment domain 11
CBCL	primary cutaneous B-cell lymphoma
CDKN2A	cyclin-dependent kinase inhibitor 2A
CGH	comparative genomic hybridization
CSR	class switch recombination
CT scan	computed tomography scan
CTCL	primary cutaneous T-cell lymphoma
DLBCL	diffuse large B-cell lymphoma
DNA	deoxyribonucleic acid
EBV	Epstein Barr virus
EORTC	European Organization for the Treatment of Cancer
FFPE	formalin-fixed and paraffin-embedded
FOXP1	forkhead box P1
FT-CGH	fine-tiling comparative genomic hybridization (DNA array)
GCB	germinal center B-cell
IgM	immunoglobulin M
IHC	immunohistochemistry
IKK	I $\kappa$ B kinase
IRF4	interferon regulatory factor 4
miR	microRNA
MLPA	multiplex ligation-dependent probe amplification
mRNA	messenger RNA
MS-MCA	methylation-specific melting curve analysis
MUM1	multiple myeloma oncogene 1
MYD88	myeloid differentiation primary response domain 88
MTX	methotrexate
NF- $\kappa$ B	nuclear factor-kappa B







1

## General introduction





## Introduction

Primary cutaneous lymphomas are malignant lymphoproliferative disorders presenting in the skin without evidence of extracutaneous disease at the time of diagnosis. A diagnosis of primary cutaneous lymphoma can only be made after excluding extracutaneous localizations by adequate staging procedures, comprising physical examination, total blood count, bone marrow aspiration/biopsy and computed tomography (CT) scan. It is important to separate primary cutaneous lymphoma from nodal non-Hodgkin lymphoma (NHL) that secondarily involve the skin, as these usually have a different clinical behavior and prognosis, and therefore might require different treatment strategies. For that reason, primary cutaneous lymphomas have been included as distinct disease entities in the recent classification systems for lymphoid malignancies, such as the World Health Organization (WHO)-European Organization for Treatment of Cancer (EORTC) classification<sup>1</sup> and WHO classification.<sup>2</sup>

While nodal NHL are predominantly of B-cell origin, primary cutaneous B-cell lymphomas (CBCL) only constitute a minority (20-25%) of all primary cutaneous lymphomas, the remaining 75-80% being primary cutaneous T-cell lymphomas (CTCL).<sup>1</sup> According to the latest WHO-EORTC classification, the group of CBCL encompasses primary cutaneous marginal zone B-cell lymphoma (PCMZBL), primary cutaneous follicle center lymphoma (PCFCL) and primary cutaneous diffuse large B-cell lymphoma, leg type (PCLBCL-LT).<sup>1</sup> The main clinicopathologic, immunophenotypic and molecular features of PCMZBL, PCFCL and PCLBCL-LT are summarized in Table 1. Histologically, PCMZBL is composed of a mixed infiltrate containing small malignant B-cells, morphologically resembling marginal zone cells, lymphoplasmacytoid cells and plasma cells. The plasma cells typically show monotypic intracytoplasmic immunoglobulin staining by immunohistochemistry. PCMZBL is an indolent type of NHL, with a 5 year disease-specific survival (DSS) of approximately 98%.<sup>3</sup> Histologically, the tumor cells of PCFCL show a predominance of medium-sized to large centrocytes (cleaved cells) and variable numbers of centroblasts. They can show a follicular, follicular and diffuse, but in most cases a diffuse growth pattern, a feature not related to prognosis.<sup>3</sup> Clinically, PCFCL commonly presents with localized skin lesions on the head, in particular the scalp, or the trunk, is highly responsive to radiotherapy and has an excellent prognosis (see Table 1). PCLBCL-LT characteristically shows a diffuse infiltrate of centroblasts and/or immunoblasts (cells with round nuclear configuration), and generally few admixed reactive T-cells. PCLBCL-LT usually presents on one or both legs in elderly patients, has an aggressive clinical course (5 year overall survival (OS) approximately 37%<sup>3</sup>), and should be treated with R-CHOP (rituximab, cyclophosphamide, hydroxydaunorubicin, oncovin and prednisone). However, new therapeutic targets are wanted. Differentiation between PCFCL with a diffuse growth pattern and PCLBCL-LT can sometimes be difficult.

Recent reports have described a novel type of B-cell lymphoproliferative disorder (B-LPD) associated with the chronic use of immunosuppression, and more specifically with the use of methotrexate (MTX).<sup>4</sup> As there have only been a few reports on this type of lymphoma occurring in the skin,<sup>5-9</sup> it is not well characterized, which may cause a delay in its recognition.

This thesis includes a number of clinicopathologic, immunophenotypic and molecular genetic studies in different subtypes of CBCL. The aims were (1) to define additional diagnostic markers that could aid in the differential diagnosis of PCFCL with a diffuse growth pattern from PCLBCL-LT, (2) to investigate molecular and genetic alterations in PCLBCL-LT underlying the pathogenesis of this type of lymphoma, and (3) to better define the group of MTX-associated B-LPD presenting in the skin, in order to find clinicopathologic and/or

immunophenotypical characteristics that can be helpful in the early recognition of this rare type of lymphoma and are separate from PCFCL and/or PCLBCL-LT.

For the understanding of B-cell NHL in general, knowledge of physiological B-cell development is crucial to gain insight into the classification of these lymphomas and the molecular pathways involved in their pathogenesis. Therefore, this introductory chapter starts with an overview of normal B-cell development, the molecular alterations involved, and its relationship with the different subtypes of B-cell NHL, including CBCL. Next, the difficulties in differentiating PCFCL with a diffuse growth pattern from PCLBCL-LT are discussed. This is followed by a short overview of the current treatment options for PCLBCL-LT and the nuclear factor (NF)- $\kappa$ B signaling pathway is summarized, as a potential pathway for upcoming targeted treatments. Finally, the rare entity MTX-associated DLBCL presenting the skin is discussed along with outstanding diagnostic issues with regard to its separation from PCFCL with a diffuse growth pattern and/or PCLBCL-LT.

### **Normal B-cell development**

The normal development of B-cells from hematopoietic stem cells in the bone marrow with multilineage potential to effector B-cells in the peripheral blood or lymphoid tissues is characterized by the formation of clonally diverse cell surface and secreted immunoglobulin B-cell receptors (BCR) which bind with high affinity to a specific antigenic epitope. Many molecular genetic processes to establish these diverse BCR take place in different stages of the developmental pathway of B-cells. These different stages are not only characterized by the processes involved in BCR generation and diversity, but also have an inherent morphology and a distinct protein expression profile. An overview of the different stages of normal B-cell development is depicted in Figure 1.

#### *Antigen-independent B-cell development*

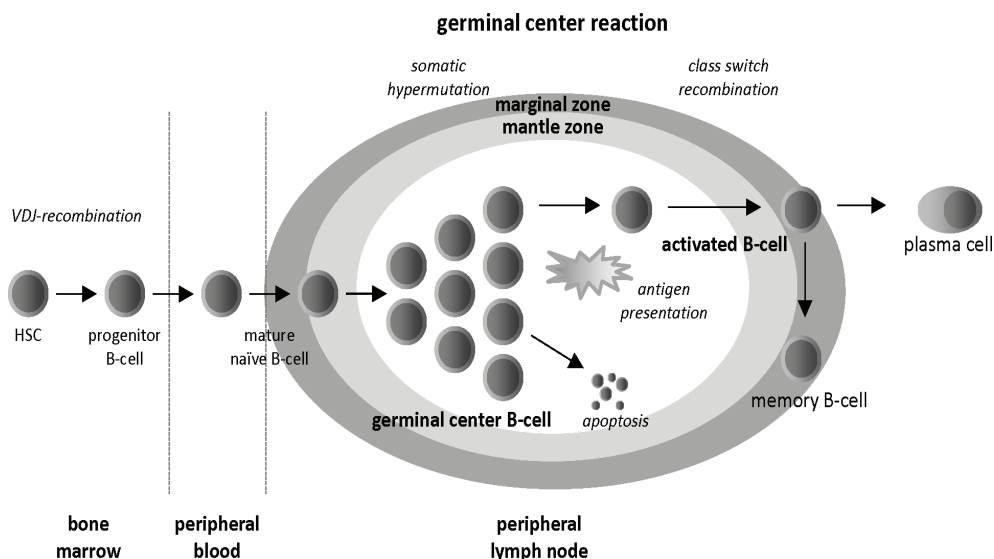
Immature B-cells are produced in the bone marrow and arise from hematopoietic stem cells in coordination with transcription factors early B-cell factor (EBF) and the E box protein E2A. EBF and E2A activate the B-cell gene expression program and initiate the process of VDJ-recombination,<sup>10</sup> comprising extensive rearrangements of the variable (V), diversity (D) and joining (J) segments of the heavy chain gene on chromosome 14 (VDJ-recombination). This first step in B-cell development is amongst others coordinated by the expression of recombination activation genes 1 and 2 (RAG1 and RAG2) which are required for VDJ-recombination.<sup>11</sup> The human immunoglobulin heavy chain consists of several different V-gene segments, D-gene segments and J-gene segments. Recombination between any D- and J-gene segments occurs by excision of the non-coding DNA and gene segments in between, followed by joining of any one of the V-segments to the rearranged DJ-segment (see Figure 2A). All gene segments in between that are not involved in these rearrangements will be deleted during VDJ-recombination. These events will create a vast amount of diversity of the heavy chain gene, which is even more enhanced by terminal deoxynucleotidyl transferase (TdT), which adds nucleotides to the 3' terminus of the V, D and J exons during recombination, creating additional junctional diversity.<sup>12</sup>

**Table 1.** Main clinicopathologic, immunophenotypical and molecular genetic features of the three subtypes of primary cutaneous B-cell lymphoma according to the WHO-EORTC classification<sup>1</sup>

	<b>PZMZL</b>	<b>PCFCL</b>	<b>PCLBCL-LIT</b>
<b>Clinical features</b>			
- lesions	solitary or multiple papules/nodules	solitary or multiple tumors	solitary or multiple tumors
- site of primary presentation	trunk and/or extremities	head and/or trunk	one or both leg(s)
- cutaneous relapse	57%	30%	69%
- nodal / visceral dissemination	rarely	10%	47%
- 5 year OS / DSS	94% / 98%	87% / 95%	37% / 50%
- first choice treatment	local excision / radiotherapy	local radiotherapy	R-CHOP
<b>Histopathology</b>			
- infiltrate	patchy or diffuse	diffuse or (partly) follicular	diffuse
- B-cell morphology	marginal zone (centrocyte-like) cells, lymphoplasmacytoid cells, plasma cells	centrocytes (cleaved)	centroblasts / immunoblasts (round)
- T-cell admixture	abundant	abundant	sparse
<b>Immunohistochemistry</b>			
- B-cells			
B-cell lineage markers	CD20+, CD79a+, PAX5+, monotypic clg	CD20+, CD79a+, PAX5+	CD20+, CD79a+, PAX5+
germinal center markers	BCL2+, BCL6-, CD10-	BCL2-, BCL6+, CD10-/+	BCL2+, BCL6+/-, CD10-
activation markers	IRF4/MUM1-, FOXP1-	IRF4/MUM1-, FOXP1-	IRF4/MUM1+, FOXP1+
- background	CD21 and CD35 show reactive follicles	CD21 and CD35: (remnants of) follicular dendritic networks	CD21 and CD35: no (remnants of) follicular dendritic networks
<b>Molecular genetics</b>			
- copy number alterations	not available	amplification 2p16.1 region, deletion 14q11.2-q12	deletion 6q arm, deletion 9p21.3 region
- gene expression profiling	not available	high expression <i>SPINK2</i>	high expression <i>GHM, PIM1, PIM2, IRF4</i> and <i>OCT2</i>

OS: overall survival; DSS: disease-specific survival; clg: intracytoplasmic immunoglobulin; R-CHOP: rituximab, cyclophosphamide, hydroxydaunorubicin, oncovin, prednisone.

Figure 1. Normal B-cell development



The normal B-cell development from hematopoietic stem cell (HSC) in the bone marrow to effector cells in the peripheral lymphoid tissue and/or blood is depicted (adapted from: Kuppers et al, Nat Rev Immunol 2005).

Following VDJ-recombination, a pre B-cell receptor will now be assembled at the B-cell membrane, consisting of a rearranged heavy chain, a not yet rearranged lambda light chain, and signaling molecules  $Ig\alpha$  and  $Ig\beta$ .<sup>13</sup> After recombination of the heavy chain gene, the produced mu chain will induce recombination of the light chain genes in a same manner, although these genes lack D segments, and therefore only undergo VJ-recombination, before generating transcripts linking the VJ-segment to the kappa or lambda constant region ( $C\kappa$  or  $C\lambda$ ). Firstly, the kappa light chain on chromosome 2 will be rearranged. If non-productive, the second allele of the gene will undergo the same process. The lambda light chain gene on chromosome 22 will only undergo VJ-recombination if VJ-recombination of both alleles of the kappa light chain gene is unproductive.<sup>14</sup> After successful VJ-recombination the light chain is complete. At this stage the B-cell receptor will be assembled at the B-cell receptor membrane, defining the immature B-cell stage.<sup>15</sup> From this moment on transcripts from the rearranged heavy gene region will have VDJ segments joined to both the constant mu and the constant delta chain ( $C_{\mu}$  and  $C_{\delta}$ ). By alternative splicing this will lead to expression of  $IgM$  and  $IgD$  subtypes of the B-cell receptor on the B-cell membrane. At this developmental stage, the B-cells are negatively selected for autoreactivity, and then enter the peripheral blood to migrate to peripheral lymphoid tissue.

#### Antigen-dependent B-cell development

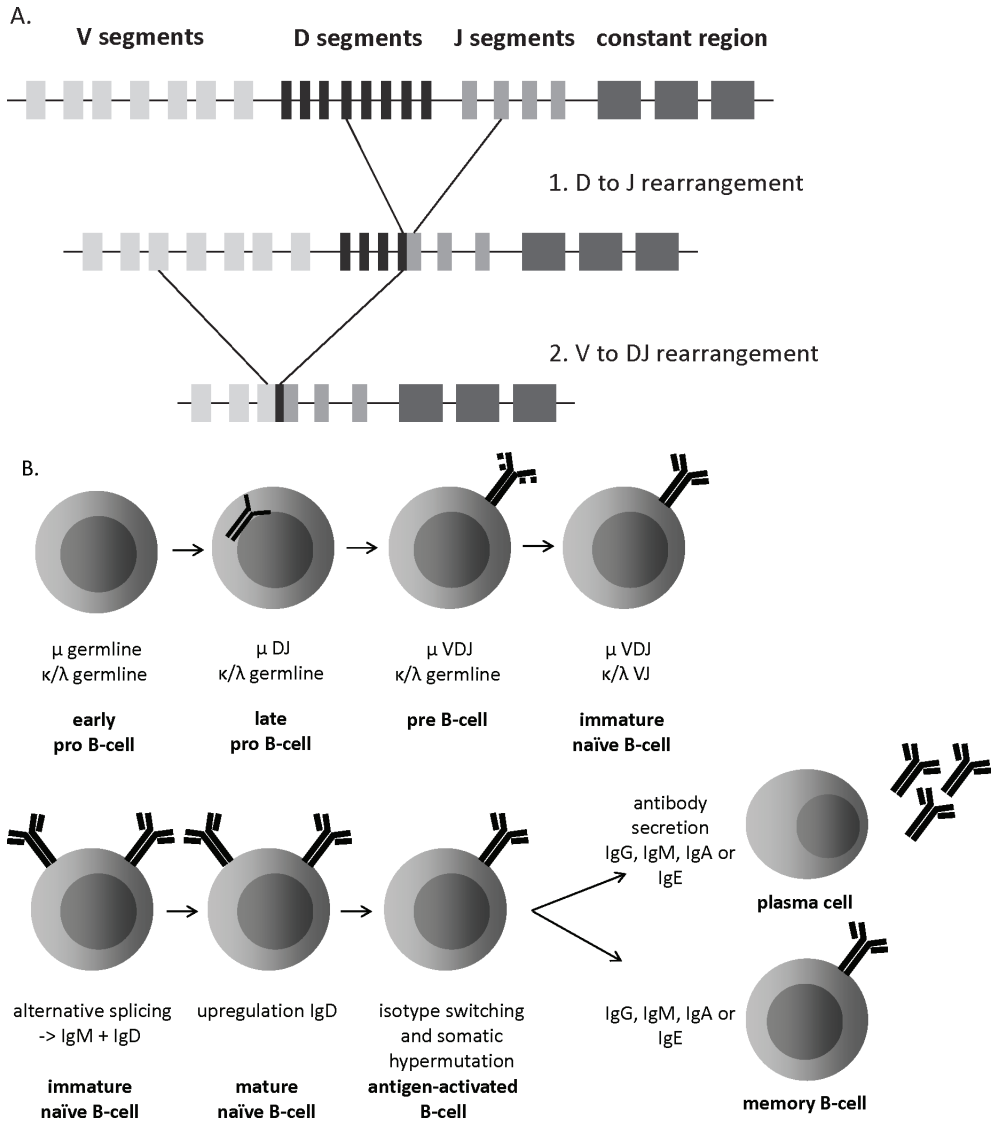
Reaching secondary or peripheral lymph nodes, in the mantle of the germinal center, the B-cells are still called naïve, as they have not encountered an antigen yet. Subsequently, antigen is presented to the B-cells by follicular dendritic cells, aided by follicular helper T-cells ( $T_{FH}$ ) residing in the primary follicle. These  $T_{FH}$  produce vast amounts of the cytokine  $IL-21$ ,<sup>16</sup>

inducing transcription of the enzyme activation-induced cytidine deaminase (AID)<sup>17</sup> and germinal center protein B-cell lymphoma 6 (BCL6).<sup>18</sup> The B-cells enter the primary follicle, where they rapidly proliferate as centroblasts. BCL6 controls B-cell activation, differentiation, susceptibility to DNA damage and apoptosis during this proliferative phase of the germinal center reaction.<sup>19</sup> By proliferating, the centroblasts form germinal centers and push out the naïve, non-antigen triggered B-cells to the periphery of this germinal center, forming a mantle zone. Characteristic for this developmental stage, the centroblasts undergo somatic hypermutation (SHM) during proliferation, leading to subclones of the immunoglobulin gene with increased affinity for the antigen. This process involves the introduction of point mutations in the V gene segments of the heavy and light chain genes, leading to further diversity of the antigen receptor, coupled with selection of the B-cell with the highest affinity B-cell receptor for the presented antigen. The presence of AID is required for SHM to occur,<sup>20</sup> and catalyzes the initiation of SHM by deaminating cytidines on DNA. Subsequently, error-prone repair mechanisms will introduce somatic mutations.<sup>21</sup> After this proliferative phase and the process of SHM, the centroblasts differentiate into centrocytes, which migrate to the opposite side of the germinal center. There, the antigen is again presented to the B-cells with help of T<sub>FH</sub> and follicular dendritic cells. Centrocytes with insufficient affinity maturation for the selected antigen will undergo apoptosis, but centrocytes with high affinity will undergo class switch recombination (CSR). This is a process in which the entire VDJ gene segment of the immunoglobulin heavy chain gene is transferred to a constant region downstream of the C<sub>μ</sub>, deleting all DNA in between. The VDJ gene segment is then linked to either the C<sub>γ</sub>, C<sub>μ</sub>, C<sub>α</sub>, or C<sub>ε</sub> gene segment, finally leading to production of either IgG, IgM, IgA, or IgE, respectively. Like for SHM, without the presence of AID CSR cannot occur,<sup>20</sup> although separate domains of AID are required for both processes.<sup>22</sup> The activated and class-switched B-cells finally become effector B-cells (plasma cell or memory B-cell), either secreting these immunoglobulins (plasma cells) or expressing immunoglobulins as surface receptor (memory B-cells). The transition from centrocyte to effector B-cell is coordinated by combined B-cell receptor signaling and CD40 triggering through immune cells in the germinal center. This activation induces transcription factors nuclear factor-κB (NF-κB) and interferon regulatory factor 4 (IRF4), which in turn inhibit transcription of BCL6.<sup>23</sup> If transcription factor paired box protein 5 (PAX5) is not downregulated, centrocytes differentiate into memory B-cells.<sup>24</sup> On the other hand, downregulation of PAX5 by a not yet elucidated mechanism in activated centrocytes leads to the release of repression of X-box binding protein 1 (XBP1) and J chain and concomitant upregulation of PRDM1 (PR domain containing 1, with ZNF domain)/Blimp1 (B-lymphocyte-induced maturation protein 1) and IRF4 that drives the B-cells further towards plasma cell differentiation.<sup>25</sup>

### *Stages of B-cell development and corresponding non-Hodgkin lymphomas*

At several stages of normal B-cell development, B-cells are at risk to acquire genetic lesions that can facilitate malignant transformation, as the genetic mechanisms responsible for generating BCR diversity also induce deleterious genetic events. The B-cell NHL usually shows morphological, immunohistochemical and molecular resemblance to a specific B-cell developmental stage, which consequently is its normal counterpart (Figure 3). Therefore knowledge of normal B-cell development is crucial to understand B-cell lymphomagenesis and classification.

Figure 2. V(D)J recombination and B-cell development



(A) In VDJ rearrangement, joining of a D segment to a J segment (DJ-recombination) is the first to occur, followed by joining of a V segment to this newly formed DJ-segment. (B) Heavy and light chain proteins are assembled from the late pro B-cell phase on, occurring after DJ-recombination has finished, and at the pro B-cell phase, these proteins reside in the cytoplasm. Pre B-cells express a pre B-cell receptor on the cell surface containing a germline light chain. The actual B-cell receptor with rearranged heavy and light chain is expressed from the stage of immature naïve B-cell. After antigen-activation, isotype switching of the B-cell receptor occurs, leading to secretion of IgG, IgA, IgM or IgE in effector plasma cells, or expression of one of these four isotypes on the surface of effector memory B-cells (adapted from: The Immune System 3<sup>rd</sup> Ed, Garland Science 2009).

The presumed cell of origin is reflected in the neoplastic cells by tumor cell morphology, immunophenotype and gene expression profile. Consistently, PCFCL tumor cells have the morphology of large follicle center cells, express germinal center marker BCL6<sup>26</sup> and show the gene expression profile of a germinal center B-cell (GCB).<sup>27</sup> PCLBCL-LT has the tumor cell morphology of an immunoblast (lymphocytes that are antigen-activated and will under normal circumstances further differentiate into effector B-cells), demonstrates immunohistochemical expression of B-cell activation-related markers IRF4/multiple myeloma oncogene 1 (MUM1) and forkhead box protein 1 (FOXP1)<sup>28</sup> and has the gene expression profile of an activated B-cell (ABC).<sup>27</sup> The large group of nodal DLBCL can also be subdivided into two groups with the germinal center B-cell or the activated B-cell as postulated normal counterpart (GCB-DLBCL and ABC-DLBCL, respectively).<sup>29</sup> As in primary cutaneous large B-cell lymphoma, nodal GCB-DLBCL has a more favorable prognosis as compared to ABC-DLBCL, although this difference is less pronounced (80% versus 45% 5 year OS, respectively).<sup>30</sup>

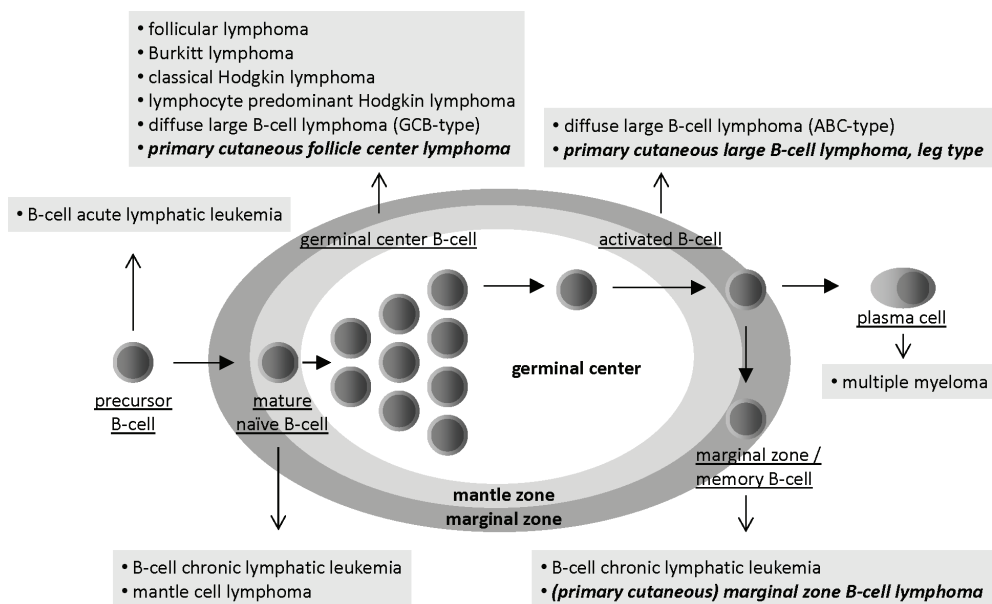
#### *Maturation arrest in primary cutaneous large B-cell lymphoma, leg type*

The ABC-like genotype of both PCLBCL-LT and ABC-DLBCL implies that both types of NHL are derived from B-cells that are blocked in differentiation in the transitional stage between germinal center B-cell and plasma cell.<sup>27,29</sup> In nodal DLBCL, several genetic mechanisms have been described that might (in part) be responsible for this differentiation arrest. In nodal ABC-DLBCL several inactivating genetic events occur in *PRDM1*, of which PRDM1 or Blimp1 is the functional protein and which is essential for plasma cell differentiation, including mutations and chromosomal deletions.<sup>31,32</sup> Other molecules driving B-cells towards plasma cell differentiation include FOXP1 and IRF4, and sporadic genetic alterations, such as translocations involving these genes, also occur in nodal DLBCL.<sup>33,34</sup>

Previous immunohistochemical studies of PCLBCL-LT have shown that BCL6 is expressed in more than half of the cases, IRF4 and FOXP1 are nearly always expressed by the tumor cells, and that no substantial expression of Blimp1 could be detected.<sup>28</sup> In the context of normal B-cell development, the expression of germinal center marker BCL6 together with post-germinal center/B-cell activation markers IRF4 and/or FOXP1 seems aberrant, and also, the absence of Blimp1 expression despite expression of IRF4 and/or FOXP1 is unexpected, as it is normally induced by both transcription factors. However, knowledge of potential underlying genetic mechanisms explaining the aberrant immunohistochemical expression of these transcription factors in PCLBCL-LT is limited.



**Figure 3.** B-cell development and concordant (non) Hodgkin lymphomas, including primary cutaneous large B-cell lymphomas



Adapted from: Kuppers et al, Nat Rev Immunol 2005.

### Differentiation between PCFCL and PCLBCL-LT

Both PCFCL with a diffuse growth pattern and PCLBCL-LT show a diffuse population of large neoplastic B-cells, and differentiation between conditions, which is important from a therapeutic and prognostic point of view, can sometimes be difficult. While in the EORTC classification distinction between PCFCL and PCLBCL-LT was primarily based on site (leg versus non-leg),<sup>35</sup> in the WHO-EORTC classification<sup>1</sup> and the WHO 2008 classification<sup>2</sup> differentiation is mainly based on cell morphology, i.e. large cells with cleaved nuclei (centrocytes) in PCFCL and large B-cells with round nuclei (centroblasts and immunoblasts) in PCLBCL-LT.

The anatomical location of the cutaneous lesions can still be a helpful characteristic, but is not decisive. However, the predominant morphological subtype is sometimes a matter of debate. In such difficult cases the presence of a considerable number of admixed T-cells, the presence of a stromal reaction, as well as demonstration of (remnants of) follicular dendritic cell networks by staining with appropriate immunohistochemical antibodies (CD35 or CD21) may serve as useful additional arguments suggesting a diagnosis of PCFCL. Moreover, as PCLBCL-LT, unlike PCFCL, characteristically shows strong expression of B-cell lymphoma 2 (BCL2), IRF4/MUM1 and FOXP1, this phenotypic profile may be used as a helpful adjunct supporting a diagnosis of PCLBCL-LT.<sup>26,28</sup> Still, as BCL2, MUM1 and FOXP1 are also expressed by a small minority of PCFCL, these markers cannot be used as a golden standard to differentiate between both conditions. In Table 1 the differences between PCFCL and PCLBCL-LT in the current classification systems are summarized. In a minority of cases these clinical, histopathological and immunohistochemical features are still insufficient to

distinguish the two subtypes of PCLBCL.<sup>36</sup>

### *Molecular genetic studies*

Genetic differences between PCFCL and PCLBCL-LT have also been observed. Array-based comparative genomic hybridization (CGH) studies showed more frequent amplification of chromosomal region 2p16.1 and loss of 14q11.2-q12 in PCFCL, while deletion of complete chromosome arm 6q and of a region corresponding to chromosome region 9p21.3 were preferentially detected in PCLBCL-LT.<sup>37</sup> Detailed molecular analysis of this region by multiplex ligation-dependent probe amplification (MLPA) in combination with promoter hypermethylation assays in a relatively large cohort of PCLBCL-LT furthermore showed that inactivation of cyclin-dependent kinase inhibitor 2A (CDKN2A), situated on 9p21.3, was associated with an unfavorable 5 year disease specific survival.<sup>38</sup> The gene expression profiles of PCFCL and PCLBCL-LT are to a considerable extent concordant with normal germinal center B-cells/GCB-DLBCL and activated B-cells/ABC-DLBCL, respectively. Differences in gene expression between the two subtypes of PCLBCL include higher expression of immunoglobulin mu heavy chain enhancer and constant region (*IGHM*), proto-oncogenes Pim kinases 1 and 2 (*PIM1* and *PIM2*), and transcription factors *IRF4* and octamer transcription factor 2 (*OCT2*) in PCLBCL-LT. Serine protease inhibitor, Kazal type 2 (*SPINK2*) showed higher expression in PCFCL.<sup>27</sup> A summary of the most relevant differences between PCFCL and PCLBCL-LT is represented in Table 1.

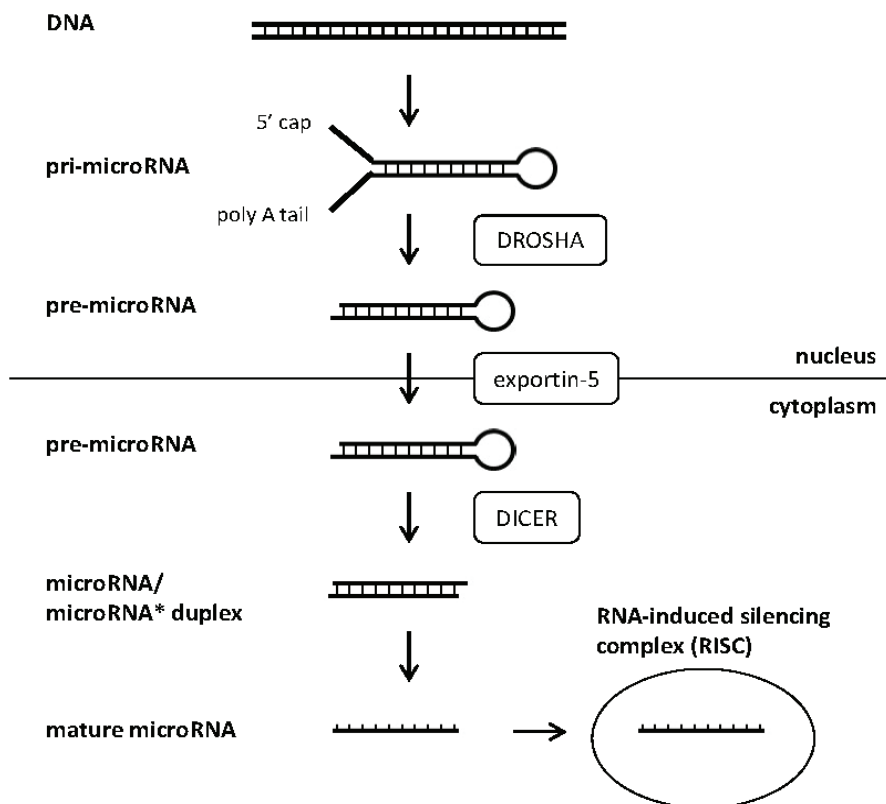
### *MicroRNAs*

Differences in microRNA profiles can be detected between various types of tumors and might therefore be helpful in the differential diagnosis between tumor subtypes. MicroRNAs are approximately 22 nucleotide long non-coding RNAs. They are transcribed from their DNA locus by RNA polymerase II in a primary microRNA (pri-microRNA) complex consisting of a loop and two strands containing a regular and a complementary star microRNA sequence. The RNase III enzyme Drosha subsequently recognizes and cleaves this structure, forming a hairpin structure (pre-microRNA). Exportin 5 then exports the pre-microRNA to the cytoplasm, where the RNase enzyme Dicer cleaves off the loop of the hairpin, releasing both microRNA sequences, which are now called mature microRNAs. Potentially, both microRNA variants of one locus can be functional, but usually one variant dominates. The mature microRNA is finally incorporated into a RNA-induced silencing complex (RISC) to exert its function. Through this RISC, microRNAs have the potential to regulate gene expression of their target genes. They are known to be able to inhibit translational initiation by blocking ribosomes. They can also directly target mRNA at the 3 prime untranslated region leading to degradation of the molecule.<sup>39</sup> These interactions usually rather lead to fine-tuning of protein levels than complete silencing of the target gene.<sup>40</sup> An overview of the biogenesis of microRNAs is depicted in Figure 4.

MicroRNAs play a role in normal human hematopoiesis, which was firstly demonstrated by the detection of three microRNAs (miR-142, miR-181 and miR-223) which were specifically encountered in hematopoietic tissues.<sup>41</sup> In B-cell development, a crucial role is found for miR-150, which is not expressed in progenitor B-cells, but shows high expression levels in mature B-cells. MiR-150 controls B-cell differentiation by targeting transcription factor and proto-oncogene c-MYB,<sup>42</sup> which, amongst others, is one of the critical master regulators of B-cell proliferation in germinal centers.<sup>43</sup> The miR-17~92 cluster (containing miR-17, miR-18a,

miR-19, miR-20a and miR-92a) is also essential for B-cell development, as absence of these microRNAs in mice leads to a block of the differentiation from pro B-cell to pre B-cell phase.<sup>44</sup>

Figure 4. MicroRNA biogenesis



The potential role of microRNAs in oncogenesis is emphasized by reports of several cancer types showing microRNA profiles that are significantly different as compared to normal cells from the same tissue type, which also accounts for hematopoietic tumors (reviewed in <sup>45</sup>). In nodal DLBCL, microRNA research has to a large extent been focused on the identification of microRNAs separating GCB-type from ABC-type DLBCL for diagnostic purposes. Although conflicting results have been reported, the most frequently encountered microRNA alterations are upregulation of miR-155, miR-21, miR-221 and miR-222 in ABC-type DLBCL as compared to GCB-type DLBCL as detected by microarray profiling and/or Real Time-polymerase chain reaction (RT-PCR).<sup>46-54</sup> Furthermore, upregulated expression of miR-21 has been reported to have an adverse prognostic impact in nodal DLBCL.<sup>50</sup>

The microRNA profiles of PCFCL and PCLBCL-LT are to a large extent unknown. A recently published study did perform quantitative PCR (qPCR) for a limited set of microRNAs on a group of PCFCL with the focus on comparison with PCMZL. A trend of higher expression miR-155-5p and miR-150-5p associated with shorter progression-free survival was reported.<sup>55</sup>

## New therapeutic targets for PCLBCL-LT

For a long time, optimal chemotherapy treatment regime for all PCLBCL-LT patients has been the same: CHOP or CHOP-like chemotherapy, concordant with treatment of nodal DLBCL. A recent improvement in CHOP chemotherapy has been the introduction of rituximab (monoclonal anti-CD20 antibody) to the chemotherapy regimens since 2001. Overall survival of nodal DLBCL has since then improved with 15 percent.<sup>56</sup> One study in PCLBCL-LT concerning the addition of rituximab to polychemotherapy also showed an increase in complete response rate and 3-year specific survival rate in patients receiving additional rituximab,<sup>57</sup> and treatment with rituximab-CHOP (R-CHOP) has been widely accepted as first choice treatment option.<sup>36</sup>

For a large part, the unfavorable clinical outcome of PCLBCL-LT seems to be related to the aggressive nature of the disease. Despite initial response to treatment with polychemotherapy, many patients have rapid recurrences, show progressive disease with secondary nodal and visceral involvement and eventually succumb to the disease. Unfortunately, due to age or age-related comorbidity, not all patients are eligible for polychemotherapy. Both the inadequacy of current chemotherapy treatment in some patients and the not being eligible for chemotherapy in others, urges for new, additional treatment options in PCLBCL-LT.

In general in cancer research, the majority of new potential targets for treatment are elaborately tested in cell lines of the tumor type investigated. Unfortunately, no cell lines of PCLBCL-LT are currently available, hampering research options for treatment improvement. Due to previously mentioned similarities between PCLBCL-LT and nodal ABC-DLBCL, treatments that are experimentally investigated in this type of nodal lymphoma, might also be of interest in PCLBCL-LT. Therefore, it is of great interest to further investigate to what extent PCLBCL-LT actually resembles nodal ABC-DLBCL and whether therapeutic targets in ABC-DLBCL can also be targeted in PCLBCL-LT to optimize treatment outcome.

### *Nuclear factor- $\kappa$ B*

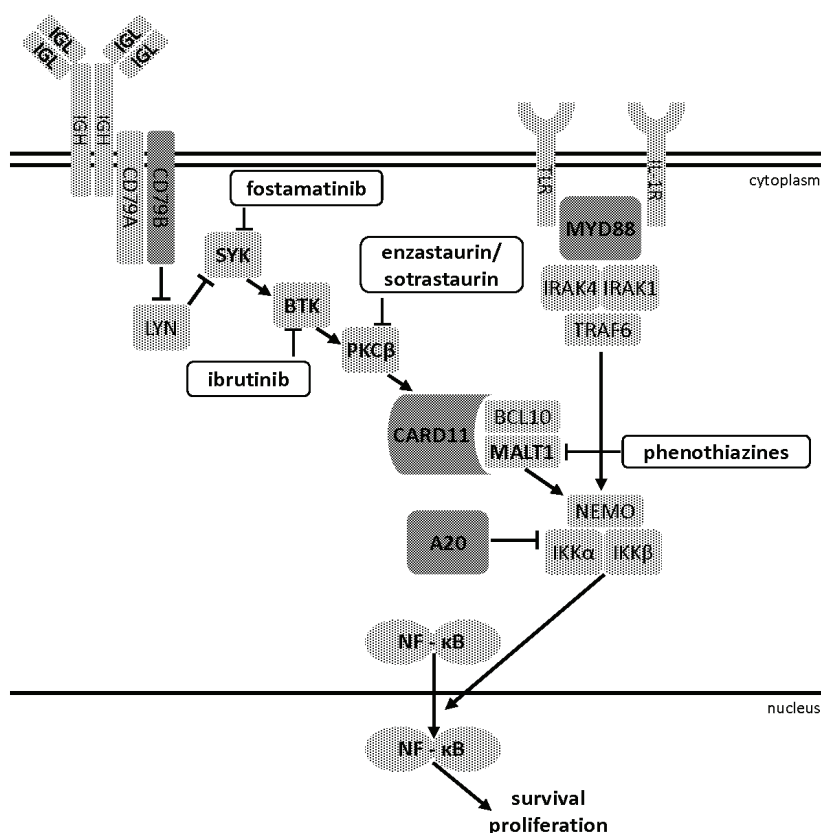
Nuclear factor- $\kappa$ B (NF- $\kappa$ B) comprises a family of transcription factors controlling genes that play a critical role in B-cell activation, proliferation and resistance to apoptosis. The NF- $\kappa$ B family has five members: p65 (RelA), p50 (NF- $\kappa$ B1), p52 (NF- $\kappa$ B2), RelB and c-Rel. In non-stimulated cells, these NF- $\kappa$ B proteins and their precursor proteins reside in the cytoplasm in an inactive form bound to NF- $\kappa$ B inhibitory proteins (I $\kappa$ Bs). The NF- $\kappa$ B pathway signals downstream after activation through various surface receptors, including the B-cell receptor. Two major signalling pathways account for the activation of NF- $\kappa$ B (Figure 5). In the canonical signalling pathway, signal transduction events lead to activation of the I $\kappa$ B kinase (IKK) complex resulting in phosphorylation and proteasomal degradation of I $\kappa$ B. Heterodimers and homodimers of p50, p65 and c-Rel can then be translocated to the nucleus to regulate gene transcription. The alternative pathway is characterized by I $\kappa$ B kinase complex activation through NF- $\kappa$ B induced kinase (NIK), eventually leading to processing of the p52 precursor subunit into active p52, which translocates to the nucleus and forms a heterodimeric complex with RelB.<sup>58,59</sup>

The NF- $\kappa$ B pathway has been implicated to play a role in the pathogenesis of different types of haematological malignancies, including nodal DLBCL. NF- $\kappa$ B activation is characteristic for ABC-DLBCL, although it is also encountered in a minority of GCB-DLBCL.<sup>60</sup> Constitutive activation of the pathway is required for survival of ABC-DLBCL cells in vitro.<sup>61</sup> ABC-DLBCLs

preferentially express known NF- $\kappa$ B target genes,<sup>62</sup> which amongst others include members of the anti-apoptotic families BCL2<sup>63</sup> and IAP,<sup>64</sup> and proliferation-related genes such as c- MYC<sup>65</sup> and IRF4.<sup>61</sup> Furthermore, a small molecule inhibitor of I $\kappa$ B kinase, an essential molecule in the activation of NF- $\kappa$ B, is selectively toxic to ABC-DLBCL cell lines.<sup>66</sup>

Mutations of several of the genes involved in the NF- $\kappa$ B pathway cause activation of NF- $\kappa$ B in DLBCL.<sup>60</sup> The genes most frequently affected by genetic aberrations are TNFAIP3 (A20), CD79B, CARD11 (CARMA1), and MYD88, which all can contribute to constitutive activation of the NF- $\kappa$ B pathway. In two-third of investigated cases of nodal ABC-type DLBCL, one or more of these genes are affected.<sup>67</sup> The NF- $\kappa$ B pathway inhibitor TNFAIP3 is commonly downregulated by (chromosomal) homozygous deletion or hemizygous deletion and hypermethylation of the promoter region of the remaining allele,<sup>60,68</sup> while the CD79B, CARD11, and MYD88 genes are frequently targeted by mutations that lead to activation of the NF- $\kappa$ B pathway.<sup>67,69,70</sup>

Figure 5. The nuclear factor- $\kappa$ B signaling pathway in diffuse large B-cell lymphoma



The activation of the NF- $\kappa$ B pathway in diffuse large B-cell lymphomas via the B-cell receptor and the Toll-like receptor (TLR) and IL-1 receptor (IL-1R) is depicted. The genes that commonly show genetic aberrations in nodal DLBCL and lead to constitutive pathway activation are dark grey. Signaling proteins that are under investigation for therapeutic targeting and thereby inhibiting the NF- $\kappa$ B pathway are represented by gene names in bold and a selection of NF- $\kappa$ B pathway blockers are depicted in black-lined boxes.

Together, these results suggest that activation of the NF- $\kappa$ B pathway is involved in the pathogenesis of ABC-type DLBCL and that this pathway can serve as a potential therapeutic target in DLBCL. Indeed, several signalling proteins in the NF- $\kappa$ B pathway have already been selectively targeted *in vitro* and *in vivo* to explore potential new treatment strategies, including SYK (by fostamatinib),<sup>71</sup> BTK (ibrutinib),<sup>72,73</sup> PKC $\beta$  (enzastaurin/sotrastaurin),<sup>74,75</sup> and MALT1 (phenothiazines)<sup>76,77</sup> (see Figure 5). Moreover, the mutational status of especially CARD11 and CD79B and to a lesser extent MYD88 has been linked to sensitivity or resistance to drugs targeting the NF- $\kappa$ B pathway,<sup>74,78</sup> and their role therefore seems essential in tumor cell survival in nodal ABC-type DLBCL.

### **Methotrexate-associated B-cell lymphoproliferative disorders presenting in the skin**

PCLBCL-LT should be differentiated not only from PCFCL with a diffuse proliferation of large B-cells, but also from DLBCL secondarily involving the skin and from immunodeficiency-associated B-cell lymphoproliferative disorders (B-LPD) with large tumor cell morphology, such as methotrexate (MTX)-associated B-LPD. The drug MTX was primarily developed as an inhibitor of the dihydrofolatereductase enzyme, thereby inhibiting cell cycle division, and therapeutically used in high doses in acute leukemias.<sup>79</sup> Later on, it was discovered that low dose MTX therapy was effective in treating autoimmune diseases, such as rheumatoid arthritis and psoriasis.<sup>80</sup> While MTX was first reported to be administered in patients with rheumatoid arthritis and psoriasis in 1951,<sup>80</sup> specific MTX-associated B-LPD were not described until 1985.<sup>4</sup> Since that time, several reports of MTX-related NHL have been published, especially in patients with underlying rheumatoid arthritis. Most of these lymphomas were B-cell NHL, mainly DLBCL, that could be Epstein Barr virus (EBV)-related and -unrelated.<sup>81</sup> Of interest, there are several reports of spontaneous regression of NHL after withdrawal of MTX, underlining the potential pathogenetic role of MTX in these lymphomas.<sup>82</sup> Furthermore, these reports of spontaneous regression warrant for a careful wait-and-see approach in these patients, before considering more aggressive treatment regimens containing polychemotherapy and/or radiotherapy.

Reports of MTX-therapy associated B-LPD primarily or secondarily involving the skin are very rare, in particular those presenting with only skin lesions.<sup>6-9,83</sup> To ensure optimal management and avoid overtreatment, MTX-associated B-LPD presenting in the skin should be differentiated from PCFCL with a diffuse growth pattern, and from PCLBCL-LT. However, not much is known about histomorphological and/or immunophenotypical features of these cases that might facilitate recognition of this rare type of lymphoma and separate them from the 'regular' types of PCLBCL.

### **Thesis outline**

As differentiation between PCFCL with a diffuse growth pattern and PCLBCL-LT can sometimes be difficult, in **chapter 2** the previously described higher expression of IGHM by gene expression profiling in PCLBCL-LT as compared to PCFCL<sup>27</sup> is validated on a large cohort of PCFCL and PCLBCL-LT, in search for an adjunct immunohistochemical diagnostic marker distinguishing the two subtypes of CBCL. Formalin-fixed and paraffin-embedded (FFPE) tumor biopsy specimens were immunohistochemically stained for heavy chain and light chains, including immunohistochemistry for IgM.

In **chapter 3** the complete microRNA profiles of both PCFCL and PCLBCL-LT are determined by next generation high-throughput sequencing on frozen tumor biopsies and compared with the profile of in vitro activated B-cells, aiming to detect microRNA signatures associated with diagnosis and/or prognosis. The results are validated by qPCR on FFPE tumor biopsy specimens. Furthermore, this chapter explores whether these differences are similar to the differences in microRNA profiles found between nodal GCB-DLBCL and ABC-DLBCL.

In **chapter 4** the genes that show genetic aberrancies in nodal DLBCL and lead to constitutive activation of the NF- $\kappa$ B pathway are explored for deletions, mutations and/or epigenetic silencing in a set of PCLBCL-LT by fine-tiling comparative genomic hybridization (FT-CGH), DNA sequencing and/or methylation specific melt curve analysis (MS-MCA). The aim is to find out whether aberrant NF- $\kappa$ B pathway activation is a feature of PCLBCL-LT, and whether treatment targeting specific molecules in this pathway might be suitable for patients with PCLBCL-LT.

**Chapter 5** investigates whether maturation arrest of PCLBCL-LT in the activated B-cell stage might be related to (genetic) aberrancies in transcription factors that are involved in maturation of the B-cells beyond this stage, including FOXP1, PRDM1/Blimp1 and IRF4. We therefore assess alterations in these transcription factors in a set of PCLBCL-LT by FT-CGH, DNA sequencing, qPCR, and immunohistochemistry.

**Chapter 6** explores the clinical, pathological and immunophenotypical characteristics of MTX-associated DLBCLs presenting in the skin and compares these features with those of PCFCL and PCLBCL-LT, aiming to find differences that could aid in the differential diagnosis of these NHL.

**Chapter 7** summarizes and discusses the results of the studies described in the preceding chapters.

## References

1. Willemze R, Jaffe ES, Burg G, et al. (2005) WHO-EORTC classification for cutaneous lymphomas. *Blood* 105: 3768-85.
2. Swerdlow SH, Campo E, Harris NL, et al. (2008) WHO Classification of Tumours Haematopoietic and Lymphoid Tissues. Geneva, Switzerland: WHO PRESS.
3. Senff NJ, Hoefnagel JJ, Jansen PM, et al. (2007) Reclassification of 300 primary cutaneous B-Cell lymphomas according to the new WHO-EORTC classification for cutaneous lymphomas: comparison with previous classifications and identification of prognostic markers. *J Clin Oncol* 25: 1581-7.
4. Weinstein A, Marlowe S, Korn J, Farouhar F (1985) Low-dose methotrexate treatment of rheumatoid arthritis. Long-term observations. *Am J Med* 79: 331-7.
5. Verma S, Frambach GE, Seilstad KH, et al. (2005) Epstein-Barr virus-associated B-cell lymphoma in the setting of iatrogenic immune dysregulation presenting initially in the skin. *J Cutan Pathol* 32: 474-83.
6. Pfistershammer K, Petzelbauer P, Stingl G, et al. (2010) Methotrexate-induced primary cutaneous diffuse large B-cell lymphoma with an 'angiocentric' histological morphology. *Clin Exp Dermatol* 35: 59-62.
7. Tournadre A, D'Incan M, Dubost JJ, et al. (2001) Cutaneous lymphoma associated with Epstein-Barr virus infection in 2 patients treated with methotrexate. *Mayo Clin Proc* 76: 845-8.
8. Chai C, White WL, Shea CR, Prieto VG (1999) Epstein Barr virus-associated lymphoproliferative-disorders primarily involving the skin. *J Cutan Pathol* 26: 242-7.
9. Rausch T, Cairoli A, Benhattar J, et al. (2013) EBV+ cutaneous B-cell lymphoproliferation of the leg in an elderly patient with mycosis fungoides and methotrexate treatment. *APMIS* 121: 79-84.
10. Goebel P, Janney N, Valenzuela JR, et al. (2001) Localized gene-specific induction of accessibility to V(D)J recombination induced by E2A and early B cell factor in nonlymphoid cells. *J Exp Med* 194: 645-56.
11. Oettinger MA, Schatz DG, Gorka C, Baltimore D (1990) RAG-1 and RAG-2, adjacent genes that synergistically activate V(D)J recombination. *Science* 248: 1517-23.
12. Desiderio SV, Yancopoulos GD, Paskind M, et al. (1984) Insertion of N regions into heavy-chain genes is correlated with expression of terminal deoxytransferase in B cells. *Nature* 311: 752-5.
13. Martensson IL, Rolink A, Melchers F, et al. (2002) The pre-B cell receptor and its role in proliferation and Ig heavy chain allelic exclusion. *Semin Immunol* 14: 335-42.
14. Mostoslavsky R, Alt FW, Rajewsky K (2004) The lingering enigma of the allelic exclusion mechanism. *Cell* 118: 539-44.
15. Rolink AG, Schaniel C, Andersson J, Melchers F (2001) Selection events operating at various stages in B cell development. *Curr Opin Immunol* 13: 202-7.
16. Bryant VL, Ma CS, Avery DT, et al. (2007) Cytokine-mediated regulation of human B cell differentiation into Ig-secreting cells: predominant role of IL-21 produced by CXCR5+ T follicular helper cells. *J Immunol* 179: 8180-90.
17. Ettinger R, Sims GP, Fairhurst AM, et al. (2005) IL-21 induces differentiation of human naive and memory B cells into antibody-secreting plasma cells. *J Immunol* 175: 7867-79.
18. Ozaki K, Spolski R, Ettinger R, et al. (2004) Regulation of B cell differentiation and plasma cell generation by IL-21, a novel inducer of Blimp-1 and Bcl-6. *J Immunol* 173: 5361-71.
19. Basso K, Dalla-Favera R (2010) BCL6: master regulator of the germinal center reaction and key oncogene in B cell lymphomagenesis. *Adv Immunol* 105: 193-210.
20. Muramatsu M, Kinoshita K, Fagarasan S, et al. (2000) Class switch recombination and hypermutation require activation-induced cytidine deaminase (AID), a potential RNA editing enzyme. *Cell* 102: 553-63.
21. Di Noia JM, Neuberger MS (2007) Molecular mechanisms of antibody somatic hypermutation. *Annu Rev Biochem* 76: 1-22.
22. Shinkura R, Ito S, Begum NA, et al. (2004) Separate domains of AID are required for somatic hypermutation and class-switch recombination. *Nat Immunol* 5: 707-12.



23. Saito M, Gao J, Basso K, et al. (2007) A signaling pathway mediating downregulation of BCL6 in germinal center B cells is blocked by BCL6 gene alterations in B cell lymphoma. *Cancer Cell* 12: 280-92.
24. Cobaleda C, Schebesta A, Delogu A, Busslinger M (2007) Pax5: the guardian of B cell identity and function. *Nat Immunol* 8: 463-70.
25. Kallies A, Hasbold J, Fairfax K, et al. (2007) Initiation of plasma-cell differentiation is independent of the transcription factor Blimp-1. *Immunity* 26: 555-66.
26. Hoefnagel JJ, Vermeer MH, Jansen PM, et al. (2003) Bcl-2, Bcl-6 and CD10 expression in cutaneous B-cell lymphoma: further support for a follicle centre cell origin and differential diagnostic significance. *Br J Dermatol* 149: 1183-91.
27. Hoefnagel JJ, Dijkman R, Basso K, et al. (2005) Distinct types of primary cutaneous large B-cell lymphoma identified by gene expression profiling. *Blood* 105: 3671-8.
28. Hoefnagel JJ, Mulder MM, Dreef E, et al. (2006) Expression of B-cell transcription factors in primary cutaneous B-cell lymphoma. *Mod Pathol* 19: 1270-6.
29. Alizadeh AA, Eisen MB, Davis RE, et al. (2000) Distinct types of diffuse large B-cell lymphoma identified by gene expression profiling. *Nature* 403: 503-11.
30. Gutierrez-Garcia G, Cardesa-Salzman T, Climent F, et al. (2011) Gene-expression profiling and not immunophenotypic algorithms predicts prognosis in patients with diffuse large B-cell lymphoma treated with immunochemotherapy. *Blood* 117: 4836-43.
31. Pasqualucci L, Compagno M, Houldsworth J, et al. (2006) Inactivation of the PRDM1/BLIMP1 gene in diffuse large B cell lymphoma. *J Exp Med* 203: 311-7.
32. Mandelbaum J, Bhagat G, Tang H, et al. (2010) BLIMP1 is a tumor suppressor gene frequently disrupted in activated B cell-like diffuse large B cell lymphoma. *Cancer Cell* 18: 568-79.
33. Salaverria I, Philipp C, Oschlies I, et al. (2011) Translocations activating IRF4 identify a subtype of germinal center-derived B-cell lymphoma affecting predominantly children and young adults. *Blood* 118: 139-47.
34. Goatly A, Bacon CM, Nakamura S, et al. (2008) FOXP1 abnormalities in lymphoma: translocation breakpoint mapping reveals insights into deregulated transcriptional control. *Mod Pathol* 21: 902-11.
35. Willemze R, Kerl H, Sterry W, et al. (1997) EORTC classification for primary cutaneous lymphomas: a proposal from the Cutaneous Lymphoma Study Group of the European Organization for Research and Treatment of Cancer. *Blood* 90: 354-71.
36. Senff NJ, Noordijk EM, Kim YH, et al. (2008) European Organization for Research and Treatment of Cancer and International Society for Cutaneous Lymphoma consensus recommendations for the management of cutaneous B-cell lymphomas. *Blood* 112: 1600-9.
37. Dijkman R, Tensen CP, Jordanova ES, et al. (2006) Array-based comparative genomic hybridization analysis reveals recurrent chromosomal alterations and prognostic parameters in primary cutaneous large B-cell lymphoma. *J Clin Oncol* 24: 296-305.
38. Senff NJ, Zoutman WH, Vermeer MH, et al. (2009) Fine-mapping chromosomal loss at 9p21: correlation with prognosis in primary cutaneous diffuse large B-cell lymphoma, leg type. *J Invest Dermatol* 129: 1149-55.
39. Bartel DP (2004) MicroRNAs: genomics, biogenesis, mechanism, and function. *Cell* 116: 281-97.
40. Bartel DP, Chen CZ (2004) Micromanagers of gene expression: the potentially widespread influence of metazoan microRNAs. *Nat Rev Genet* 5: 396-400.
41. Chen CZ, Li L, Lodish HF, Bartel DP (2004) MicroRNAs modulate hematopoietic lineage differentiation. *Science* 303: 83-6.
42. Xiao C, Calado DP, Galler G, et al. (2007) MiR-150 controls B cell differentiation by targeting the transcription factor c-Myb. *Cell* 131: 146-59.
43. Lefebvre C, Rajbhandari P, Alvarez MJ, et al. (2010) A human B-cell interactome identifies MYB and FOXM1 as master regulators of proliferation in germinal centers. *Mol Syst Biol* 6: 377.
44. Ventura A, Young AG, Winslow MM, et al. (2008) Targeted deletion reveals essential and overlapping functions of the miR-17 through 92 family of miRNA clusters. *Cell* 132: 875-86.

45. Calin GA, Croce CM (2006) MicroRNA signatures in human cancers. *Nat Rev Cancer* 6: 857-66.
46. Culpin RE, Proctor SJ, Angus B, et al. (2010) A 9 series microRNA signature differentiates between germinal centre and activated B-cell-like diffuse large B-cell lymphoma cell lines. *Int J Oncol* 37: 367-76.
47. Huang X, Shen Y, Liu M, et al. (2012) Quantitative proteomics reveals that miR-155 regulates the PI3K-AKT pathway in diffuse large B-cell lymphoma. *Am J Pathol* 181: 26-33.
48. Jima DD, Zhang J, Jacobs C, et al. (2010) Deep sequencing of the small RNA transcriptome of normal and malignant human B cells identifies hundreds of novel microRNAs. *Blood* 116: e118-e127.
49. Lawrie CH, Chi J, Taylor S, et al. (2009) Expression of microRNAs in diffuse large B cell lymphoma is associated with immunophenotype, survival and transformation from follicular lymphoma. *J Cell Mol Med* 13: 1248-60.
50. Lawrie CH, Soneji S, Marafioti T, et al. (2007) MicroRNA expression distinguishes between germinal center B cell-like and activated B cell-like subtypes of diffuse large B cell lymphoma. *Int J Cancer* 121: 1156-61.
51. Malumbres R, Sarosiek KA, Cubedo E, et al. (2009) Differentiation stage-specific expression of microRNAs in B lymphocytes and diffuse large B-cell lymphomas. *Blood* 113: 3754-64.
52. Montes-Moreno S, Martinez N, Sanchez-Espiridon B, et al. (2011) miRNA expression in diffuse large B-cell lymphoma treated with chemoimmunotherapy. *Blood* 118: 1034-40.
53. Roehle A, Hoefig KP, Reptsilber D, et al. (2008) MicroRNA signatures characterize diffuse large B-cell lymphomas and follicular lymphomas. *Br J Haematol* 142: 732-44.
54. Zhong H, Xu L, Zhong JH, et al. (2012) Clinical and prognostic significance of miR-155 and miR-146a expression levels in formalin-fixed/paraffin-embedded tissue of patients with diffuse large B-cell lymphoma. *Exp Ther Med* 3: 763-70.
55. Monsalvez V, Montes-Moreno S, Artiga MJ, et al. (2013) MicroRNAs as prognostic markers in indolent primary cutaneous B-cell lymphoma. *Mod Pathol* 26: 171-81.
56. Flowers CR, Sinha R, Vose JM (2010) Improving outcomes for patients with diffuse large B-cell lymphoma. *CA Cancer J Clin* 60: 393-408.
57. Grange F, Maubec E, Bagot M, et al. (2009) Treatment of cutaneous B-cell lymphoma, leg type, with age-adapted combinations of chemotherapies and rituximab. *Arch Dermatol* 145: 329-30.
58. Perkins ND (2007) Integrating cell-signalling pathways with NF-kappaB and IKK function. *Nat Rev Mol Cell Biol* 8: 49-62.
59. Sun SC, Ley SC (2008) New insights into NF-kappaB regulation and function. *Trends Immunol* 29: 469-478.
60. Compagno M, Lim WK, Grunn A, et al. (2009) Mutations of multiple genes cause deregulation of NF-kappaB in diffuse large B-cell lymphoma. *Nature* 459: 717-21.
61. Davis RE, Brown KD, Siebenlist U, Staudt LM (2001) Constitutive nuclear factor kappaB activity is required for survival of activated B cell-like diffuse large B cell lymphoma cells. *J Exp Med* 194: 1861-74.
62. Ngo VN, Davis RE, Lamy L, et al. (2006) A loss-of-function RNA interference screen for molecular targets in cancer. *Nature* 441: 106-10.
63. Zheng Y, Vig M, Lyons J, Van Parijs L, Beg AA (2003) Combined deficiency of p50 and cRel in CD4+ T cells reveals an essential requirement for nuclear factor kappaB in regulating mature T cell survival and in vivo function. *J Exp Med* 197: 861-74.
64. Wang CY, Mayo MW, Korneluk RG, Goeddel DV, Baldwin AS, Jr. (1998) NF-kappaB antiapoptosis: induction of TRAF1 and TRAF2 and c-IAP1 and c-IAP2 to suppress caspase-8 activation. *Science* 281: 1680-3.
65. Grumont RJ, Strasser A, Gerondakis S (2002) B cell growth is controlled by phosphatidylinositol 3-kinase-dependent induction of Rel/NF-kappaB regulated c-myc transcription. *Mol Cell* 10: 1283-94.
66. Lam LT, Davis RE, Pierce J, et al. (2005) Small molecule inhibitors of IkappaB kinase are selectively toxic for subgroups of diffuse large B-cell lymphoma defined by gene expression profiling. *Clin Cancer Res* 11: 28-40.
67. Ngo VN, Young RM, Schmitz R, et al. (2011) Oncogenically active MYD88 mutations in human lymphoma. *Nature* 470: 115-9.

68. Honma K, Tsuzuki S, Nakagawa M, et al. (2009) TNFAIP3/A20 functions as a novel tumor suppressor gene in several subtypes of non-Hodgkin lymphomas. *Blood* 114: 2467-75.
69. Davis RE, Ngo VN, Lenz G, et al. (2010) Chronic active B-cell-receptor signalling in diffuse large B-cell lymphoma. *Nature* 463: 88-92.
70. Lenz G, Davis RE, Ngo VN, et al. (2008) Oncogenic CARD11 mutations in human diffuse large B cell lymphoma. *Science* 319: 1676-9.
71. Friedberg JW, Sharman J, Sweetenham J, et al. (2010) Inhibition of Syk with fostamatinib disodium has significant clinical activity in non-Hodgkin lymphoma and chronic lymphocytic leukemia. *Blood* 115: 2578-85.
72. Advani RH, Buggy JJ, Sharman JP, et al. (2013) Bruton tyrosine kinase inhibitor ibrutinib (PCI-32765) has significant activity in patients with relapsed/refractory B-cell malignancies. *J Clin Oncol* 31: 88-94.
73. Yang Y, Shaffer AL, III, Emre NC, et al. (2012) Exploiting synthetic lethality for the therapy of ABC diffuse large B cell lymphoma. *Cancer Cell* 21: 723-37.
74. Naylor TL, Tang H, Ratsch BA, et al. (2011) Protein kinase C inhibitor sotrastaurin selectively inhibits the growth of CD79 mutant diffuse large B-cell lymphomas. *Cancer Res* 71: 2643-53.
75. Robertson MJ, Kahl BS, Vose JM, et al. (2007) Phase II study of enzastaurin, a protein kinase C beta inhibitor, in patients with relapsed or refractory diffuse large B-cell lymphoma. *J Clin Oncol* 25: 1741-6.
76. Fontan L, Yang C, Kabaleeswaran V, et al. (2012) MALT1 small molecule inhibitors specifically suppress ABC-DLBCL in vitro and in vivo. *Cancer Cell* 22: 812-4.
77. Nagel D, Spranger S, Vincendeau M, et al. (2012) Pharmacologic inhibition of MALT1 protease by phenothiazines as a therapeutic approach for the treatment of aggressive ABC-DLBCL. *Cancer Cell* 22: 825-37.
78. Wilson WH, Gerecitano JF, Goy A, et al. (2012) The Bruton's Tyrosine Kinase (BTK) Inhibitor, Ibrutinib (PCI-32765), Has Preferential Activity in the ABC Subtype of Relapsed/Refractory De Novo Diffuse Large B-Cell Lymphoma (DLBCL): Interim Results of a Multicenter, Open-Label, Phase 2 Study. *Blood (ASH Annual Meeting Abstracts)* 120: 4039.
79. Pierce M, Alt H (1948) Treatment of acute leucemia with aminopterin (4-amino-pteroylglutamic acid). *J Lab Clin Med* 33: 1642.
80. Gubner R, August S, Ginsberg V (1951) Therapeutic suppression of tissue reactivity. II. Effect of aminopterin in rheumatoid arthritis and psoriasis. *Am J Med Sci* 221: 176-82.
81. Tran H, Nourse J, Hall S, et al. (2008) Immunodeficiency-associated lymphomas. *Blood Rev* 22: 261-81.
82. Rizzi R, Curci P, Delia M, et al. (2009) Spontaneous remission of "methotrexate-associated lymphoproliferative disorders" after discontinuation of immunosuppressive treatment for autoimmune disease. Review of the literature. *Med Oncol* 26: 1-9.
83. Verma S, Frambach GE, Seilstad KH, et al. (2005) Epstein-Barr virus-associated B-cell lymphoma in the setting of iatrogenic immune dysregulation presenting initially in the skin. *J Cutan Pathol* 32: 474-83.





# 2

## **IgM expression on paraffin sections distinguishes primary cutaneous large B-cell lymphoma, leg type from primary cutaneous follicle center lymphoma**

*The American Journal of Surgical Pathology 2010;  
34(7): 1043-1048*

Lianne Koens, MD<sup>1</sup>

Maarten H. Vermeer, MD, PhD<sup>2</sup>

Rein Willemze, MD, PhD<sup>2</sup>

Patty M. Jansen, MD, PhD<sup>1</sup>

Departments of <sup>1</sup>Pathology and <sup>2</sup>Dermatology, Leiden University  
Medical Center, Leiden, The Netherlands



## Abstract

*In the World Health Organization (WHO) 2008 classification 2 main types of primary cutaneous large B-cell lymphomas (PCLBCLs) are distinguished: primary cutaneous follicle center lymphoma (PCFCL) and primary cutaneous large B-cell lymphoma, leg type (PCLBCL-LT). PCFCL has a 5-year overall survival rate of 95%, and PCLBCL-LT of approximately 50%. Expression profiling studies have shown higher RNA expression of the IgM heavy chain in PCLBCL-LT compared with PCFCL. To find out whether this difference could also be demonstrated at the protein level, we performed immunohistochemical staining for B-cell receptor heavy and light chains on skin biopsies from 53 patients with PCFCL and 40 patients with PCLBCL-LT. All 40 cases of PCLBCL-LT consistently showed cytoplasmic staining for IgM, in 18 of them with co-expression of IgD. In contrast, only 5 of the PCFCL cases showed cytoplasmic staining for IgM and/or IgD, including all 3 PCFCLs presenting on the leg. Hence, staining for IgM on paraffin-embedded sections seems to be an additional tool for differentiating between the 2 entities in clinical pathology practice. Analogous to other nodal and extranodal large B-cell lymphomas, expression of IgM in PCLBCL seems to be related to an activated B cell-like phenotype. Finally, the expression of IgM (and IgD) in this type of lymphoma might imply defective class switch recombination.*

## Introduction

Primary cutaneous large B-cell lymphomas (PCLBCLs) are a group of malignant lymphoproliferative disorders presenting in the skin with no evidence of extracutaneous disease at the time of diagnosis.<sup>1</sup> In the World Health Organization (WHO)-European Organization for Research and Treatment of Cancer (EORTC) classification<sup>2</sup> and the WHO 2008 classification<sup>3</sup> 2 main types of PCLBCL are distinguished: primary cutaneous follicle center lymphoma (PCFCL) and primary cutaneous diffuse large B-cell lymphoma, leg-type (PCLBCL-LT). PCFCL is considered an indolent type of lymphoma (5-y survival > 95%), predominantly presenting with localized skin lesions on the head or the trunk,<sup>4</sup> whereas PCLBCL-LT has a more aggressive clinical course (5-y survival approximately 50%) and most often presents on the legs.<sup>5</sup> Distinction between the different subtypes of PCLBCL is important, as it dictates the first choice of treatment, that is, radiotherapy in PCFCL and the combination of anthracyclin-based chemotherapy and rituximab in PCLBCL-LT.<sup>6</sup> In the EORTC classification of 1997, the subdivision was made solely on the localization of the tumor (head/trunk versus legs).<sup>1</sup> In the WHO-EORTC classification of 2005 and WHO classification of 2008, distinction is primarily based on morphological criteria, namely the absence or presence of confluent sheets of centroblasts and/or immunoblasts, designated previously as cleaved cell versus round cell morphology.<sup>7</sup> Differentiation on the basis of morphology is sometimes a matter of debate. In such difficult cases the presence of a considerable number of admixed T-cells, the presence of a stromal reaction as well as demonstration of (remnants of) follicular dendritic cell networks by staining with appropriate antibodies (CD35 or CD21) may serve as useful additional criteria suggesting a diagnosis of PCFCL. Moreover, as PCLBCL-LT, unlike PCFCL, characteristically shows strong expression of BCL2, IRF4/MUM1 and FOXP1, this phenotype profile may be used as a useful adjunct supporting a diagnosis of PCLBCL-LT.<sup>2</sup> However, as BCL2, MUM-1 and FOXP-1 are also expressed by a small minority of PCFCL, these markers cannot be used as a golden standard to differentiate between both conditions.<sup>6,8</sup>

Although PCLBCLs are suggested to have a distinct relationship with different stages of normal B-cell development, surprisingly little is known about the composition of the B-cell



receptor (BCR) of this type of lymphoma. Expression profiling studies of our group have shown higher RNA expression levels of the IgM heavy chain of the BCR in PCLBCL-LT as compared with PCFCL.<sup>9</sup> The aim of our current study was to find out whether this difference in expression level could also be detected at the protein level by immunohistochemical staining. Differences in immunohistochemical IgM expression could be of additional diagnostic value, as it is an easy procedure to perform in daily clinical pathology practice.

## Materials and methods

### *Patient Selection*

Forty patients with PCLBCL-LT and 53 patients with PCFCL were selected from the archive of the Dutch Cutaneous Lymphoma Group. Characteristically, 33 of 40 cases of PCLBCL-LT presented with skin lesions on one or both legs, whereas 7 patients presented with skin lesions at other sites including the trunk (3 cases), head (3 cases), and arm (1 case). In the group of PCFCL 44 patients presented with localized skin lesions on the head or trunk, 6 had more generalized lesions, but without involvement of the leg, while 3 patients had skin lesions on 1 or 2 legs at presentation. All cases had been classified by a panel of hematopathologists and dermato(patho)logists according to the criteria of the WHO-EORTC classification.<sup>1</sup> All patients were adequately staged; physical examination, blood count, computed tomography scan, and bone marrow biopsy were performed and showed no signs of extracutaneous disease manifestation at the time of diagnosis. Of all the patients, formalin-fixed and paraffin-embedded pretreatment biopsy or excision tumor tissue was collected from different hospitals in the Netherlands.

### *Antibodies and immunohistochemistry*

Immunohistochemical staining was performed on 4  $\mu$ m sections using standard procedures. After antigen retrieval by boiling for 10 minutes in 1.0 mmol/L ethylenediamine tetra-acetic acid (pH 8.0) for IRF4/MUM1 and BCL6, and in 10 mmol/L citrate buffer (pH 6.0) for  $\kappa$ ,  $\lambda$ , IgM, IgG, IgA, IgD, and BCL2, tissue sections were incubated overnight with the different antibodies, listed in Table 1. Sections were then incubated for 30 minutes with PowerVision Poly-horseradish peroxidase. Subsequently, a 10-minute incubation with diaminobenzidine (DAB) solution (Sigma-Aldrich, Zwijndrecht, The Netherlands) for IRF4/MUM1, Bcl2 and Bcl6 was performed, whereas slides with  $\kappa$ ,  $\lambda$ , IgM, IgG, IgA, and IgD were incubated with DAB+ chromogen (K-3468, DAKO, Glostrup, Denmark) for 10 minutes. Finally, all slides were counterstained with Mayer's haematoxylin.

### *Data analysis*

The data were analyzed with SPSS version 16.0. Descriptive statistics were used to describe the characteristics of the study population. Differences in immunohistochemical positivity for IgM, Bcl2, and IRF4/MUM1 between the 2 diagnosis groups were calculated with the  $\chi^2$  test. Binary logistic univariate and multivariate regression modeling was used to determine the extent to which patient characteristics (independent variables) could differentiate between the diagnosis of PCFCL or PCLBCL-LT (dependent variable). In the multiple regression analysis, gender, age over 70, tumor localization on the leg(s), and immunohistochemical positivity for BCL2, IRF4/MUM1 and IgM were entered in a forward stepwise method with likelihood

ratio test, to assort the most optimal and feasible combination of parameters to predict the final diagnosis in patients with PCLBCL. *P*-values lower than 0.05 were considered to indicate statistical significance.

**Table 1.** Antibodies used in this study

Protein	Clone	Source	Dilution
κ	rabbit polyclonal	DAKO, Glostrup, Denmark	1:16000
λ	rabbit polyclonal	DAKO, Glostrup, Denmark	1:16000
IgM	rabbit polyclonal	DAKO, Glostrup, Denmark	1:8000
IgG	rabbit polyclonal	DAKO, Glostrup, Denmark	1:8000
IgA	rabbit polyclonal	DAKO, Glostrup, Denmark	1:8000
IgD	rabbit polyclonal	DAKO, Glostrup, Denmark	1:4000
BCL2	mouse monoclonal	DAKO, Glostrup, Denmark	1:200
BCL6	mouse monoclonal	DAKO, Glostrup, Denmark	1:50
IRF4/MUM1	mouse monoclonal	DAKO, Glostrup, Denmark	1:100

## Results

A summary of relevant clinical and follow-up data of the different groups is given in Table 2. Table 3 summarizes the results of the immunohistochemical staining.

### *PCLBCL-LT*

In all 40 cases of PCLBCL-LT there was moderate to strong cytoplasmatic staining for IgM of almost all tumor cells. Of these cases, 18 showed coexpression of IgD, mainly with weak staining intensity (Figs. 1A-C). Except for 1 case without any detectable light chain expression of the tumor cells, all cases showed either monotypic κ (*n* = 26) or λ (*n* = 13) expression. The 7 cases classified as PCLBCL-LT with presentation on the head, trunk, or arm showed similar results as the PCLBCL-LT presenting on the legs (Table 3). Membranous expression of BCL2 was detected in most cases of PCLBCL-LT (36/40), as was nuclear expression of IRF4/MUM1 (35/40), both of which were independent of the site of presentation. Nuclear expression of BCL6 was detected in approximately half of the cases (18/40).

### *PCFCL*

Out of 50 cases of PCFCL presenting on the head or trunk 2 cases showed moderately strong cytoplasmatic staining of virtually all of the tumor cells for IgM, combined with coexpression of IgD. Except for 4 cases showing questionable expression of IgG or IgA in combination with monotypic κ or λ light chain restriction, 43 cases showed no expression of heavy or light chains at all (Figs. 1D-F). One case showed monotypic κ light chain expression without expression of a specific heavy chain. The IgM and IgD-negative cases showed evident positive internal controls, as the remains of the mantle zone in between the neoplastic cells did show expression of these 2 markers, sparing the neoplastic cells. In contrast, all 3 cases presenting on one or both legs showed strong cytoplasmatic expression of IgM and of κ (*n* = 2) or λ (*n* = 1) light chain (Figs. 1G-I). There was no coexpression of IgD in these cases.

Table 2. Characteristics of the study population

	PCLBCL-LT		PCFCL	
	leg	head/trunk	leg	head/trunk
Number of cases	33	7	3	50
Sex				
- male	12	5	1	39
- female	21	2	2	11
Age (years)				
- median	78	80	70	58
- range	47-92	60-86	68-83	21-81
Initial therapy				
- radiotherapy	13	5	3	40
- polychemotherapy	12	1	0	3
- chemoradiation	4	0	0	3
- none	3	0	0	1
- other	1	1	0	3
Follow-up (months)				
- median	19	26	30	54
- range	2-121	5-72	26-32	1-264
Current status				
- A <sup>0</sup>	7	5	0	32
- A <sup>+</sup>	5	2	0	11
- D <sup>0</sup>	4	0	2	6
- D <sup>+</sup>	17	0	1	0
- unknown	0	0	0	1

A<sup>+</sup> indicates alive with disease; A<sup>0</sup>, alive without disease; D<sup>+</sup>, death with disease; D<sup>0</sup>, death without disease; PCLBCL-LT, primary cutaneous B-cell lymphoma- leg type; PCFCL, primary cutaneous follicle center lymphoma.

The 2 patients with tumors on the head or trunk that expressed IgM and IgD were treated with radiotherapy and are still alive without evidence of disease activity after 102 and 161 months, respectively. One of these patients had a cutaneous relapse after 46 months of follow-up that was treated with chemotherapy resulting in complete remission. Two of the 3 patients with PCFCL presenting on the leg died 26 and 30 months after radiation of the primary tumor due to causes unrelated to the disease. In one of these patients, a cutaneous relapse occurred after 9 months of follow-up, which was successfully treated with additional radiotherapy. The third patient with PCFCL presenting on the leg was treated with radiotherapy resulting in complete remission. However, he died with disseminated lymphoma 32 months after initial diagnosis.

Twenty-two cases of PCFCL showed a (partly) follicular growth pattern of the neoplastic cells, whereas the remaining 31 cases, including the ones presenting on the leg(s), exhibited a diffuse growth pattern. Expression of IgM (and IgD) was not restricted to either growth pattern. Membranous expression of BCL2 was detected in 9/50 cases presenting on the head or trunk, but in none of the 3 cases presenting on the leg(s). Nuclear expression of IRF4/MUM1 was

detected in only 1 PCFCL, presenting on the leg. Nuclear expression of BCL6 was detected in almost all cases (51/53).

**Table 3.** Results of immunohistochemical staining procedures

Diagnosis	Total No.	Heavy Chains				Light Chains		BCL2+	BCL6+	Mum1+
		IgM+	IgD+	IgG+	IgA+	κ+	λ+			
PCLBCL-LT	40	40 (100%)	18 (45%)	0	0	26 (65%)	13 (33%)	36 (90%)	18 (45%)	35 (88%)
presenting on leg (s)	33	33 (100%)	17 (52%)	0	0	21 (64%)	11 (33%)	30 (91%)	15 (45%)	30 (91%)
presenting on head/trunk	7	7 (100%)	1 (14%)	0	0	5 (71%)	2 (29%)	6 (86%)	3 (43%)	5 (71%)
PCFCL	53	5 (9%)	2 (4%)	3 (6%)	1 (2%)	8 (15%)	2 (4%)	9 (17%)	51 (96%)	1 (2%)
presenting on leg (s)	3	3 (100%)	0	0	0	2 (67%)	1 (33%)	0	1 (33%)	1 (33%)
presenting on head/trunk	50	2 (4%)	2 (4%)	3 (6%)	1 (2%)	6 (12%)	1 (2%)	9 (18%)	50 (100%)	0

For BCL2 and BCL6 cases were considered positive if more than 50% of the tumor cells showed expression, the cut-off point for positivity of IRF4/MUM1 was 30%.

K indicates kappa light chain; λ, lambda light chain; Mum1, IRF4/MUM1; PCLBCL-LT, primary cutaneous B-cell lymphoma, leg type; PCFCL, primary cutaneous follicle center lymphoma.

### Discriminative characteristics

Expression of BCL2, IRF4/MUM1, and IgM was significantly different between PCFCL and PCLBCL-LT ( $P = 0.000$ ). These 3 factors were also indicative for diagnosis in a univariate logistic regression model, with an accurate prediction percentage of 94.6% for IgM, 93.5% for IRF4/MUM1, and 86% for BCL2 in our series. The clinical parameter tumor localization on the leg(s) was also correlated with the final diagnosis (accurate prediction 89.2%). In a logistic multiple regression model, using both clinical features and immunohistochemical staining procedures, positive staining for IgM and BCL2 was the most optimal combination to correctly classify cases of PCLBCL, with an accurate prediction of 95.7% in our series, which was only slightly more predictive than positive staining for IgM alone.

### Discussion

In this study, intracytoplasmic expression of IgM was demonstrated to be significantly different between the 2 types of PCLBCL, which are, PCFCL and PCLBCL-LT. All PCLBCL-LT showed strong protein expression of IgM, whereas only a minority (5/53) of PCFCL demonstrated detectable intracytoplasmic IgM. This is consistent with previous reports demonstrating a notable difference in IgM heavy chain gene expression between both entities.<sup>9</sup> Moreover, using array-based comparative genomic hybridization, our group has shown loss of chromosome 14q32.33 containing the immunoglobulin heavy chain locus in 13 of 19 PCFCL, but only in 3 of the 12 PCLBCL-LTs.<sup>10</sup> In the present study, not only PCLBCL-LT presenting on the

leg, but also PCLBCL-LT presenting on the trunk or head, showed strong expression of IgM, implying that for lesions on the trunk and head IgM expression might be used as an additional marker in differentiating between PCFCL and PCLBCL-LT. Of note, the 3 PCFCLs that presented on the leg(s) also expressed IgM. Therefore, IgM expression does not seem to discriminate between both PCLBCL entities when presenting on the leg.

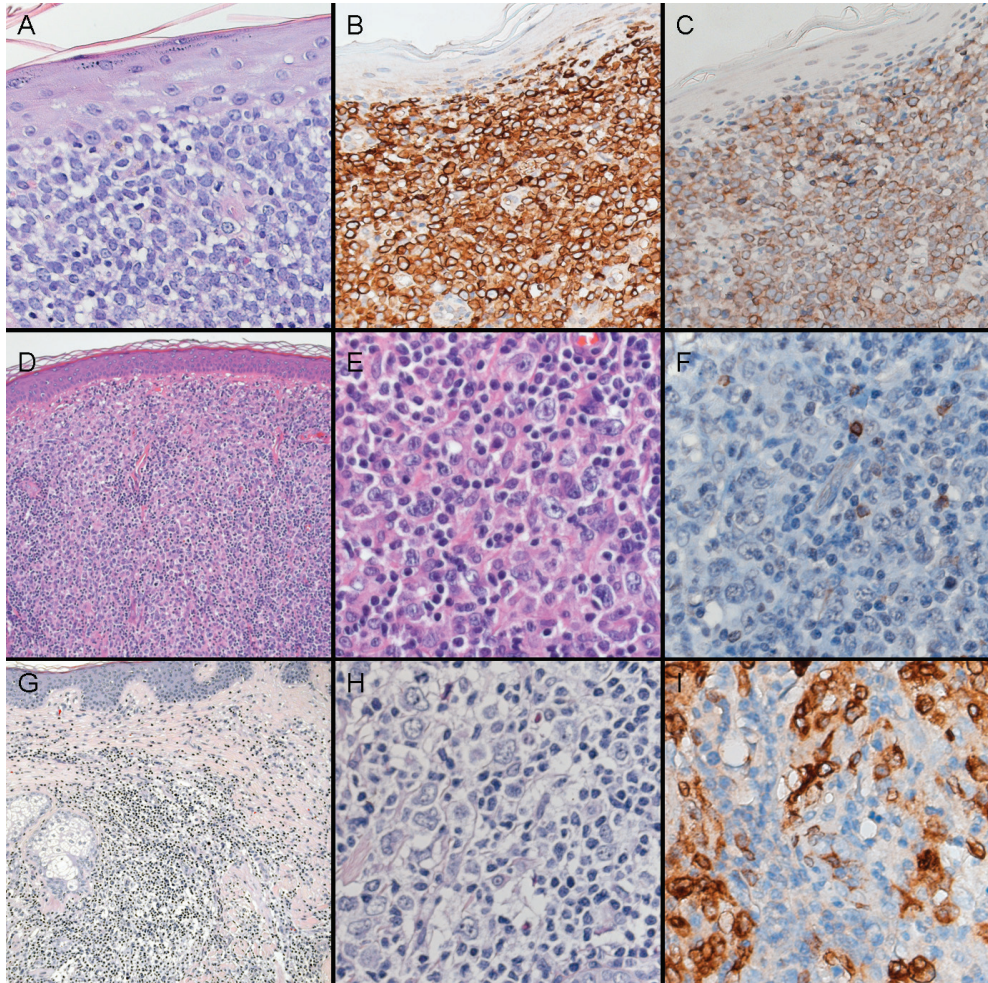
Because of these results, we considered the possibility that the 3 cases of PCFCL presenting on the leg were classified incorrectly, but are nonetheless convinced that a diagnosis of PCFCL is justified. All cases showed a predominantly cleaved morphology, lacked cohesive sheets of centroblasts and/or immunoblasts, were negative for BCL2 (3/3) and MUM1/IRF4 (2/3), and were admixed with a considerable amount of small reactive T-cells. Moreover, 2 of the 3 cases showed (remnants of) follicular dendritic networks, which also supports a diagnosis of PCFCL.

We previously reported that PCFCLs presenting on the leg have a significantly worse prognosis than their counterparts on the head or trunk, with a 5-year disease specific survival of approximately 46%.<sup>6</sup> It can therefore be argued that the expression of IgM in these PCFCL on the legs is part of a phenotype that shows a more malignant behavior than PCFCL occurring on the head or trunk. Hence, as exact classification of the type of PCLBCL Over 50% of nodal DLBCLs show immunohistochemical expression of IgM in the tumor cells.<sup>11,12</sup> Furthermore, IgM expression was reported as an independent adverse prognostic parameter in all patients with DLBCL.<sup>11</sup> High levels of IgM RNA are more frequently encountered in activated B-cell (ABC)-type DLBCL than in germinal center B-cell (GCB)-type DLBCL,<sup>13</sup> which might in part explain the prognostic impact of IgM expression, as ABC-type DLBCL has a worse overall survival compared with GCB-type DLBCL.<sup>14</sup> Previous reports have shown immunoglobulin expression in primary extranodal large B-cell lymphomas at other sites than the skin. Primary central nervous system (CNS) large B-cell lymphomas showed transcripts of IgM and IgD, confirmed at protein level by immunohistochemical staining for IgM in 11 out of 11 cases, with consistent absence of IgG.<sup>15</sup> Primary testicular large B-cell lymphoma also showed consistent immunohistochemical expression of IgM,<sup>16</sup> although some cases were reported to coexpress IgA or IgG. Both primary CNS large B-cell lymphoma and primary testicular large B-cell lymphoma almost invariably have an ABC-like phenotype.<sup>17,18</sup> In contrast, primary large B-cell lymphoma of the bone does not show immunohistochemical IgM expression, but rather expression of IgG.<sup>19</sup> However, this type of lymphoma is known for its predominant GCB phenotype and favorable survival.<sup>20</sup> So, expression of IgM is encountered in both ABC-type DLBCL as well as some extranodal large B-cell lymphomas at immunoprivileged sites, which are also known for an ABC-like phenotype and decreased survival as compared with other large B-cell lymphomas. This is consistent with our finding that IgM is expressed in PCLBCL-LT and not in PCFCL, as PCLBCL-LT shows an ABC-like phenotype<sup>9</sup> and is a more aggressive type of PCLBCL.

In normal B-cell maturation the BCR characteristically shows stepwise alterations.<sup>21</sup> Mature naive B cells express membrane-bound IgM and IgD molecules, composed of rearranged, but unmutated Ig variable heavy chain and light chain genes. In secondary lymphoid tissues, these B cells encounter antigens in the germinal centers of secondary follicles. During the subsequent cell divisions, somatic hypermutations (SHM) diversify the variable region of the Ig genes. This process of so-called affinity maturation finally leads to selection for B cells with high affinity for the recognized antigens. Subsequently, these selected B cells receive growth and differentiation signals that promote class switch recombination (CSR) of the Ig heavy chain constant region by deletional recombination, leading to Ig heavy chain isotype

switching. This process, yielding different classes of immunoglobulins, determines the final effector functions of the secreted immunoglobulin.

**Figure 1.** Primary cutaneous large B-cell lymphomas



Primary cutaneous large B-cell lymphoma, leg type (A-C). High power view showing a dense infiltrate of large non-cleaved lymphoid cells (A) (haematoxylin and eosin). The neoplastic cells show strong staining intensity for IgM (B) and moderate strong staining intensity for IgD (C).

Primary cutaneous follicle center lymphoma (D-F). Low (D) and high (E) power view showing a diffuse infiltrate of large cleaved lymphocytes admixed with scattered small lymphocytes. Immunohistochemistry for IgM (F) shows strong staining of some of the small lymphocytes and negativity for the large, neoplastic cells.

Primary cutaneous follicle center lymphoma presenting on the leg (G-I). Low (G) and high (H) power view showing a diffuse infiltrate of large cleaved lymphocytes admixed with a considerable amount of small lymphocytes. Immunohistochemistry for IgM (I) shows strong staining of the large, neoplastic lymphocytes, sparing most of the small lymphocytes in between.

2

Gene expression profiling,<sup>9</sup> the presence of SHM<sup>22</sup> and expression of activation-induced cytidine deaminase (AID)<sup>22</sup> and BCL6 strongly imply a germinal center experience in PCLBCL-LT. The coexpression of BCL2 and IRF4/MUM1 seems aberrant in this context. However, coexpression of BCL2, BCL6 and IRF4/MUM1 is also frequently encountered in ABC-type DLBCL,<sup>23</sup> and may be part of a malignant deregulating phenotype. Given this presumed germinal center experience, the absence of CSR in PCLBCL-LT is surprising and might indicate a defect in the CSR mechanism. Derivation of PCLBCL-LT from the recently described subpopulation of memory B cells expressing IgM and IgD<sup>24</sup> seems unlikely as this subpopulation consistently expresses CD27 and the tumor cells of PCLBCL in our study did not (5 cases of PCFCL and 5 cases of PCLBCL-LT, data not shown). Collectively, these data point to a germinal center origin of PCLBCL-LT and defective CSR.

The RNA-editing enzyme AID is essential for CSR and deficiency of the AID is associated with impairment of CSR.<sup>25</sup> AID expression was demonstrated in PCLBCL and levels of AID in PCLBCL-LT seem to be higher than in PCFCL and normal lymph node tissue,<sup>22</sup> so the absence of CSR in PCLBCL-LT cannot be explained by shortage of AID. Moreover, AID is required for CSR as well as for SHM,<sup>25</sup> so AID must at least be partly functional in PCLBCL-LT, as this type of lymphoma shows evidence of SHM.<sup>22</sup> In ABC-type DLBCL as well as in primary CNS large B-cell lymphoma it was suggested that CSR was impaired due to the high frequency of mutations in the switch regions of the constant chain, comprising both intra-S $\mu$  and intra-S $\gamma$  deletion/recombination events.<sup>15,26</sup>

In summary, we reported immunohistochemical staining for IgM on paraffin-embedded sections to be an easy additional tool to differentiate between PCFCL and PCLBCL-LT in clinical pathology practice. Analogous to other nodal and extranodal large B-cell lymphomas, expression of IgM in PCLBCL appears to be related to an ABC-like phenotype. Finally, the expression of IgM (and IgD) in this type of lymphoma might imply defective CSR.

## References

1. Willemze R, Jaffe ES, Burg G, et al. (2005) WHO-EORTC classification for cutaneous lymphomas. *Blood* 105: 3768-85.
2. Willemze R, Kerl H, Sterry W, et al. (1997) EORTC classification for primary cutaneous lymphomas: a proposal from the Cutaneous Lymphoma Study Group of the European Organization for Research and Treatment of Cancer. *Blood* 90: 354-71.
3. Swerdlow SH, Campo E, Harris NL, et al. (2008) WHO Classification of Tumours Haematopoietic and Lymphoid Tissues. Geneva, Switzerland: WHO PRESS.
4. Rijlaarsdam JU, Toonstra J, Meijer OW, et al. (1996) Treatment of primary cutaneous B-cell lymphomas of follicle center cell origin: a clinical follow-up study of 55 patients treated with radiotherapy or polychemotherapy. *J Clin Oncol* 14: 549-55.
5. Vermeer MH, Geelen FA, van Haselen CW, et al. (1996) Primary cutaneous large B-cell lymphomas of the legs. A distinct type of cutaneous B-cell lymphoma with an intermediate prognosis. Dutch Cutaneous Lymphoma Working Group. *Arch Dermatol* 132: 1304-8.
6. Senff NJ, Noordijk EM, Kim YH, et al. (2008) European Organization for Research and Treatment of Cancer and International Society for Cutaneous Lymphoma consensus recommendations for the management of cutaneous B-cell lymphomas. *Blood* 112: 1600-9.
7. Grange F, Bekkenk MW, Wechsler J, et al. (2001) Prognostic factors in primary cutaneous large B-cell lymphomas: a European multicenter study. *J Clin Oncol* 19: 3602-10.
8. Kodama K, Massone C, Chott A, et al. (2005) Primary cutaneous large B-cell lymphomas: clinicopathologic features, classification, and prognostic factors in a large series of patients. *Blood* 106: 2491-7.
9. Hoefnagel JJ, Dijkman R, Basso K, et al. (2005) Distinct types of primary cutaneous large B-cell lymphoma identified by gene expression profiling. *Blood* 105: 3671-8.
10. Dijkman R, Tensen CP, Jordanova ES, et al. (2006) Array-based comparative genomic hybridization analysis reveals recurrent chromosomal alterations and prognostic parameters in primary cutaneous large B-cell lymphoma. *J Clin Oncol* 24: 296-305.
11. Miyazaki K, Yamaguchi M, Suguro M, et al. (2008) Gene expression profiling of diffuse large B-cell lymphoma supervised by CD21 expression. *Br J Haematol* 142: 562-70.
12. Ogawa S, Yamaguchi M, Oka K, et al. (1990) CD21S antigen expression in tumour cells of diffuse large B-cell lymphomas is an independent prognostic factor indicating better overall survival. *Br J Haematol* 125: 180-6.
13. Wright G, Tan B, Rosenwald A, et al. (2003) A gene expression-based method to diagnose clinically distinct subgroups of diffuse large B cell lymphoma. *Proc Natl Acad Sci U S A* 100: 9991-6.13.
14. Alizadeh AA, Eisen MB, Davis RE, et al. (2000) Distinct types of diffuse large B-cell lymphoma identified by gene expression profiling. *Nature* 403: 503-11.
15. Montesinos-Rongen M, Schmitz R, Courts C, et al. (2005) Absence of immunoglobulin class switch in primary lymphomas of the central nervous system. *Am J Pathol* 166: 1773-9.
16. Wilkins BS, Williamson JM, O'Brien CJ. (1989) Morphological and immunohistological study of testicular lymphomas. *Histopathology* 15: 147-56.
17. Booman M, Douwes J, Glas AM, et al. (2006) Primary testicular diffuse large B-cell lymphomas have activated B-cell-like subtype characteristics. *J Pathol* 210: 163-71.
18. Camilleri-Broet S, Criniere E, Broet P, et al. (2006) A uniform activated B-cell-like immunophenotype might explain the poor prognosis of primary central nervous system lymphomas: analysis of 83 cases. *Blood* 107: 190-6.



19. Pettit CK, Zukerberg LR, Gray MH, et al. (1990) Primary lymphoma of bone. A B-cell neoplasm with a high frequency of multilobated cells. *Am J Surg Pathol* 14: 329-34.
20. Heyning FH, Hogendoorn PC, Kramer MH, et al. (2009) Primary lymphoma of bone: extranodal lymphoma with favourable survival independent of germinal centre, post-germinal centre or indeterminate phenotype. *J Clin Pathol* 62: 820-4.
21. Rajewsky K. (1996) Clonal selection and learning in the antibody system. *Nature* 381: 751-8.
22. Dijkman R, Tensen CP, Buettner M, et al. (2006) Primary cutaneous follicle center lymphoma and primary cutaneous large B-cell lymphoma, leg type, are both targeted by aberrant somatic hypermutation but demonstrate differential expression of AID. *Blood* 107: 4926-9.
23. Hans CP, Weisenburger DD, Greiner TC, et al. (2004) Confirmation of the molecular classification of diffuse large B-cell lymphoma by immunohistochemistry using a tissue microarray. *Blood* 103: 275-82.
24. Seifert M, Kuppers R. (2009) Molecular footprints of a germinal center derivation of human IgM+(IgD+)CD27+ B cells and the dynamics of memory B cell generation. *J Exp Med* 206: 2659-69.
25. Muramatsu M, Kinoshita K, Fagarasan S, et al. (2000) Class switch recombination and hypermutation require activation-induced cytidine deaminase (AID), a potential RNA editing enzyme. *Cell* 102: 553-63.
26. Lenz G, Nagel I, Siebert R, et al. (2007) Aberrant immunoglobulin class switch recombination and switch translocations in activated B cell-like diffuse large B cell lymphoma. *J Exp Med* 204: 633-43.





## MicroRNA profiling of primary cutaneous large B-cell lymphomas

*Public Library of Science ONE 2013;  
8(12): e82471*

Lianne Koens<sup>1</sup>

Yongjun Qin<sup>2,3</sup>

Wai Y. Leung<sup>3</sup>

Willem E. Corver<sup>1</sup>

Patty M. Jansen<sup>1</sup>

Rein Willemze<sup>3</sup>

Maarten H. Vermeer<sup>3</sup>

Cornelis P. Tensen<sup>3</sup>

Departments of <sup>1</sup>Pathology; and <sup>3</sup>Dermatology, Leiden University Medical Center, Leiden, The Netherlands;

<sup>2</sup>Biotechnology Center, Shanxi Academy of Agricultural Sciences, Taiyuan, China



## Abstract

*Aberrant expression of microRNAs is widely accepted to be pathogenetically involved in nodal diffuse large B-cell lymphomas (DLBCLs). However, the microRNAs profiles of primary cutaneous large B-cell lymphomas (PCLBCLs) are not yet described. Its two main subtypes, i.e., primary cutaneous diffuse large B-cell lymphoma, leg type (PCLBCL-LT) and primary cutaneous follicle center lymphoma (PCFCL) are characterized by an activated B-cell (ABC)-genotype and a germinal center B-cell (GCB)-genotype, respectively. We performed high-throughput sequencing analysis on frozen tumor biopsies from 19 cases of PCFCL and PCLBCL-LT to establish microRNA profiles. Cluster analysis of the complete microRNome could not distinguish between the two subtypes, but 16 single microRNAs were found to be differentially expressed. Single microRNA RT-qPCR was conducted on formalin-fixed paraffin-embedded tumor biopsies of 20 additional cases, confirming higher expression of miR-9-5p, miR-31-5p, miR-129-2-3p and miR-214-3p in PCFCL as compared to PCLBCL-LT. MicroRNAs previously described to be higher expressed in ABC-type as compared to GCB-type nodal DLBCL were not differentially expressed between PCFCL and PCLBCL-LT. In conclusion, PCFCL and PCLBCL-LT differ in their microRNA profiles. In contrast to their gene expression profile, they only show slight resemblance with the microRNA profiles found in GCB- and ABC-type nodal DLBCL.*

3

## Introduction

Primary cutaneous large B-cell lymphomas (PCLBCLs) are a group of malignant lymphoproliferative disorders presenting in the skin with no evidence of extracutaneous disease at the time of diagnosis.<sup>1</sup> In the latest World Health Organization (WHO) 2008 classification two main types of PCLBCL are distinguished: primary cutaneous follicle center lymphoma (PCFCL) and primary cutaneous diffuse large B-cell lymphoma, leg type (PCLBCL-LT).<sup>2</sup> PCFCL is considered an indolent type of lymphoma (5 year overall survival (OS) > 95%), whereas PCLBCL-LT has a more aggressive clinical course (5 year OS approximately 40%).<sup>3</sup> The two subtypes also show marked differences at a molecular level by array comparative genomic hybridization<sup>4</sup> and gene expression profiling. PCFCL and PCLBCL-LT have gene expression profiles corresponding to germinal center B-cell (GCB)-type diffuse large B-cell lymphoma (DLBCL) and activated B-cell (ABC)-type nodal DLBCL, respectively.<sup>5</sup> Clinical distinction at the time of first diagnosis between these different subtypes of PCLBCL is important, as the first choice of treatment differs between the two entities. PCFCL can be adequately treated with radiotherapy, but the more aggressive behavior of PCLBCL-LT warrants for treatment with anthracyclin-based chemotherapy combined with rituximab.<sup>6</sup>

MicroRNAs are approximately 22 nucleotides long non-coding RNA molecules that can regulate translation of several specific target messenger RNAs (mRNAs). The two major responsible mechanisms are inhibition of translational initiation by blocking ribosomes and direct targeting of mRNA at the 3 prime untranslated region leading to degradation of the molecule.<sup>7</sup> Alterations in the expression of microRNAs contribute to the pathogenesis of different types of malignancies, including malignant lymphomas, but are also involved in normal development of hematopoietic cells.<sup>8</sup> Although a role for microRNAs in the pathogenesis of nodal DLBCLs is generally recognized, little is known about the presence and significance of microRNAs in PCLBCL. In one recently published study, a limited set of microRNAs was investigated in PCFCL.<sup>9</sup>

In nodal DLBCL, much effort has been given to differentiate between the two major molecular subtypes, i.e. GCB-type DLBCL and ABC-type or non-GCB-type DLBCL, by means of expression of specific microRNAs or microRNA profiles. However, conflicting results concerning this topic have been published. The most frequently encountered microRNA alterations are upregulation of miR-155, miR-21, miR-221 and miR-222 in ABC-type DLBCL as compared to GCB-type DLBCL as detected by microarray profiling and/or Real Time quantitative PCR (RT-qPCR).<sup>10-19</sup> To date, the prognostic value of expression levels of specific microRNAs in nodal DLBCL remains unclear. Although higher expression of miR-222 correlating to a shorter progression-free survival (PFS) was reproduced in more than one study,<sup>12,15,20</sup> a correlation was not consistently found for other microRNAs. In addition, reported microRNA profiles generated by complete microRNA profiling that would distinguish between the two subtypes of nodal DLBCL have no substantial similarities (Supplemental Table 1).<sup>12,14-18,21</sup> To some extent, the observed variations might be explained by the different techniques used to quantify microRNAs, i.e. different microarrays or varying reference RNAs in RT-PCR experiments. Furthermore, the techniques used to distinguish the two molecular subtypes from each other are not uniform. The encountered differences might on the other hand also reflect the profound tumor heterogeneity within the group of nodal DLBCLs.

In search of differences in the pathogenesis of PCFCL and PCLBCL-LT we investigated the microRNA profiles in PCLBCL by performing microRNA high-throughput sequencing. Several single microRNAs that were differentially expressed between PCFCL and PCLBCL-LT in our high-throughput sequence data were validated by RT-qPCR. Furthermore, we were interested in comparing the microRNA profiles of PCFCL and PCLBCL-LT with the (known) microRNA profiles of GCB- and ABC-type nodal DLBCL, in search for common pathogenetical pathways and common targets for tailored therapy.

## Materials and methods

### *Tumor samples*

Frozen skin biopsy or excision material from primary tumors was collected from 6 patients with PCFCL and 13 patients with PCLBCL-LT from the archives of the Leiden University Medical Center (Leiden, The Netherlands). Formalin-fixed and paraffin-embedded (FFPE) skin biopsy material was available from 5 of these patients (2 PCFCL and 3 PCLBCL-LT cases) and an additional 8 patients with PCFCL and 7 patients with PCLBCL-LT. The diagnosis was based on the criteria of the WHO-EORTC and WHO 2008 classifications,<sup>1,22</sup> and confirmed by a panel of hematopathologists and dermatologists, aided by several additional immunohistochemical stainings. The clinical data and expression of relevant immunohistochemical markers are summarized in Table 1. In all cases physical examination, computed tomography scan, bone marrow examination and peripheral blood counts did not show extracutaneous disease. Furthermore, FFPE lymph node excisions of 34 cases of nodal DLBCL were collected from the Leiden University Medical Center, the Diaconessenhuis (Leiden, The Netherlands) and the Reinier de Graaf Hospital (Delft, The Netherlands). Of those, 19 were ABC-type and 11 were GCB-type, according to both Hans and Choi immunohistochemical algorithms,<sup>23,24</sup> the four samples with discrepancy between the two algorithms were discarded from further analysis. The tumor cell percentage was at least 75% in every tumor specimen, as shown by immunohistochemistry for CD20 and CD3. All tissue samples were handled in a coded fashion, according to the Dutch National Ethical guidelines (Code for Proper Secondary Use of Human Tissue, Dutch Federation of Medical Scientific Societies), waving the need for specific

approval of the study by the ethical committee and patient informed consent.

Human B-cells were purified from peripheral blood mononuclear cells isolated from buffy coats obtained from anonymous blood donors (Sanquin Bloodbank, Nijmegen, The Netherlands) and were *in vitro* activated subsequently (details are given in Supplemental Materials and Methods).

#### *MicroRNA library preparation, high-throughput sequencing and data analysis*

Total RNA was extracted from the frozen tumor samples and activated B-cells using TRIzol and according to the protocol described by the supplier (Invitrogen, Carlsbad, CA, USA). Library preparation was to a large extent based on the SOLiD Total RNA-Seq Kit protocol (SREK protocol, Applied Biosystems, Nieuwerkerk a/d IJssel, The Netherlands) as described previously (Supplemental Materials and Methods).<sup>25</sup> Subsequently, 0.5 nM per sample of the cDNA clusters generated was loaded onto the flow cells for massively parallel high-throughput sequencing using the Illumina Genome Analyzer II (Illumina) performing sequencing-by-synthesis technology. The raw sequencing data were extracted through standard Illumina pipelines. The primary sequencing data are publicly available through the Gene Expression Omnibus (GEO) archive through accession GSE51359. Illumina sequence reads were aligned to the human genome (GRCh37/hg19) using the miRDeep2.0 algorithm,<sup>26</sup> which predicts precursor sequences and matches them to precursor microRNAs enlisted in the miRBase 18.0 database (<http://www.mirbase.org>). Only sequences with a minimum sequence length of 17 bases were analyzed, allowing for a maximum mismatch of one base. Samples with less than 100,000 microRNA reads were discarded from further analyses.<sup>27</sup> The different microRNAs were only included in the analyses if in at least half of the samples of at least one of the three analyzed groups (PCFCL, PCLBCL-LT or activated B-cells) the single microRNA read number exceeded 0,01% of the total number of microRNA reads (100 reads/million). The samples were then analyzed for differential expression between the groups by the Bioconductor package EdgeR,<sup>28</sup> considering only mature microRNAs. Differential expression was considered statistically significant when a *p*-value below 0.05 was reached after multiple testing correction according to the Benjamini-Hochberg method.<sup>29</sup> EdgeR transformed, normalized microRNA expression (in counts per million reads) were used for unsupervised hierarchical clustering, running under R 2.14.2 software (<http://www.r-project.org>). The NormFinder version 0.953 algorithm<sup>30</sup> was used on high-throughput sequencing data to identify the most stably expressed microRNAs within and between the analyzed subgroups suitable for RT-qPCR normalization.<sup>31</sup>

#### *MicroRNA real-time qPCR*

Total RNA was isolated from 10  $\mu$ m sections of FFPE tumor samples. Approximately 300 ng of total RNA from each sample (FFPE or frozen, same isolation as for the high-throughput sequencing) was reverse transcribed using the microRNA reverse transcription kit (Applied Biosystems). RT-qPCR was performed in duplicate using Taqman microRNA and control assays (Applied Biosystems). The output data were analyzed using CFX Manager software (Bio-Rad). The expression of the different microRNAs was analyzed using the  $\Delta\Delta$ Ct method expressed relative to the most stably expressed endogenous controls according to GeNorm.<sup>32</sup> For more details see Supplemental Materials and Methods. Statistical analyses were performed using the Mann Whitney U test in IBM SPSS version 20 (SPSS Inc., Chicago, IL, USA) and the data were visualized in GraphPad Prism (GraphPad Software Inc, CA, USA).



Table 1. Patient characteristics

Case	Experiment	Sex	Age at diagnosis	Primary tumor	BCL2	BCL6	CD10	IRF4	BCR	Initial therapy	Recurrence	PFS (months)	Follow-up (months)	Current status
1 FC	HTS & RT-PCR	f	81	head	-	+	-	-	-	RT	yes	62	86	A <sup>0</sup>
2 FC	HTS & RT-PCR	m	71	trunk	-	+	-	-	-	RT + o.p.	no	89	90	A <sup>0</sup>
3 FC	HTS	f	71	head	-	+	-	-	-	RT	no	55	56	A <sup>0</sup>
4 FC	HTS	m	72	head	+	+	-	-	-	RT	no	32	33	A <sup>0</sup>
5 FC	HTS	m	67	head	-	+	-	-	-	RT	no	55	56	A <sup>0</sup>
6 FC	HTS	m	59	arm	-	+	-	-	NA	RT	yes	8	9	A <sup>0</sup>
7 FC	RT-PCR	f	53	head	-	+	-	-	IgM, IgD	RT	yes	46	128	A <sup>0</sup>
8 FC	RT-PCR	m	33	trunk	+	+	-	-	IgM, IgD, λ	RT	yes	60	185	A <sup>+</sup>
9 FC	RT-PCR	m	55	trunk	-	NA	-	-	-	RT	yes	5	105	A <sup>0</sup>
10 FC	RT-PCR	f	50	trunk	-	+	-	-	-	RT	no	63	64	A <sup>0</sup>
11 FC	RT-PCR	m	47	trunk	-	+	-	-	-	RT	yes	7	68	A <sup>+</sup>
12 FC	RT-PCR	m	44	head	-	+	-	-	-	RT	no	52	53	A <sup>0</sup>
13 FC	RT-PCR	m	35	trunk	-	+	-	-	-	RT + PCT	no	20	26	A <sup>0</sup>
14 FC	RT-PCR	m	66	trunk	-	+	-	-	-	RT	yes	11	36	A <sup>+</sup>
1 LT	HTS & RT-PCR	m	88	leg	+	+	-	+	IgM, IgD, κ	PCT	yes	2	12	D <sup>+</sup>
2 LT	HTS & RT-PCR	m	81	leg	+	+	+	+	IgM, IgD, λ	None	no	0	2	D <sup>+</sup>
3 LT	HTS & RT-PCR	m	68	leg	+	+	-	+	IgM, IgD, λ	PCT	yes	17	60	D <sup>+</sup>
4 LT	HTS	f	89	leg	+	NA	-	+	NA	RT	yes	21	32	A <sup>+</sup>
5 LT	HTS	f	84	leg	+	+	-	+	IgM, IgD, κ	RT	no	0	2	D <sup>0</sup>
6 LT	HTS	f	83	leg	+	+	-	+	IgM, IgD, κ	RT + PCT	yes	34	38	D <sup>+</sup>
7 LT	HTS	m	83	leg	+	+	-	+	IgM, IgD, κ	RT	no	49	50	A <sup>0</sup>
8 LT	HTS	f	76	leg	+	-	-	+	IgM, κ	RT	no	0	13	D <sup>+</sup>
9 LT	HTS	m	77	both legs	+	+	-	+	IgM, IgD	RT	no	0	3	D <sup>+</sup>
10 LT	HTS	f	79	leg	+	+	-	+	IgM, κ	RT	?	>20	32	A <sup>+</sup>
11 LT	HTS	f	81	leg	+	-	-	+	IgM	RT + PCT	yes	20	39	D <sup>+</sup>
12 LT	RT-PCR	f	73	leg	+	+	-	+	IgM, IgD, κ	PCT	no	79	85	D <sup>0</sup>
13 LT	RT-PCR	f	71	leg	+	+	-	+	IgM, λ	PCT	yes	34	73	A <sup>0</sup>
14 LT	RT-PCR	m	47	leg	+	+	-	+	IgM, IgD, λ	PCT	no	43	49	A <sup>0</sup>
15 LT	RT-PCR	f	75	leg	+	+	-	-	κ <sup>a</sup>	PCT	yes	2	29	D <sup>+</sup>
16 LT	RT-PCR	f	77	leg	+	-	-	+	IgM, λ	PCT	yes	10	19	D <sup>+</sup>
17 LT	RT-PCR	f	75	both legs	+	+	-	+	IgM, IgD, κ	PCT	yes	1	12	D <sup>+</sup>
18 LT	RT-PCR	f	84	leg	+	+	-	+	IgM, IgD, κ	None	no	0	3	D <sup>+</sup>

Legend to Table 1.: FC: primary cutaneous follicle center lymphoma; PCLBCL-LT: primary cutaneous large B-cell lymphoma, leg type; BCR: B-cell receptor; PFS: progression-free survival; f: female; HTS: high-throughput sequencing; RT-PCR: Real Time polymerase chain reaction; m: male; NA: not assessed; RT: radiotherapy; o.p.: oral prednisone; PCT: polychemotherapy; A<sup>+</sup>: alive with disease; A<sup>0</sup>: alive without disease; D<sup>+</sup>: death with disease; D<sup>0</sup>: death without disease; <sup>a</sup> heavy chains not assessed.

## Results

### *High-throughput sequencing*

From 19 tumor samples (13 samples of PCLBCL-LT and 6 samples of PCFCL) and 4 samples of activated B-cells, microRNA libraries were generated and sequenced. Of these, two PCLBCL-LT samples yielded less than 100,000 total microRNA reads (7,302 and 55,383 reads) and were discarded from further analyses.<sup>27</sup> Mean microRNA read number in the other samples was 4,139,515 (standard deviation 9,348,501). After alignment of the sequence reads in miRDeep 2.0, 1921 different known precursor microRNAs were identified to be expressed in at least one sample. 328 precursor loci were identified as putative novel microRNAs. After discarding precursor microRNAs that showed low expression levels (see Materials and Methods), a total number of 238 different precursor microRNAs were included for further analysis.

### *MicroRNA profiles of PCFCL and PCLBCL-LT*

The most abundantly expressed microRNAs of the analyzed subgroups are represented in Figure 1. In PCLBCL-LT, miR-19b-3p and miR-19a-3p show the highest expression levels, and comprise 12% and 11% of the total microRNome, respectively. In PCFCL, these microRNAs also constitute a substantial part of the microRNome (7% and 6%, respectively), but miR-150-5p is most abundantly expressed. The activated B-cells are to a large extent represented by miR-150-5p, comprising approximately one-fifth of the microRNome. Using NormFinder, miR-148b-3p, miR-25-3p, let-7c and let-7e-5p were the most stably expressed microRNAs in our complete study cohort (Supplemental Figure 1).

Unsupervised hierarchical clustering analysis of all samples using the 238 mature microRNAs of the precursor sequences identified did not result into distinct clustering of the two tumor types and/or the activated B-cells (Supplemental Figure 2).

### *Differential microRNA expression in PCLBCLs*

Table 2 shows an overview of mature microRNAs that showed statistically significantly differential expression between PCFCL and PCLBCL-LT. Under the given conditions (allowing a mismatch of 1 base pair), MiRDeep 2.0 did not categorize miR-129-1-3p and miR-129-2-3p as separate microRNAs. Recounting of both variants in the aligned sequence data derived from miRDeep 2.0 showed a markedly higher expression of miR-129-2-3p in PCFCL as compared to PCLBCL-LT. Similarly, miRDeep 2.0 was not able to differentiate between miR-9-1, -2 and -3 variants, because of the relatively short aligned sequences (no sequences containing (part of) the precursor microRNA outside the mature microRNA region). For the 16 differentially expressed microRNAs, unsupervised hierarchical clustering analysis was applied (Figure 2). According to this analysis, two groups are separated from each other, one containing all cases of PCFCL and two cases of PCLBCL-LT, the other group comprising of the remaining cases of PCLBCL-LT. The two cases of PCLBCL-LT clustering with the PCFCL cases showed a clinical presentation, tumor cell morphology and immunohistochemical profile with classical features of PCLBCL-LT. One of the patients received polychemotherapy combined with radiotherapy and died of lymphoma after 38 months; the other patient was solely treated with radiotherapy and is still alive without disease recurrence after 50 months of follow-up.

**Table 2.** High-throughput sequencing: differential expression of microRNAs between PCFCL and PCLBCL-LT

MicroRNA		Reads per million, mean (SD)		Adjusted <i>p</i> -value <sup>a</sup>
		PCFCL	PCLBCL-LT	
miR-129-2-3p	<sup>b</sup>	1.668 (3.260)	4 (8)	5.74E-15
miR-129-1-3p		184 (269)	18 (21)	2.10E-14
miR-1246		0 (0)	26 (45)	1.42E-5
miR-214-3p	<sup>b</sup>	8.620 (14.534)	1.174 (1.232)	7.24E-4
miR-574-3p	<sup>b</sup>	12.079 (14.180)	1.951 (1.392)	0.00266
miR-4485		6 (8)	77 (127)	0.00321
miR-222-5p		16 (14)	142 (126)	0.0108
miR-31-5p	<sup>b</sup>	1.729 (995)	346 (385)	0.0129
miR-486-3p	<sup>b</sup>	196 (194)	40 (43)	0.0133
miR-363-3p	<sup>b</sup>	37 (27)	288 (535)	0.0153
miR-99a-5p	<sup>b</sup>	9.843 (9.113)	2.168 (1.155)	0.0184
miR-574-5p		289 (184)	1.996 (5.654)	0.0442
miR-100-5p	<sup>b</sup>	8.849 (6.850)	2.318 (1.400)	0.0442
miR-205-5p	<sup>b</sup>	11.492 (12.787)	3.059 (2.818)	0.0442
miR-342-3p	<sup>b</sup>	22.775 (24.636)	6.079 (3.992)	0.0442
miR-9-5p	<sup>b</sup>	273 (309)	73 (74)	0.0442

<sup>a</sup> *p*-values Benjamini-Hochberg corrected; <sup>b</sup> microRNA included in RT-qPCR validation; PCFCL: primary cutaneous follicle center lymphoma, PCLBCL-LT: primary cutaneous large B-cell lymphoma, leg type.

### MicroRNA RT-qPCR validation

A selection of 11 differentially expressed microRNAs (marked in Table 3) was used for validation in a novel group of test cases. MiR-129-1-3p, miR-1246, miR-4485 and miR-222-5p were not validated because of the relatively low counts in both PCFCL and PCLBCL-LT samples. Of miR-574-5p, no Taqman PCR primer assay was available, because of dinucleotide repeats in the microRNA sequence that could interfere with the PCR. Assays for miR-148b-3p, miR-25-3p, let-7c and let-7e-5p were included as reference microRNAs, along with widely used reference RNAs U6 and RNU48. Of these six, miR-148b-3p, let-7e-5p and miR-25-3p were most stably expressed in the RT-qPCR experiments (according to GeNorm) and therefore used for normalization of the data. The expression of U6 and RNU48 was very variable in this sample set. Comparison of RT-qPCR performed on both RNA of frozen tumor material isolated for high-throughput sequence analysis and RNA isolated from FFPE sections of the same tumor sample (2 cases of PCFCL and 3 cases of PCLBCL-LT) showed high concordance (Supplemental Figure 3). With inclusion of all 20 FFPE PCLBCL samples in the analysis, including 10 PCFCL and 10 PCLBCL-LT cases, we confirmed higher expression of miR-129-2-3p, miR-214-3p, miR-31-5p and miR-9-5p in PCFCL as compared to PCLBCL-LT ( $p < 0.05$ ) (Figure 3). For the other seven microRNAs, no statistically significantly differential expression was found between PCFCL and PCLBCL-LT. In addition to these differentially expressed microRNAs resulting from the deep sequence analysis, we tested whether four microRNAs frequently reported to show higher expression in ABC-type compared GCB-type nodal DLBCL (miR-21-5p, miR-155-5p, miR-221-3p and miR-222-3p) were higher expressed in PCLBCL-LT.

Figure 1. Most abundantly expressed microRNAs

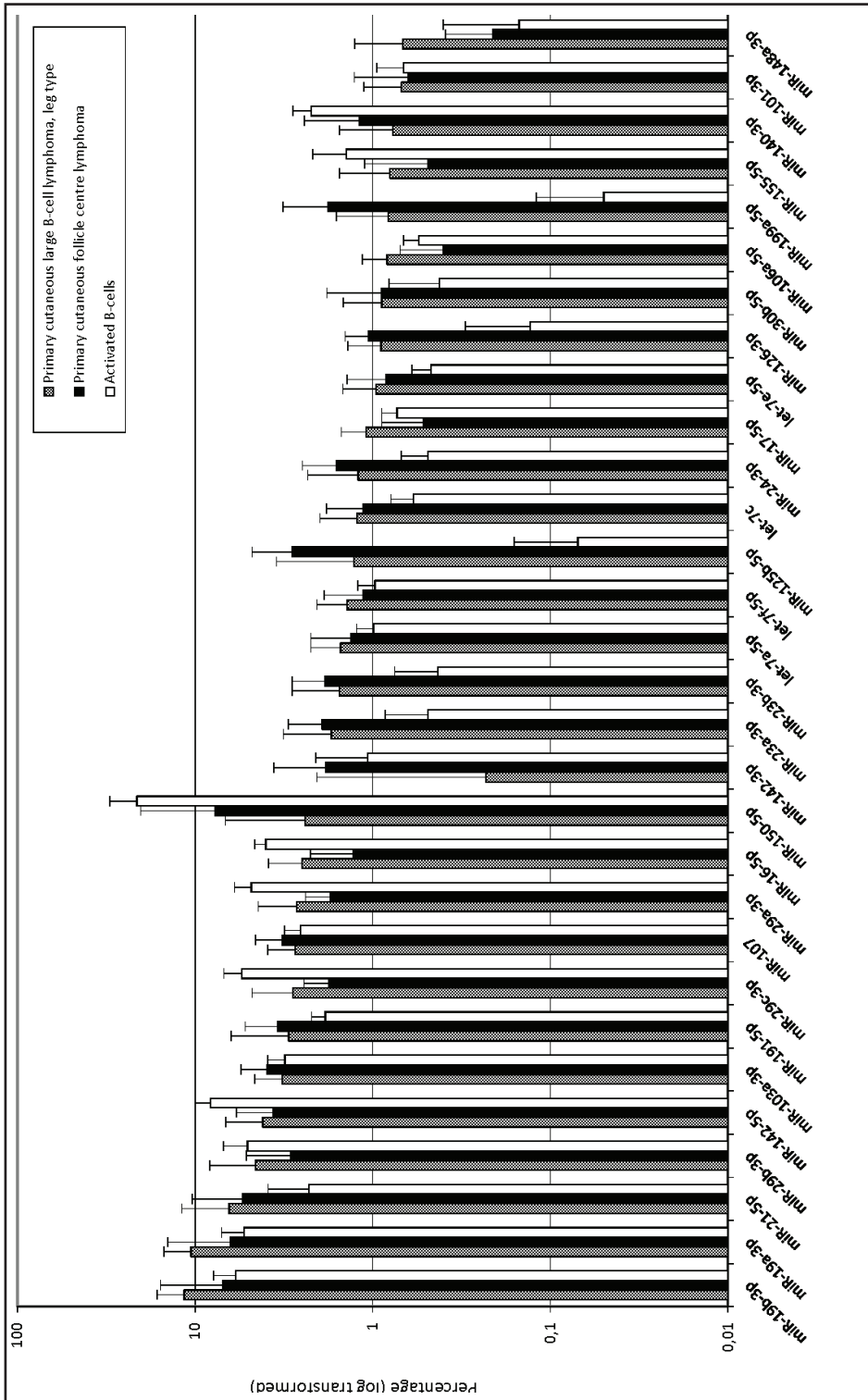
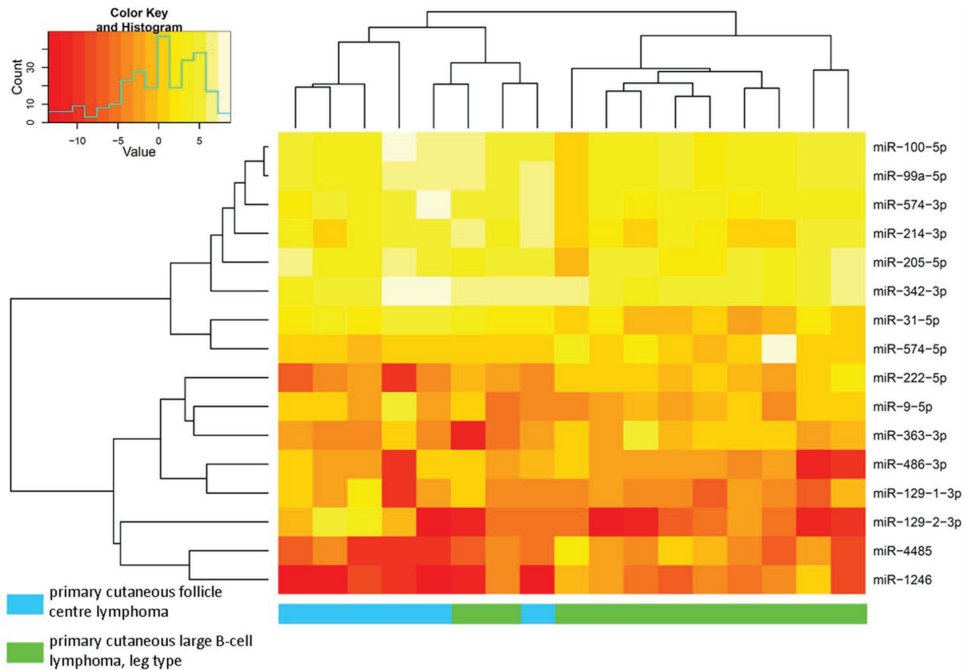


**Figure 2.** Unsupervised hierarchical clustering analysis in PCLBCL samples of high-throughput sequencing, using 16 differentially expressed microRNAs



PCFCL and PCLBCL-LT tend to cluster together in two subgroups, with only 2 cases of PCLBCL-LT clustering together with the PCFCL cases.

However, no differential expression between PCLBCL-LT and PCFCL of these four microRNAs was observed (Figure 4). Above that, unsupervised hierarchical clustering analysis of the high-throughput sequence data of our PCLBCLs using microRNA signature profiles that should be able to distinguish GCB-type from ABC-type DLBCL<sup>12,14,17</sup> did not set apart PCFCL from PCLBCL-LT.

#### *MicroRNA RT-qPCR analysis of GCB- and ABC-subtypes of nodal DLBCLs*

Because of the inconsistencies in literature concerning microRNA profiling of nodal DLBCL and the varying references used in these studies, a set of well-defined GCB- and ABC-subtype nodal DLBCLs was subjected to microRNA RT-qPCR analysis, using the same conditions as for our PCLBCL FFPE samples. As in PCLBCL, GeNorm analysis showed that miR-148b-3p, miR-25-3p, let-7e-5p were most stably expressed, and these three microRNAs were therefore used as reference microRNAs. We evaluated the expression of the four microRNAs that showed significantly higher expression in PCFCL as compared to PCLBCL-LT in our nodal DLBCL samples. The expression of miR-129-2-3p was indeed higher in GCB-type DLBCL as compared to the ABC-type ( $p=0.00$ ), while the expression of miR-214-3p, miR-31-5p and miR-9-5p did not show statistically significant differences between both nodal subtypes. Four microRNAs frequently reported to show higher expression in ABC-type than in GCB-type nodal DLBCL (miR-21-5p, miR-155-5p, miR-221-3p and miR-222-3p) were included in the RT-qPCR analy-

sis. However, in our group of nodal DLBCLs, of these four microRNAs, we could only confirm higher expression levels of miR-155-5p ( $p=0.01$ ) and miR-222-5p ( $p=0.05$ ) in ABC-type as compared to GCB-type DLBCL (Figure 4).

**Table 3.** MicroRNAs in RT-qPCR validation: predicted targets

MicroRNA	Location <sup>a</sup>	Up <sup>b</sup>	Potential target(s) and function	
miR-129-2-3p	11p11.2	PCFCL	SOX4 CDK6	(B-cell) transcription factor regulator of cell cycle progression
miR-214-3p	1q24.3	PCFCL	PTEN EZH2	negative regulator of cell cycle progression polycomb group gene silencer
miR-574-3p	4p14	PCFCL	IL6	involved in NF- $\kappa$ B signaling
miR-31-5p	9p21.3	PCFCL	PIK3C2A CXCL12 RhoA NIK	PI3K pathway component chemokine attractant metastasis promoting gene NF- $\kappa$ B signaling
miR-486-3p	8p11.21	PCFCL	PTEN E2F1	negative regulator of cell cycle progression regulator of cell cycle progression
miR-99a-5p	21q21.1	PCFCL	mTOR	PI3K family member
miR-100-5p	11q24.1	PCFCL	mTOR	PI3K family member
miR-205-5p	1q32.2	PCFCL	PTEN E2F1	negative regulator of cell cycle progression regulator of cell cycle progression
miR-342-3p	14q32.2	PCFCL	BCL2L10	BCL2 family member
miR-9-5p	1q22/5q14.3/15q26.1	PCFCL	PRDM1/BLIMP1 FOXP1 NF $\kappa$ B1 = p50	B-cell transcription factor (B-cell) transcription factor NF- $\kappa$ B signaling
miR-363-3p	Xq26.2	PCLBCL-LT	CDKN1A = p21	regulator of cell cycle progression

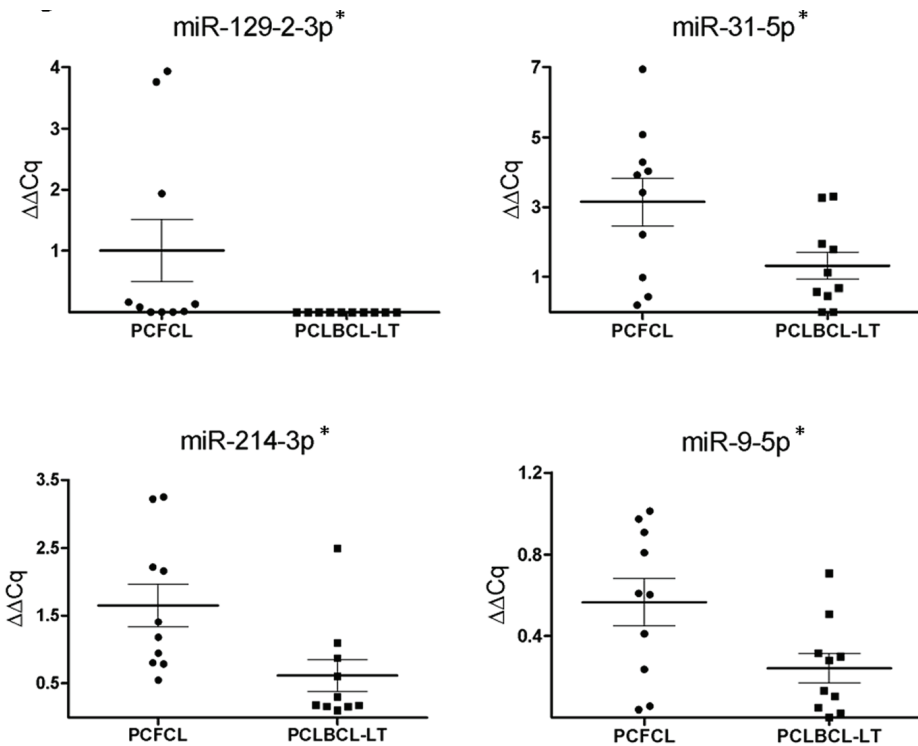
<sup>a</sup> chromosomal location microRNA gene; <sup>b</sup> higher expression in subgroup of PCLBCL; PCFCL: primary cutaneous follicle center lymphoma; PCLBCL-LT: primary cutaneous diffuse large B-cell lymphoma, leg type.

## Discussion

This is the first study to report complete genome-wide microRNA profiles of PCLBCLs, and comparing PCFCL and PCLBCL-LT subtypes. By use of next generation high-throughput microRNA sequence analysis, we provided microRNA profiles of these tumors on frozen biopsy samples, accurately exploring both quantitative and qualitative aspects of all microRNAs. The complete microRNomes of PCLBCL-LT and PCFCL did not allow their separation by unsupervised hierarchical clustering, and PCLBCL-LT did not cluster together with activated B-cells, its postulated normal counterpart (Supplemental Figure 1). The list of expressed and quantified microRNAs generated from this experiment was the basis for selecting specific microRNAs for RT-qPCR confirmation on FFPE tumor tissue of both lymphoma subtypes. The use of high-throughput

sequencing also enabled us to identify 328 putative novel microRNAs expressed in our samples, of which further validation was not performed and is warranted. Furthermore, these sequence data were also instrumental in selecting stably expressed reference microRNAs for subsequent confirmation experiments. We identified four microRNAs (miR-129-2-3p, miR-214-3p, miR-31-5p and miR-9-5p) of which statistically significantly higher expression in PCFCL as compared to PCLBCL-LT in high-throughput sequencing could be confirmed by RT-qPCR on a new FFPE study cohort.

Figure 3. RT-qPCR expression in FFPE samples (1)



The expression of the 4 microRNAs showing statistically significantly higher expression in PCFCL as compared to PCLBCL-LT are represented in dot plots.  $\Delta\Delta Cq$  was calculated with miR-148b-3p, let-7e-5p and miR-25-3p as stably expressed reference microRNAs. \*P-value < 0.05 (Mann Whitney U test).

#### MicroRNomes of PCFCL and PCLBCL-LT

Considering all samples analyzed, miR-19a-3p and miR-19b-3p constituted a significant part of the microRNA profile, up to 12% for miR-19b-3p of the complete profile of PCLBCL-LT. Both microRNAs are members of the miR-17~92 cluster, the presence of which is critical for normal B-cell development.<sup>33</sup> It also acts as a potential oncogenic cluster in B-cell non-Hodgkin lymphomas,<sup>34</sup> with miR-19 components being essential in this oncogenic potential.<sup>35</sup> The other members of this cluster, miR-17-5p, miR-18a-5p, miR-20a-5p and miR-92a-3p, only

made up a very small proportion of the complete microRNome (with a maximum of 1%). The relatively low expression of miR-92a-3p was most remarkable, as this microRNA was found to be one of the most abundantly expressed microRNA in a recent study on nodal DLBCL and primary central nervous system DLBCL, an extranodal DLBCL with an ABC-like genotype.<sup>36</sup> Although in PCFCL, miR-19a-3p and miR-19b-3p also made up a substantial part of the microRNome, miR-150-5p was most abundantly expressed. MiR-150-5p is involved in normal B-cell development, targeting transcription factor and proto-oncogene c-MYB.<sup>37</sup>

#### *Differentially expressed microRNAs*

By performing RT-qPCR in an independent cohort of FFPE tumor samples, the higher expression of miR-129-2-3p, miR-214-3p, miR-31-5p and miR-9-5p in PCFCL as compared to PCLBCL-LT in high-throughput sequence data could be confirmed.

MiR-129-2-3p targets transcription factor SOX4, which was validated in endometrial cancer.<sup>38</sup> SOX4 also has a critical function in normal B-cell development.<sup>39</sup> Because of the dichotomy in expression of miR-129-2-3p (11 cases without and 9 cases with expression of this microRNA in RT-qPCR), immunohistochemical staining for SOX4 was performed. However, no inverse correlation between RT-qPCR expression of miR-129-2-3p and immunohistochemical expression of SOX4 was observed (data not shown).

A previous array-based comparative genomic hybridization study performed by our group, showed low copy number gains of 1q23-q25 in PCFCL, but not in PCLBCL-LT cases.<sup>5</sup> The miR-214 gene is located in this chromosomal region and correspondingly, higher levels of miR-214-3p were observed in PCFCL compared to PCLBCL-LT. MiR-214-3p has been reported as oncogenic microRNA in T-cells, negatively regulating tumor suppressor gene phosphate and tensin homolog (PTEN),<sup>40</sup> and is involved in controlling cell cycle regulation. However, miR-214-3p has also been described to exert a tumor suppressor function in breast cancer cell lines, where reduced levels of this microRNA result in increased proliferation and invasion and in accumulation of EZH2,<sup>41</sup> a polycomb group protein with the potential to promote cell proliferation.<sup>42</sup>

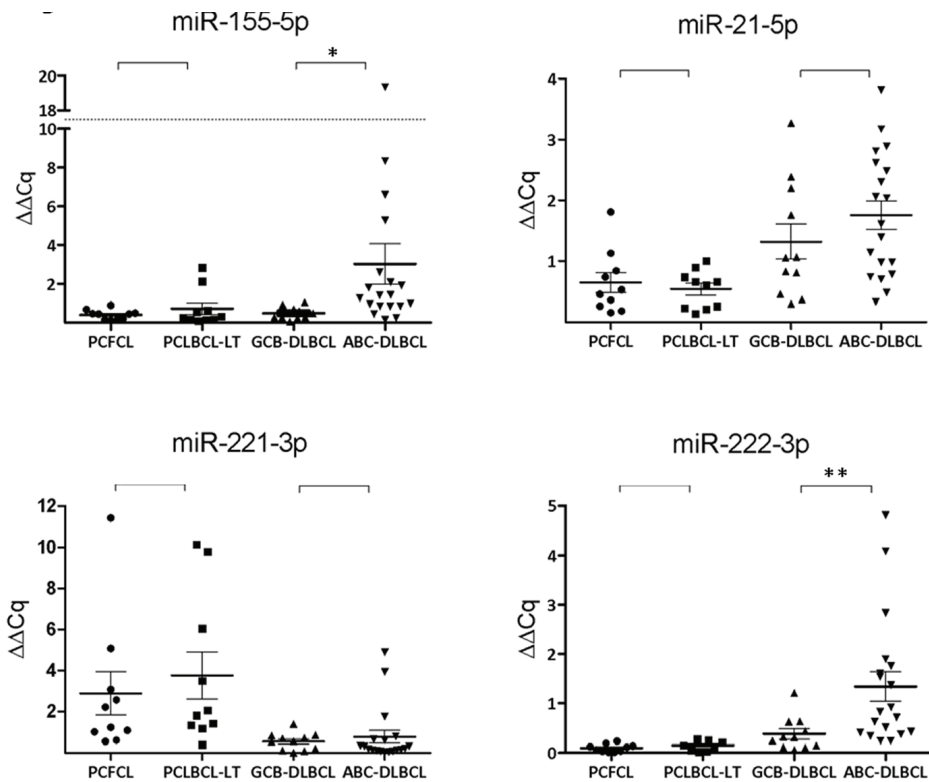
The miR-31 gene is located on 9p21.3. This chromosomal region is often targeted by mono-allelic or biallelic deletions in PCLBCL-LT, but not in PCFCL.<sup>4,43</sup> In accordance, the expression of miR-31-5p was lower in PCLBCL-LT in proportion to PCFCL. Correlation of previous multiplex ligation probe-dependent assay results of chromosomal location 9p21.3<sup>43</sup> to the current results showed that two of the PCLBCL-LT samples tested here had deletions in this region and low expression of miR-31-5p, while four samples did not have deletions and showed higher expression of this specific microRNA. Well characterized genes involved in this deletion are CDKN2A and CDKN2B, tumor suppressor genes involved in cell cycle control.<sup>44</sup> We previously reported that inactivation of CDKN2A in PCLBCL-LT is associated with inferior survival.<sup>4,43</sup> It is however not clear whether the miR-31 gene is also part of the 9p21.3 deletion involved in this more aggressive behavior. Downregulation of miR-31-5p has been described in different types of T-cell non-Hodgkin lymphomas.<sup>45</sup> In these lymphomas, miR-31-5p was shown to be associated with activation of the nuclear factor (NF)- $\kappa$ B pathway, a signaling pathway often deregulated in several types of malignancies, by targeting NF- $\kappa$ B inducing kinase.<sup>45</sup>

MiR-9-5p is involved in normal B-cell development, negatively regulating transcription factor PRDM1, an essential driver of plasma cell differentiation. In accordance, this microRNA



is more abundantly expressed in normal germinal center B-cells than plasma cells.<sup>21</sup> As PCLBCL-LT is thought to be derived from B-cells in a stage just beyond the germinal center reaction, tending towards plasma cell differentiation, the lower expression of miR-9-5p might reflect a normal biological stage in B-cell maturation. In ovarian cancer, miR-9-5p has been demonstrated to act as a tumor suppressor microRNA by targeting the NF- $\kappa$ B family member NF $\kappa$ B1/p50.<sup>46</sup> Since the NF- $\kappa$ B pathway has a well-known oncogenic potential in ABC-type nodal DLBCL,<sup>47</sup> it can be speculated that downregulation of miR-9-5p might have a pathogenic effect in PCLBCL-LT through reduced inhibition of NF- $\kappa$ B signaling.

Figure 4. RT-qPCR expression in FFPE samples (2)



The expression of the 4 microRNAs that are repeatedly reported in previous studies to be more abundantly expressed in ABC-type than GCB-type nodal DLBCL are represented in dot plots.  $\Delta\Delta Cq$  was calculated with miR-148b-3p, let-7e-5p and miR-25-3p as stably expressed reference microRNAs. \*P-value < 0.05; \*\* P-value = 0.05 (Mann Whitney U test).

#### Correlation with nodal DLBCL subtypes

PCFCL and PCLBCL-LT have a very distinct gene expression profile, corresponding with gene expression profiles of GCB- and ABC-type nodal DLBCL.<sup>5</sup> We therefore were interested in comparing both subtypes of PCLBCL with their molecular counterparts of nodal DLBCL. However, literature concerning microRNA expression in nodal DLBCL shows inconsistent results. Taken together, the most frequently reported microRNAs showing higher expression

in ABC-type as compared to GCB-type nodal DLBCL are miR-155-5p, miR-21-5p and miR-221-3p and miR-222-3p.<sup>11,12,15-19,48</sup> In our PCLBCL samples, expression of these four microRNAs did not show significant differences between the two subtypes in both high-throughput sequencing and RT-qPCR. To accurately compare our PCLBCL samples with nodal DLBCL, and exclude external influences such as differing reference microRNAs, we performed RT-qPCR on well-defined subgroups of nodal DLBCL by using a set of three microRNAs (miR-148b-3p, let-7e-5p and miR-25-3p) that were stably expressed in our PCLBCL sequencing studies as a reference. These microRNAs were, in contrast to widely used references U6 and RNU48, stably expressed in our nodal DLBCLs. By using this approach of matching conditions, we confirmed higher expression of miR-155-5p and miR-222-3p in ABC-type as compared to GCB-type nodal DLBCL, but not of miR-21-5p and miR-221-3p.

The absence of higher expression of miR-155-5p in PCLBCL-LT as compared to PCFCL was most noteworthy. The role miR-155-5p has been studied extensively in nodal B-cell non-Hodgkin lymphomas and is linked to activation of the intracellular signaling pathway PI3K-Akt pathway<sup>10</sup> and increased lymphoma cell motility,<sup>49</sup> and its expression is associated with NF- $\kappa$ B activity in nodal DLBCL.<sup>48</sup> The finding that miR-155-5p was not elevated in PCLBCL-LT as compared to PCFCL suggests at least partially different pathogenetic mechanisms in PCLBCL-LT as compared to its nodal molecular counterpart.

In summary, we presented the first microRNA profiling results by next generation high-throughput sequencing and RT-qPCR comparing PCFCL and PCLBCL-LT. These two subtypes of PCLBCL did not show entirely distinct microRNA profiles, but could be distinguished by differential expression of microRNAs miR-129-2-3p, miR-214-3p, miR-31-5p and miR-9-5p. We also showed that the hitherto described microRNA signature of GCB- and ABC-subtype nodal DLBCLs could not be extrapolated to PCFCL and PCLBCL-LT. Therefore, we conclude that although PCFCL and PCLBCL-LT show strong resemblance at gene expression level with GCB- and ABC-type nodal DLBCL, respectively, their microRNA profiles are at least partially disparate from their nodal counterparts, suggesting distinct pathogenetic mechanisms.

## References

1. Willemze R, Jaffe ES, Burg G, et al. (2005) WHO-EORTC classification for cutaneous lymphomas. *Blood* 105: 3768-85.
2. Swerdlow SH, Campo E, Harris NL, et al. (2008) WHO Classification of Tumours Haematopoietic and Lymphoid Tissues. Geneva, Switzerland: WHO PRESS.
3. Senff NJ, Hoefnagel JJ, Jansen PM, et al. (2007) Reclassification of 300 primary cutaneous B-Cell lymphomas according to the new WHO-EORTC classification for cutaneous lymphomas: comparison with previous classifications and identification of prognostic markers. *J Clin Oncol* 25: 1581-7.
4. Dijkman R, Tensen CP, Jordanova ES, et al. (2006) Array-based comparative genomic hybridization analysis reveals recurrent chromosomal alterations and prognostic parameters in primary cutaneous large B-cell lymphoma. *J Clin Oncol* 24: 296-305.
5. Hoefnagel JJ, Dijkman R, Basso K, et al. (2005) Distinct types of primary cutaneous large B-cell lymphoma identified by gene expression profiling. *Blood* 105: 3671-8.
6. Senff NJ, Noordijk EM, Kim YH, et al. (2008) European Organization for Research and Treatment of Cancer and International Society for Cutaneous Lymphoma consensus recommendations for the management of cutaneous B-cell lymphomas. *Blood* 112: 1600-9.
7. Bartel DP (2004) MicroRNAs: genomics, biogenesis, mechanism, and function. *Cell* 116: 281-97.
8. Garzon R, Croce CM (2008) MicroRNAs in normal and malignant hematopoiesis. *Curr Opin Hematol* 15: 352-8.
9. Monsalvez V, Montes-Moreno S, Artiga MJ, et al. (2013) MicroRNAs as prognostic markers in indolent primary cutaneous B-cell lymphoma. *Mod Pathol* 26: 171-81.
10. Huang X, Shen Y, Liu M, et al. (2012) Quantitative proteomics reveals that miR-155 regulates the PI3K-AKT pathway in diffuse large B-cell lymphoma. *Am J Pathol* 181: 26-33.
11. Zhong H, Xu L, et al. (2012) Clinical and prognostic significance of miR-155 and miR-146a expression levels in formalin-fixed/paraffin-embedded tissue of patients with diffuse large B-cell lymphoma. *Exp Ther Med* 3: 763-70.
12. Montes-Moreno S, Martinez N, Sanchez-Espiridion B, et al. (2011) miRNA expression in diffuse large B-cell lymphoma treated with chemoimmunotherapy. *Blood* 118: 1034-40.
13. Jima DD, Zhang J, Jacobs C, et al. (2010) Deep sequencing of the small RNA transcriptome of normal and malignant human B cells identifies hundreds of novel microRNAs. *Blood* 116: e118-e127.
14. Culpin RE, Proctor SJ, Angus B, et al. (2010) A 9 series microRNA signature differentiates between germinal centre and activated B-cell-like diffuse large B-cell lymphoma cell lines. *Int J Oncol* 37: 367-76.
15. Malumbres R, Sarosiek KA, Cubedo E, et al. (2009) Differentiation stage-specific expression of microRNAs in B lymphocytes and diffuse large B-cell lymphomas. *Blood* 113: 3754-64.
16. Roehle A, Hoefig KP, Repsilber D, et al. (2008) MicroRNA signatures characterize diffuse large B-cell lymphomas and follicular lymphomas. *Br J Haematol* 142: 732-44.
17. Lawrie CH, Chi J, Taylor S, et al. (2009) Expression of microRNAs in diffuse large B cell lymphoma is associated with immunophenotype, survival and transformation from follicular lymphoma. *J Cell Mol Med* 13: 1248-1260.
18. Lawrie CH, Soneji S, Marafioti T, et al. (2007) MicroRNA expression distinguishes between germinal center B cell-like and activated B cell-like subtypes of diffuse large B cell lymphoma. *Int J Cancer* 121: 1156-61.
19. Eis PS, Tam W, Sun L, et al. (2005) Accumulation of miR-155 and BIC RNA in human B cell lymphomas. *Proc Natl Acad Sci USA* 102: 3627-32.
20. Alencar AJ, Malumbres R, Kozloski GA, et al. (2011) MicroRNAs are independent predictors of outcome in diffuse

large B-cell lymphoma patients treated with R-CHOP. *Clin Cancer Res* 17: 4125-35.

21. Zhang J, Jima DD, Jacobs C, et al. (2009) Patterns of microRNA expression characterize stages of human B-cell differentiation. *Blood* 113: 4586-94.
22. Meijer CJLM, Vergier B, Duncan LM, Willemze R (2008) Primary cutaneous DLBCL, leg type. In: Swerdlow SH, Campo E, Harris NL, Jaffe ES, Pileri S et al., editors. WHO classification of tumours of haematopoietic and lymphoid tissues. Lyon: IARC Press 242.
23. Hans CP, Weisenburger DD, Greiner TC, et al. (2004) Confirmation of the molecular classification of diffuse large B-cell lymphoma by immunohistochemistry using a tissue microarray. *Blood* 103: 275-82.
24. Choi WW, Weisenburger DD, Greiner TC, et al. (2009) A new immunostain algorithm classifies diffuse large B-cell lymphoma into molecular subtypes with high accuracy. *Clin Cancer Res* 15: 5494-502.
25. Qin Y, Buermans HP, van Kester MS, et al. (2012) Deep-sequencing analysis reveals that the miR-199a2/214 cluster within DN3os represents the vast majority of aberrantly expressed microRNAs in Sezary syndrome. *J Invest Dermatol* 132: 1520-2.
26. Friedlander MR, Chen W, Adamidi C, et al. (2008) Discovering microRNAs from deep sequencing data using miRDeep. *Nat Biotechnol* 26: 407-15.
27. Volinia S, Galasso M, Sana ME, et al. (2012) Breast cancer signatures for invasiveness and prognosis defined by deep sequencing of microRNA. *Proc Natl Acad Sci USA* 109: 3024-9.
28. Robinson MD, McCarthy DJ, Smyth GK (2010) edgeR: a Bioconductor package for differential expression analysis of digital gene expression data. *Bioinformatics* 26: 139-40.
29. Benjamini YH, Y. (1995) Controlling the False Discovery Rate: A practical and powerful approach to multiple testing. *J R Statist Soc B* 57: 289-300.
30. Andersen CL, Jensen JL, Orntoft TF (2004) Normalization of real-time quantitative reverse transcription-PCR data: a model-based variance estimation approach to identify genes suited for normalization, applied to bladder and colon cancer data sets. *Cancer Res* 64: 5245-50.
31. Mestdagh P, Van Vlierberghe P, De Weer A, et al. (2009) A novel and universal method for microRNA RT-qPCR data normalization. *Genome Biol* 10: R64.
32. Vandesompele J, De Preter K, Pattyn F, et al. (2002) Accurate normalization of real-time quantitative RT-PCR data by geometric averaging of multiple internal control genes. *Genome Biol* 3: RESEARCH0034.
33. Ventura A, Young AG, Winslow MM, et al. (2008) Targeted deletion reveals essential and overlapping functions of the miR-17 through 92 family of miRNA clusters. *Cell* 132: 875-86.
34. He L, Thomson JM, et al. (2005) A microRNA polycistron as a potential human oncogene. *Nature* 435: 828-33.
35. Olive V, Bennett MJ, et al. (2009) miR19 is a key oncogenic component of mir17-92. *Genes Dev* 23: 2839-49.
36. Fischer L, Hummel M, Korfel A, et al. (2011) Differential micro-RNA expression in primary CNS and nodal diffuse large B-cell lymphomas. *Neuro Oncol* 13: 1090-8.
37. Xiao C, Calado DP, Galler G, et al. (2007) MiR-150 controls B cell differentiation by targeting the transcription factor c-Myb. *Cell* 131: 146-59.
38. Huang YW, Liu JC, Deatherage DE, et al. (2009) Epigenetic repression of microRNA-129-2 leads to overexpression of SOX4 oncogene in endometrial cancer. *Cancer Res* 69: 9038-46.
39. Smith E, Sigvardsson M (2004) The roles of transcription factors in B lymphocyte commitment, development, and transformation. *J Leukoc Biol* 75: 973-81.
40. Jindra PT, Bagley J, Godwin JG, Iacomini J (2010) Costimulation-dependent expression of microRNA-214 increases

the ability of T cells to proliferate by targeting Pten. *J Immunol* 185: 990-7.

41. Derfoul A, Juan AH, Difilippantonio MJ, et al. (2011) Decreased microRNA-214 levels in breast cancer cells coincides with increased cell proliferation, invasion and accumulation of the Polycomb Ezh2 methyltransferase. *Carcinogenesis* 32: 1607-14.
42. Muller H, Bracken AP, Vernell R, et al. (2001) E2Fs regulate the expression of genes involved in differentiation, development, proliferation, and apoptosis. *Genes Dev* 15: 267-85.
43. Senff NJ, Zoutman WH, Vermeer MH, et al. (2009) Fine-mapping chromosomal loss at 9p21: correlation with prognosis in primary cutaneous diffuse large B-cell lymphoma, leg type. *J Invest Dermatol* 129: 1149-55.
44. Kim WY, Sharpless NE (2006) The regulation of INK4/ARF in cancer and aging. *Cell* 127: 265-75.
45. Yamagishi M, Nakano K, Miyake A, et al. (2012) Polycomb-mediated loss of miR-31 activates NIK-dependent NF-kappaB pathway in adult T cell leukemia and other cancers. *Cancer Cell* 21: 121-35.
46. Guo LM, Pu Y, Han Z, et al. (2009) MicroRNA-9 inhibits ovarian cancer cell growth through regulation of NF-kappaB1. *FEBS J* 276: 5537-46.
47. Davis RE, Brown KD, Siebenlist U, Staudt LM (2001) Constitutive nuclear factor kappaB activity is required for survival of activated B cell-like diffuse large B cell lymphoma cells. *J Exp Med* 194: 1861-74.
48. Rai D, Karanti S, Jung I, Dahia PL, Aguiar RC (2008) Coordinated expression of microRNA-155 and predicted target genes in diffuse large B-cell lymphoma. *Cancer Genet Cytogenet* 181: 8-15.
49. Dagan LN, Jiang X, Bhatt S, et al. (2012) miR-155 regulates HGAL expression and increases lymphoma cell motility. *Blood* 119: 513-20.

## Supplemental Materials and Methods

### *B-cell selection and activation*

Human B-cells were purified from the separate lymphocyte fractions of peripheral blood (buffy coats) obtained from four healthy individuals by positive selection with magnetic CD19 MicroBeads (Miltenyi Biotec, Bergisch Gladbach, Germany). The B-cells were cultured in RPMI 1640 with 10% FCS and incubated with CpG (5 µg/ml) (ODN 2006, Invivogen, San Diego, USA) and monoclonal antibodies to CD40 (0.1 µg/ml) (BD Biosciences Pharmingen, Heidelberg, Germany) for 24 hours. After harvesting, a B-cell purity of more than 97% was confirmed by flow cytometric analysis with a mixture of monoclonal antibodies against B-cell (CD20, APC-H7), T-cell (CD3, PE-H7) and monocytes (CD14, APC). Simultaneously, the activation status was determined using anti-CD80 (PE) and anti-CD86 (FITC), respectively. All antibodies were obtained from BD Biosciences. Dead cells were excluded using 1 µM of DAPI. A BD Biosciences LSRII was used for acquisition. WinList 7 (Verity Software House, Topsham, ME, USA) was used for data analysis. Approximately 86% of the lymphocytes showed expression of these activation markers.

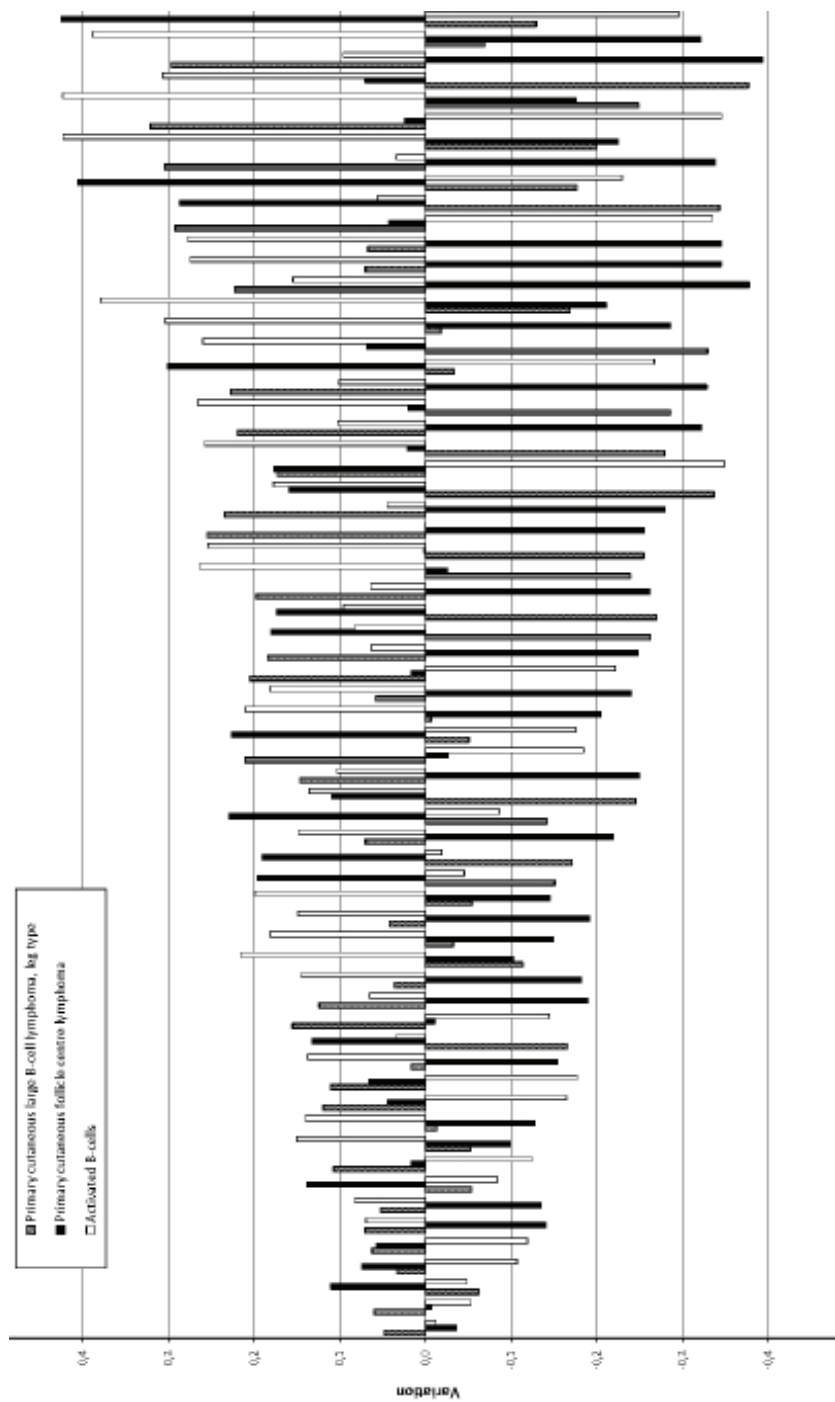
### *MicroRNA library preparation for high-throughput sequencing*

Sequencing adaptors were ligated to total RNA on both ends of the RNA molecules and reverse-transcribed. The cDNA was pre-amplified with PCR primers containing specific sequence tags making the libraries compatible with the Illumina flow cells (Illumina, Son en Breugel, The Netherlands). Polyacrylamide *gel* electrophoresis size selection was performed, excising the 95-105 bp band containing the adaptor-ligated microRNA insert. Quantification and size verification was performed using a high sensitivity DNA chip (Agilent, Amstelveen, The Netherlands).

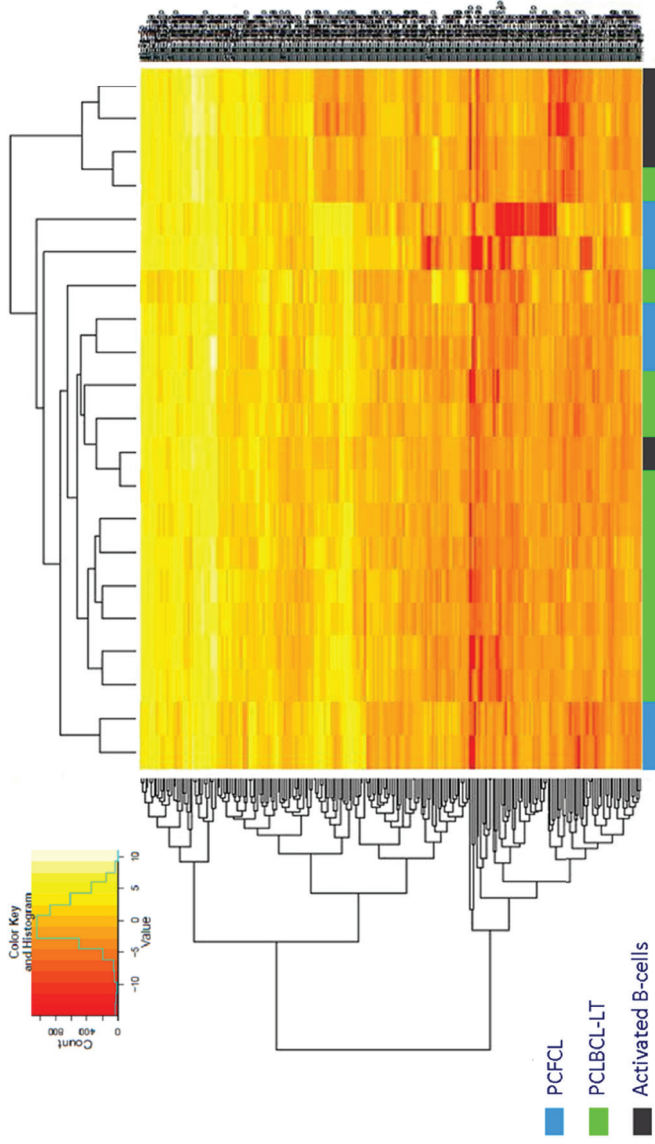
### *MicroRNA real-time qPCR*

Total RNA was isolated from 10 µm sections of FFPE tumor samples (number of sections varying from 4 to 20 sections, according to the size of the specimen) using the RecoverAll Total Nucleic Acid Extraction Kit according to manufacturer's protocol (Ambion, Warrington, UK). Approximately 300 ng of total RNA from each sample (FFPE or frozen, same isolation as for the high-throughput sequencing) was reverse transcribed using the microRNA reverse transcription kit (Applied Biosystems) combined with the stem-loop Megaplex primer pool A v2.1 (Applied Biosystems), which allowed for simultaneous reverse transcription of 377 microRNAs and 4 endogenous controls. The reverse transcription was conducted on the LightCycler480 (Roche, Almere, The Netherlands), running 40 cycles with the following conditions: 2 minutes at 16°C, 1 minutes at 42°C and 1 second at 50°C, followed by 5 minutes holding at 85°C. RT-qPCR was performed using Taqman microRNA and control assays and 2x Universal PCR mastermix (Applied Biosystems). The reactions were run in duplicate on the CFX384 RT-qPCR Detection System, according to manufacturer's protocol (Bio-Rad Laboratories, Veenendaal, the Netherlands), with the following cycle parameters: 10 min at 95 °C, followed by 50 cycles denaturing for 15 s at 95 °C and annealing and extending for 60 s at 60 °C.

Supplemental Figure 1. Most stably expressed microRNAs in high-throughput sequencing according to GeNorm

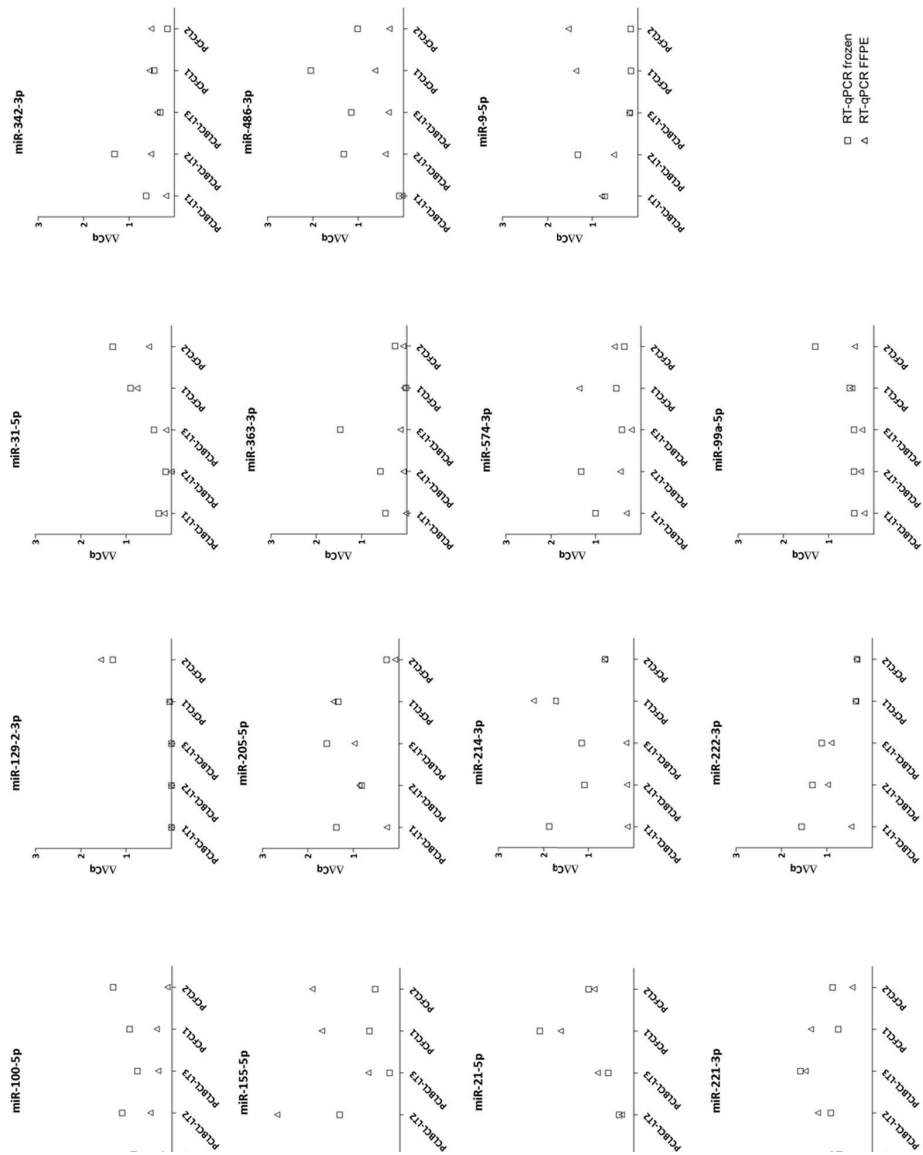


Supplemental Figure 2. Unsupervised hierarchical clustering of the normalized expression of all analyzed microRNAs of high-throughput sequencing





Supplemental Figure 3. Internal validation



Supplemental Table 1. Complete microRNA profiling of nodal DLBCL: differences between ABC- and GCB-type nodal DLBCL

Author	Journal	Year	# pt	Technique	MicroRNA ↑ in ABC- vs GCB-DLBCL	MicroRNA ↑ in GCB- vs ABC-DLBCL	Subtyping DLBCLs
Lawrie	Int J Cancer	2007	5*	miRMAX microarray (252 microRNAs)	<u>miR-155</u> , <u>miR-21</u> , <u>miR-222</u>	none	established cell lines
Roehle	Br J Haematol	2008	58	qPCR assay (157 microRNAs)	<u>miR-155</u>	miR-27b, miR-28, miR-129, miR-133a, miR-133b, miR-138, miR-151	IHC: Hans
Lawrie†	J Cell Mol Med	2009	64	custom-made microarray (464 microRNAs)	miR-518a, miR-363, miR-21, miR-132, miR-340, miR-301, miR-30d, <u>miR-221</u> , miR-422b, miR-146b, <u>miR-155</u> , miR-190, miR-194, miR-660, miR-213, <u>miR-222</u> , miR-186	miR-620, miR-616, miR-199b, miR-421, miR-569, miR-653, miR-138, miR-520h, miR-129	IHC: Hans
Malumbrest	Blood	2009	8*	LC Sciences microarray (711 microRNAs)	miR-146b-5p, miR-146a, miR-21, <u>miR-155</u> , miR-500, <u>miR-222</u> , miR-363, miR-574-5p, miR-574-3p	none	established cell lines
Zhang	Blood	2009	40	Exiqon microarray (789 microRNAs)	( <i>up- or downregulation not stated</i> ) miR-142-3p, miR-16, miR-184, miR-191, miR-19a, miR-19b, miR-299-5p, miR-32, miR-30e*, miR-151-5p, miR-583, mghv-miR-M1-7-5p, miR-142-5p, miR-106b, miR-30e, miR-140-3p, miR-20a, miR-526b*, miR-28-5p, miR-30c	miR-142-3p, miR-16, miR-184, miR-191, miR-19a, miR-19b, miR-299-5p, miR-32, miR-30e*, miR-151-5p, miR-583, mghv-miR-M1-7-5p, miR-142-5p, miR-106b, miR-30e, miR-140-3p, miR-20a, miR-526b*, miR-28-5p, miR-30c	IHC: Hans
Culpin	Int J Oncol	2010	8*	Miltenyi Biotec microarray (1860 microRNAs)	miR-17, miR-19b, miR-20a, miR-29a, none	miR-17, miR-19b, miR-20a, miR-29a, none	IHC: Hans
Montes-Moreno	Blood	2011	29	Agilent microarray (470 microRNAs)	miR-92a, miR-106a, miR-720, miR-1260, miR-1280	miR-331, miR-151, miR-28, miR-454-3p	IHC: Choi

\* cell lines; † study generated a distinct microRNA subset separating ABC- from GCB-DLBCL by unsupervised hierarchical clustering analysis; # pt: number of patients; IHC: immunohistochemistry; ABC: activated B-cell; GCB: germinal center B-cell; DLBCL: diffuse large B-cell lymphoma, qPCR: quantitative polymerase chain reaction; NGS: next generation sequencing.

Supplemental Table 2. 238 microRNAs with sufficiently high enough read counts in next generation sequencing to be included in further analysis

let-7a-5p	miR-1275	miR-152	miR-195-5p	miR-223-5p	miR-31-5p	miR-378c	miR-574-3p
let-7b-5p	miR-128	miR-155-3p	miR-197-3p	miR-224-5p	miR-32-5p	miR-378d	miR-574-5p
let-7c	miR-1280	miR-155-5p	miR-199a-3p	miR-23a-3p	miR-320a	miR-378f	miR-577
let-7d-3p	miR-129-1-3p	miR-15a-3p	miR-199a-5p	miR-23b-3p	miR-320b	miR-378g	miR-582-5p
let-7d-5p	miR-129-2-3p	miR-15a-5p	miR-199b-3p	miR-23c	miR-324-5p	miR-378i	miR-590-3p
let-7e-5p	miR-1306-5p	miR-15b-3p	miR-199b-5p	miR-24-2-5p	miR-326	miR-423-3p	miR-590-5p
let-7f-5p	miR-1307-3p	miR-15b-5p	miR-19a-3p	miR-24-3p	miR-328	miR-423-5p	miR-598
let-7g-3p	miR-1307-5p	miR-16-2-3p	miR-19b-3p	miR-25-3p	miR-330-3p	miR-424-5p	miR-625-3p
let-7g-5p	miR-130a-3p	miR-16-5p	miR-200a-3p	miR-26a-5p	miR-331-3p	miR-425-3p	miR-652-3p
let-7i-3p	miR-130b-3p	miR-17-3p	miR-200b-3p	miR-26b-5p	miR-338-3p	miR-425-5p	miR-652-5p
let-7i-5p	miR-130b-5p	miR-17-5p	miR-200c-3p	miR-27a-3p	miR-339-3p	miR-4286	miR-660-5p
miR-100-5p	miR-138-5p	miR-181a-2-3p	miR-203	miR-27b-3p	miR-339-5p	miR-4485	miR-664-3p
miR-101-3p	miR-139-5p	miR-181a-3p	miR-205-5p	miR-28-3p	miR-33a-5p	miR-451a	miR-7-1-3p
miR-103a-3p	miR-140-3p	miR-181a-5p	miR-20a-3p	miR-28-5p	miR-342-3p	miR-4521	miR-7-5p
miR-106a-5p	miR-140-5p	miR-181b-5p	miR-20a-5p	miR-296-5p	miR-342-5p	miR-454-3p	miR-720
miR-106b-3p	miR-141-3p	miR-182-5p	miR-20b-5p	miR-29a-3p	miR-345-5p	miR-455-3p	miR-744-5p
miR-106b-5p	miR-142-3p	miR-183-5p	miR-21-3p	miR-29b-2-5p	miR-34a-5p	miR-484	miR-766-3p
miR-107	miR-142-5p	miR-185-5p	miR-21-5p	miR-29b-3p	miR-361-3p	miR-486-3p	miR-874
miR-10a-5p	miR-143-3p	miR-186-5p	miR-210	miR-29c-3p	miR-361-5p	miR-486-5p	miR-9-5p
miR-10b-5p	miR-144-3p	miR-188-5p	miR-214-3p	miR-29c-5p	miR-3613-3p	miR-497-5p	miR-92a-1-5p
miR-1246	miR-145-5p	miR-188-5p	miR-214-5p	miR-301a-3p	miR-3613-5p	miR-500a-3p	miR-92a-3p
miR-1247-5p	miR-146a-5p	miR-18a-5p	miR-215	miR-301a-3p	miR-362-3p	miR-501-3p	miR-92b-3p
miR-1249	miR-146b-5p	miR-18b-5p	miR-218-5p	miR-301b	miR-363-3p	miR-502-3p	miR-93-5p
miR-125a-5p	miR-148a-3p	miR-191-5p	miR-22-3p	miR-30a-3p	miR-365a-3p	miR-505-3p	miR-941
miR-125b-5p	miR-148b-3p	miR-192-5p	miR-22-5p	miR-30a-5p	miR-365b-3p	miR-505-5p	miR-96-5p
miR-126-3p	miR-150-3p	miR-193a-3p	miR-221-3p	miR-30b-5p	miR-374a-5p	miR-5100	miR-98
miR-126-5p	miR-150-5p	miR-193a-5p	miR-221-5p	miR-30c-5p	miR-374b-5p	miR-532-3p	miR-99a-5p
miR-1260a	miR-151a-3p	miR-193b-3p	miR-222-3p	miR-30d-5p	miR-376a-3p	miR-532-5p	miR-99b-5p
miR-1260b	miR-151a-5p	miR-193b-5p	miR-222-5p	miR-30e-3p	miR-376c	miR-548h-3p	
miR-1271-5p	miR-151b	miR-194-5p	miR-223-3p	miR-30e-5p	miR-378a-3p	miR-548z	





**Nuclear Factor- $\kappa$ B pathway-activating gene  
aberrancies in primary cutaneous large B-cell  
lymphoma, leg type**

*Abridged version published:*

*Journal of Investigative Dermatology 2014;  
134(1): 290-292*

Lianne Koens<sup>1</sup>

Willem H. Zoutman<sup>2</sup>

Passorn Ngarmmlertsirichai<sup>3</sup>

Grzegorz K. Przybylski<sup>3,4</sup>

Piotr Grabarczyk<sup>3</sup>

Maarten H. Vermeer<sup>2</sup>

Rein Willemze<sup>2</sup>

Patty M. Jansen<sup>1</sup>

Christian A. Schmidt<sup>3</sup>

Cornelis P. Tensen<sup>2</sup>

Departments of <sup>1</sup>Pathology; and <sup>2</sup>Dermatology, Leiden University  
Medical Center, Leiden, The Netherlands;

<sup>3</sup>Clinic for Internal Medicine C , University Greifswald, Greifswald,  
Germany and <sup>4</sup>Instute of Human Genetics, Polish Academy of  
Sciences, Poznan, Poland



## Abstract

Primary cutaneous large B-cell lymphoma, leg type (PCLBCL-LT) is an aggressive cutaneous lymphoma with a 5-year overall survival of approximately 40%. At gene expression level, PCLBCL-LT resembles the activated B-cell (ABC) type of nodal diffuse large B-cell lymphoma (DLBCL). In ABC-DLBCL, a role for constitutive Nuclear Factor (NF)- $\kappa$ B pathway activation in tumor cell survival is generally recognized. We screened 10 cases of PCLBCL-LT for genetic alterations potentially leading to aberrant NF- $\kappa$ B activation. Tumor suppressor gene *TNFAIP3* was heterozygously deleted in four cases. No additional promoter hypermethylation was detected. A *CD79B*Y196 mutation was found in 2 cases. The coiled-coil domain of *CARD11* contained a D415E and a R423W mutation in one sample. At genomic level, the oncogenic *MYD88* L265P mutation was found in 4 cases, of which 3 showed the same mutation at transcriptional level. Combined, seven out of 10 cases of PCLBCL-LT showed genetic alterations in genes that regulate NF- $\kappa$ B activation. The percentages of mutations were highly concordant with those encountered in nodal ABC-DLBCL. Together, these findings strongly suggest a role for constitutive activation of the NF- $\kappa$ B pathway in PCLBCL-LT and provide the rationale to explore using new treatment modalities targeted at components of the NF- $\kappa$ B pathway.

## Introduction

Primary cutaneous large B-cell lymphoma, leg type (PCLBCL-LT) is an aggressive cutaneous lymphoma with a 5 year overall survival of approximately 40%.<sup>1</sup> Due to its aggressive nature, the treatment of first choice is anthracyclin-based chemotherapy combined with rituximab.<sup>2</sup> However, patients often show a progressive disease course despite treatment with polychemotherapy. Furthermore, due to age and (age-related) comorbidity, not all patients are eligible for this treatment. Therefore, new and additional therapies for PCLBCL-LT are necessary, with a focus on more specific, targeted therapies with fewer side effects than conventional chemotherapy.

At mRNA expression level, PCLBCL-LT resembles activated B-cell (ABC) type of nodal diffuse large B-cell lymphoma (DLBCL), including strong expression of known targets of the Nuclear Factor (NF)- $\kappa$ B pathway, such as interferon regulatory factor 4 (*IRF4*).<sup>3-5</sup> In nodal ABC-type/non-germinal center-type DLBCL, increased NF- $\kappa$ B activity likely plays a role in its pathogenesis, by acting as a transcription factor involved in several cellular survival mechanisms. In line with this role, in nodal ABC-type DLBCL cell lines, constitutive activation of NF- $\kappa$ B is required for tumor cell survival.<sup>3,6</sup> Studies on the molecular background of NF- $\kappa$ B pathway activation have demonstrated that mutations in multiple genes can cause deregulation of NF- $\kappa$ B signaling in nodal ABC-type DLBCL.<sup>7</sup> The genes most frequently affected by genetic aberrations are *TNFAIP3* (*A20*), *CD79B*, *CARD11* (*CARMA1*), and *MYD88*, which all can contribute to constitutive activation of the NF- $\kappa$ B pathway. In two-third of cases nodal ABC-type DLBCL, one or more of these genes are affected.<sup>8</sup> The NF- $\kappa$ B pathway inhibitor *TNFAIP3* is commonly affected by (chromosomal) deletion and hypermethylation of the second allele,<sup>7,9</sup> while the *CD79B*, *CARD11*, and *MYD88* genes are frequently targeted by mutations that lead to activation of the NF- $\kappa$ B pathway.<sup>8,10,11</sup> Together, these results suggest that activation of the NF- $\kappa$ B pathway is involved in the pathogenesis of ABC-type DLBCL and that this pathway can serve as a potential therapeutic target in DLBCL. Indeed, several molecules in the NF- $\kappa$ B pathway have already been selectively targeted *in vitro* and *in vivo* to explore potential new treatment strategies, including SYK (fostamatinib),<sup>12</sup> BTK (ibrutinib),<sup>13,14</sup> PKC $\beta$  (enzastaurin/sotrastaurin),<sup>15,16</sup> and MALT1 (phenothiazines).<sup>17,18</sup> Moreover, the mutational status of espe-



cially *CARD11* and *CD79B* and to a lesser extent *MYD88* has been linked to sensitivity or resistance to drugs targeting the NF- $\kappa$ B pathway,<sup>15,19</sup> and their role therefore seems essential in tumor cell survival in nodal ABC-type DLBCL. We performed a comprehensive investigation of genetic aberrancies in PCLBCL-LT leading to pathological NF- $\kappa$ B pathway activation, to evaluate whether aberrant NF- $\kappa$ B activation is operative in this type of lymphoma.

## Materials & Methods

### *Sample collection*

Frozen biopsy primary tumor material of 10 PCLBCL-LT cases was available from the archive of the Leiden University Medical Center (Leiden, The Netherlands). A diagnosis of PCLBCL-LT was made according to criteria of the WHO-EORTC<sup>20</sup> and WHO classification,<sup>21</sup> and confirmed by a panel of hematopathologists and dermatologists, aided by several routinely performed immunohistochemical stainings. Cases were only included when frozen biopsy material contained a tumor cell percentage of at least 75%, as assessed by immunohistochemical stainings for CD20 and CD3. In all cases physical examination, total blood count, computed tomography scan, and bone marrow did not show extracutaneous disease at inclusion. Patient characteristics are summarized in Supplemental Table 1.

### *Activated B-cells*

Human B-cells were purified from the separate lymphocyte fractions of peripheral blood (buffy coats) obtained from four healthy individuals by positive selection with magnetic CD19 MicroBeads (Miltenyi Biotec, Bergisch Gladbach, Germany). The B-cells were cultured in RPMI 1640 with 10% FCS and incubated with CpG (5  $\mu$ g/ml) (ODN 2006, Invivogen, San Diego, USA) and monoclonal antibodies to CD40 (0.1  $\mu$ g/ml) (BD Biosciences Pharmingen, Heidelberg, Germany) for 24 hours. After harvesting, a B-cell purity of more than 97% was confirmed by flow cytometric analysis with a mixture of monoclonal antibodies against B-cell (CD20, APC-H7), T-cell (CD3, PE-H7) and monocytes (CD14, APC). Simultaneously, the activation status was determined using anti-CD80 (PE) and anti-CD86 (FITC)), respectively. All antibodies were obtained from BD Biosciences. Dead cells were excluded using 1  $\mu$ M of DAPI. A BD Biosciences LSRII was used for acquisition. WinList 7 (Verity Software House, Topsham, ME, USA) was used for data analysis. Approximately 86% of the lymphocytes showed expression of these activation markers.

### *DNA and RNA isolation*

Genomic DNA was extracted using the Genomic-tip 20/G method, according to the protocol supplied by the provider (Qiagen, Hilden, Germany). RNA was isolated by the TRIzol method (Life Technologies, Carlsbad, CA, USA). 0.5  $\mu$ g of total RNA was treated with RQ1 DNase I (Promega, Madison, WI) and reverse-transcribed by use of the iScript cDNA Synthesis kit (BioRad, Veenendaal, The Netherlands).

### *TNFAIP3 gene expression*

mRNA expression of *TNFAIP3* was analyzed by quantitative PCR (qPCR). Candidate reference genes were selected by analysis of gene expression data of two sets of (extra)nodal DLBCLs,<sup>22,23</sup>

online accessible in GENEVESTIGATOR (<https://www.genevestigator.com>) and supplemented with three additional stably expressed reference genes, previously used by our group. Optimal reference genes were selected and tested as previously described.<sup>24</sup> The combination of *TMEM222*, *ZDHCC5*, and *ARF5* was identified as most optimal and used as reference gene set in all subsequent experiments. The qPCR reactions were run in triplicate with the use of iQ SYBR Green SuperMix (Bio-Rad) on the CFX384™ Real-Time System (Bio-Rad). The output data were analyzed using Bio-Rad CFX Manager software applying the  $\Delta\Delta C_q$  method. Relative expression was normalized to the determined reference gene set. Cycle parameters for all transcripts analyzed were as follows: denaturing for 15 seconds at 95 °C, and annealing and extension for 20 seconds at 60 °C, for 40 cycles. Specificity of the PCR products was confirmed by melting curve analysis. Primer sequences are listed in Supplemental Table 2.

#### *TNFAIP3 copy number variation*

A custom designed high-density fine-tiling DNA array with a resolution of 10 kB was set up for the genomic region of *TNFAIP3* (situated at chr6: 138,188,581-138,204,445; array coverage: chr6: 137,200,000- 139,200,000), according to the human genome, built 19 (February 2009; Humane Genome Browser, University of California, Santa Cruz, CA, USA). The array was prepared using Maskless Array Synthesizer Technology (NimbleGen Systems, Reykjavik, Iceland). The mean fluorescence was normalized to reference DNA (healthy donor DNA from blood, Promega, Madison, USA) and analyzed using SignalMap software (NimbleGen Systems) in order to detect copy number alteration in the chromosomal region containing the *TNFAIP3* locus.

#### *TNFAIP3 promoter methylation assay*

Using the EZ Methylation Kit (Zymo Research Corporation, Orange, CA), extracted tumor sample DNA was treated with sodium bisulfite. PCR primers annealing to sodium bisulfite-modified DNA, 5'- ATTGAAACGGGGTAAAGTAGATTG - 3' forward and 5'- CAAAATC-CCAAATCTAATCAAACA - 3' reverse, were designed. Primers were developed in such a way that both methylated and unmethylated sequences are amplified using the same bisulfite treated DNA as PCR template. These primers amplified a 236 bp genomic region (-211 bp to +26 bp from the transcription start site (ENST00000237289)) and covering the middle part of the promoter CpG island of *TNFAIP3*. Twenty-four CpGs were situated in this amplicon. PCR amplification was performed on the CFX384™ Real-Time System (Bio-Rad), and afterwards melting curves were acquired in the presence of iQ SYBR Green Supermix (Bio-Rad) during a linear temperature transition from 65 to 90 °C with increments of 0,2 °C per 10 seconds. The presence of methylated DNA in the samples was detected through a peak with a higher melting curve temperature (84.2 °C) as compared to unmethylated DNA (79.6 °C), using bisulfite converted unmethylated human semen DNA and methylated human DNA (Chemicon, Hampshire, UK) as references as described before.<sup>24</sup>

#### *TNFAIP3 alternative transcript analysis*

For isolated tumor sample DNA, the genomic region containing exons 3 and 4 and intron 3 of *TNFAIP3* was amplified. Forward primer 5'- TTGCTGGGTCTTACATGCAG - 3' and reverse primer 5'- GCTGAAAGCATTTAAGTACAGATCC - 3' were designed for PCR amplification in the presence of Advantage GC Genomic LA Polymerase Mix (Clontech, Heidelberg, Germany). PCR products

were sequenced by the 3730XL/3130XL Genetic Analyzer (LGC Genomics, Berlin, Germany). The nucleotide alterations of each gene were analyzed using Mutation Surveyor software (Softgenetic, State College, PA).

For cDNA amplification of *TNFAIP3* exon 3 to 5, 5' - ATTTGTTGAAACGGGGCTTT - 3' forward and 5' - GGCGAAATTGGAACCTGAT - 3' reverse primers were designed. Amplification was performed on the C1000 Touch™ Thermal Cycler (Bio-Rad) using a touchdown PCR protocol with the following parameters: denaturing at 95°C for 30 seconds, followed by 40 cycles of annealing at 65°C to 58°C for 20 seconds (with a 1°C decrement per cycle in the first 7 cycles) and extension at 72°C for 30 seconds. The purified PCR products were subjected to Sanger sequencing both with forward and reverse primers on the ABI 3730 (Applied Biosystems, Foster City, CA). The sequenced PCR fragments of each gene were aligned to the corresponding normal sequences (Ensembl Genome Browser 70, <http://www.ensembl.org>).

#### *Mutational analysis of CD79B and CARD11, and MYD88*

PCR was performed to amplify exon 5 of *CD79B*, exons 5 to 10 of *CARD11*, and exon 5 of *MYD88* for both DNA and cDNA (primer pairs listed in Supplemental Tables 2 and 3), on the C1000 Touch™ Thermal Cycler (Bio-Rad) using the touchdown PCR protocol as described above. The PCR products were completely sequenced in both directions on the ABI 3730 (Applied Biosystems). Mutation Surveyor software (SoftGenetic) was used for analysis of single nucleotide alterations.

## Results

### *TNFAIP3*

mRNA expression of *TNFAIP3* varied substantially among the tumor samples (Figure 1) as measured relative to stably expressed reference genes *TMEM222*, *ZDHCC5*, and *ARF5*. The high-density fine-tiling DNA array showed decreased mean fluorescence in the *TNFAIP3* chromosomal region in four tumor samples. The mean log<sub>2</sub> transformed fluorescence levels of these samples varied from -0,315 to -0,382 and were concordant with heterozygous deletion of the gene region. Above that, in all 4 samples the complete region investigated (1 MB upstream and downstream of the gene) was heterozygously deleted, confirming this deletion targeted a larger chromosomal area than the *TNFAIP3* locus alone.

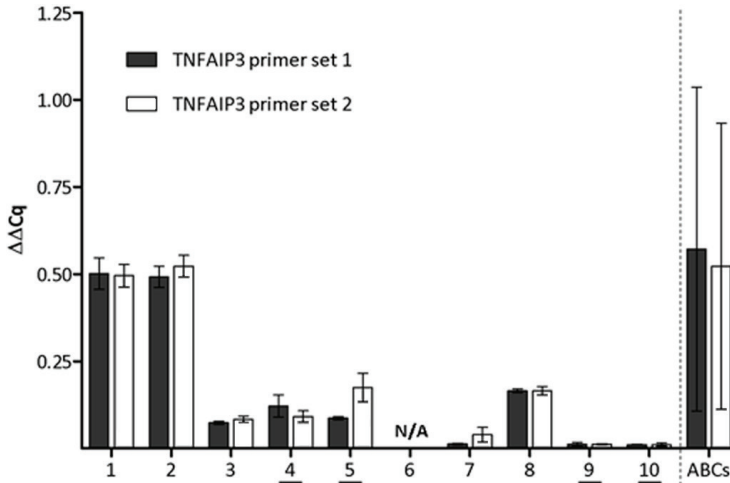
### *Mutational analysis CD79B, CARD11, and MYD88*

Two tumor samples showed a nucleotide substitution in the first immunoreceptor tyrosine-based activation motif (ITAM) of *CD79B*, the first one a c.680A>T missense mutation leading to substitution of tyrosine by phenylalanine (Y196F), the second one a c.679T>C mutation in which tyrosine will be substituted by histidine (Y196H). Both mutations were detected at genomic and transcriptional level (Supplemental Figure 1a and b).

One tumor sample showed both a c.1649C>A and a c.1671C>T mutation in *CARD11* in DNA and cDNA (Supplemental Figure 1c), leading to a substitution of aspartic acid by glutamic acid (D415E), and of arginine by tryptophan (R423W), respectively. Two additional tumor samples showed alterations in codon 415 of *CARD11*, concerning a similar silent mutation (c.1649C>T)

(Supplemental Figure 1d). One of these samples displayed this mutation in DNA and cDNA sequences. For the other sample, only cDNA was analyzed.

Figure 1. *TNFAIP3* mRNA expression (quantitative PCR)



Mean  $\Delta\Delta Cq$  for PCR with two primer sets for *TNFAIP3* relative to reference genes *TMEM222*, *ZDHHC5* and *ARF5* for 9 of 10 tumor samples and 4 samples of in vitro activated peripheral blood B-cells (ABCs). The error bars represent the standard deviation. The underlined tumor samples showed heterozygous deletion of the complete *TNFAIP3* gene region.

Methylation-specific melting curve analysis of the *TNFAIP3* promoter region showed melt curves at the temperature of unmethylated control DNA in all 9 tumor samples tested. No *TNFAIP3* intron 3 mutations or gene conversions affecting the intronic c.487-2A to c.487-1G acceptor splicing site were detected. In cDNA, PCR amplification of exon 3 to 5 of *TNFAIP3* using cDNA showed normal transcripts with a length of 212 base pairs and without replacement any of these exons.

In of four cases, a c.794T>C mutation in *MYD88* was detected in DNA (Supplemental figure 1e and f), leading to a substitution of leucine by proline (L265P). This specific mutation was also present in cDNA in 3 of these cases, but one of these four showed an unchanged cDNA sequence.

An overview of all results is given in Table 1, showing that 7 out of 10 cases contained genetic alterations involved in the regulation of the NF- $\kappa$ B pathway that could lead to constitutive activation of this signaling pathway. Off note, one of the three cases without genetic alterations showed relatively low levels of *TNFAIP3*, suggesting that NF- $\kappa$ B pathway activation is also present in these tumors. In this relatively small cohort of PCLBCL-LT cases, no correlation between genetic aberrancies and survival was found.

## Discussion

We generated a comprehensive overview of NF- $\kappa$ B-activating genetic aberrancies in PCLBCL-LT. Evident genetic alteration were encountered in 7 out of 10 samples, strongly suggesting that constitutive activation of the NF- $\kappa$ B pathway plays a role in the pathogenesis and/or tumor cell survival in PCLBCL-LT.

### *TNFAIP3*

*TNFAIP3* (*A20*) is a tumor suppressor gene, downregulating the NF- $\kappa$ B signaling pathway by deubiquitination of several target proteins involved in activation of this pathway. The *TNFAIP3* protein consists of an ovarian tumor (OTU) domain and seven Zinc finger domains, both necessary for optimal functioning.<sup>25</sup> In both nodal ABC-type DLBCL and PCLBCL-LT, chromosomal arm 6q, on which the *TNFAIP3* gene is situated, is frequently deleted.<sup>26,27</sup>

Table 1. Overview of genetic aberrancies

	TNFAIP3 / A20					CD79B		CARD11		MYD88	
	del.	hyper-methylation	qPCR ( $\Delta\Delta Cq$ )	splicing site		Y196 ITAM mutation		coiled-coil domain mutation		L265P mutation	
				mut.	splice variant	DNA	cDNA	exon 5-8 & 10	exon 9	DNA	cDNA
1	no	no	0,50	no	no	no	no	no	no	L265P	L265P
2	no	no	0,51	no	no	no	no	no	no	no	no
3	no	no	0,08	no	no	no	no	no	no	no	no
4	+/-	no	0,11	no	no	no	no	no	no	L265P	L265P
5	+/-	no	0,13	no	no	no	no	no	D415E, R423W	no	no
6	no	no	N/A	N/A	N/A	no	no	no	no <sup>1</sup>	no	no
7	no	N/A	0,03	no	no	Y196H	Y196H	no	no	L265P	no
8	no	no	0,17	no	no	Y196F	Y196F	no	no	L265P	L265P
9	+/-	N/A	0,01	no	no	N/A	no	no	no	N/A	no
10	+/-	no	0,01	no	no	no	no	no	D415D	no	no

del: deletion; mut: mutation; +/-: heterozygous deletion; N/A: not assessed; <sup>1</sup> A silent mutation (D415D) was detected.

As the mRNA expression levels of *TNFAIP3* varied amongst the tumor samples of PCLBCL-LT, we were interested in potential underlying mechanisms for these variations in PCLBCL-LT. Four cases showing heterozygous deletion of the gene region indeed showed relatively low mRNA expression levels of *TNFAIP3*. These heterozygous deletions were concordant with our previous results of conventional array comparative genomic hybridization studies in primary cutaneous large B-cell lymphomas.<sup>26</sup> Homozygous deletions that are observed in 10% of nodal ABC-type DLBCL,<sup>7</sup> were not found in PCLBCL-LT. In cases with two gene copies of *TNFAIP3* and relatively low levels of mRNA, we could not establish a negative regulatory mechanism. Epigenetic silencing through promoter hypermethylation was not detected in PCLBCL-LT, as was encountered in approximately 40 percent of nodal ABC-type DLBCLs.<sup>9</sup> Furthermore, we investigated whether the *TNFAIP3* transcripts present could give rise to functional proteins. In one-third of cases of nodal ABC-type DLBCL, intron 3 splice site mutations or gene conver-

sions disrupting the intron 3 splice site are encountered, leading to transcripts with an introduced premature stop codon. These transcripts will give rise to a truncated protein without the essential OUT and Zinc finger domains. Again we could not detect these alterations in PCLBCL-LT. As TNFAIP3 was demonstrated to influence proliferation and survival in normal B-cells in a gene-dose-dependent fashion,<sup>28</sup> the relatively low expression of *TNFAIP3* in most of the PCLBCL-LT samples still seems a relevant finding.

Altogether, the heterozygous deletions of *TNFAIP3* and reduced mRNA expression in PCLBCL-LT suggest a role for this tumor suppressor in the pathogenesis of this type of lymphoma, but the mechanisms of reduced expression of *TNFAIP3* are different from the ones encountered in nodal ABC-type DLBCL.

#### *CD79B, CARD11 and MYD88 activating mutations*

CD79B (immunoglobulin-associated beta) is a component of the B-cell receptor, and has a combined function with CD79A in the assembly and membrane expression of the B-cell receptor. The CD79A/CD79B heterodimer also initiates downstream activation of different signaling pathways, including the NF- $\kappa$ B pathway.<sup>29</sup> Somatic mutations affecting *CD79B* were detected in 18% of nodal ABC-type DLBCLs, mainly comprising recurrent mutations in the first immunoreceptor tyrosine-based activation motif (ITAM) tyrosine Y196. These mutations lead to increased surface B-cell receptor expression and downregulated Lyn kinase, a feedback inhibitor of B-cell receptor signaling.<sup>10</sup> The mechanism of activation of the NF- $\kappa$ B pathway through these mutations is called chronic active B-cell receptor signaling, and occurs in cases with wild-type *CARD11*. In our series, concordant with nodal ABC-type DLBCLs, in 20% an Y196 mutation was detected in the absence of mutations in *CARD11*, suggesting that chronic active B-cell receptor signaling is a mechanism involved in these cases of PCLBCL-LT.

*CARD11* is a signaling scaffold protein involved in coordinating the activation of the NF- $\kappa$ B pathway,<sup>11</sup> and a critical component involved in constitutive NF- $\kappa$ B activation in ABC-DLBCL,<sup>6</sup> downstream of the B-cell receptor (see Figure 2). Remarkably, in 3 out of 10 cases, we found point mutations in codon 415 of exon 9. In two of these cases, it concerned a silent mutation. Although functional consequences may seem less apparent for silent mutations, there is increasing evidence that these do have physiological effects, for example through incorrect splicing and changes in RNA structure or by altering the rate of translation.<sup>30</sup> However, as this mutation is a common single nucleotide polymorphism, the relevance of these mutations in PCLBCL-LT can be debated. The sample with a missense mutation in this codon (D415E) also showed a R423W mutation in the same exon in both DNA and cDNA. This *CARD11* R423W mutation was previously described in nodal ABC-type DLBCL.<sup>7</sup> In contrast to some known *CARD11* mutations, the functional relevance of the D415E and R423W mutations has not yet been investigated. However, mutations in the coiled-coil domain are potentially relevant in constitutive activation of the NF- $\kappa$ B pathway, as changes in this domain have the potential to disrupt the autoinhibition of *CARD11* signaling, leading to receptor-independent activation of the NF- $\kappa$ B pathway.<sup>31</sup>

Myeloid response gene 88 (MYD88) is a Toll-like receptor associated adaptor protein with many cellular functions. Amongst others, MYD88 is known to be involved in activation of different signaling pathways through the assembly of a complex containing IRAK1 and IRAK4.<sup>8</sup> Nodal ABC-type DLBCLs showed a L265P mutation in 29% of cases, and the consequent amino acid substitution in the  $\beta$ D sheet of MYD88 has been shown to be oncogenically active,

leading to aberrant activation of NF- $\kappa$ B and JAK-STAT3 signaling pathways and lymphoma cell survival,<sup>8</sup> a mechanism most likely not directly related to (chronic active) B-cell receptor signaling (see Figure 2). In primary central nervous system DLBCL, also an extranodal DLBCL of ABC-genotype, the L265P mutation was encountered in 36% of cases<sup>32</sup> and 38% of cases<sup>33</sup>. Somatic *MYD88* L265P mutations in PCLBCL-LT have been previously described in 69% of cases.<sup>34</sup> The 40% mutation rate we encountered in our series is therefore concordant with other (extra)nodal ABC-type DLBCLs. Furthermore, we showed that not all mutations in the DNA seem to be transcribed to RNA, as for one sample, the mutation was not detected in cDNA.

**Table 2.** Genetic aberrancies in PCLBCL-LT compared to nodal ABC-type DLBCL

	<b>PCLBCL-LT</b>	<b>nodal ABC-type DLBCL</b>
CD79B ITAM mutations	20%	20%
CARD11 coiled-coil domain mutations	10%	10%
MYD88 L265P mutation	30%*	40%
TNFAIP3		
- homozygous deletion	0%	10%
- heterozygous deletion	40%	40%
- epigenetic silencing	0%	40%
- alternative transcripts	0%	33%

\*30% in cDNA, 40% in DNA

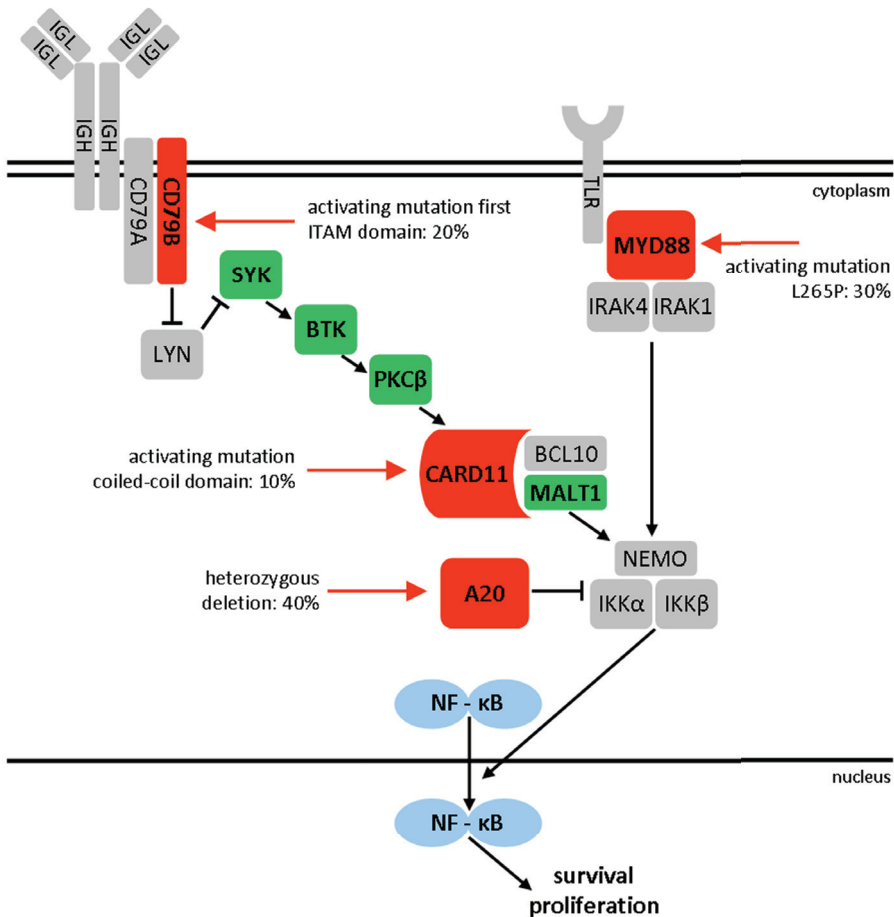
PCLBCL-LT, primary cutaneous large B-cell lymphoma, leg type; ABC-type DLBCL, activated B-cell-type diffuse large B-cell lymphoma

#### *Mutational status and therapeutic targets*

The above described specific mutations not only give more insight into the pathogenesis of (extra)nodal DLBCLs, but the relevance of these mutations for novel therapeutic strategies has also been explored. For example, sotrastaurin can interfere with NF- $\kappa$ B pathway activation, by inhibition of PKC- $\beta$ , which is required for CARD11-dependent activation of the NF- $\kappa$ B pathway.<sup>35</sup> Sotrastaurin was shown to be selectively toxic for *CD79*-mutant DLBCL in a mouse xenograft model<sup>15</sup> as compared to unmutated DLBCL, but only in presence of wild-type *CARD11*. These findings strongly suggest that sotrastaurin is especially promising in cases of DLBCL with chronic active B-cell receptor signaling. An RNA interference screen revealed that a BCR signaling component, Bruton's tyrosine kinase (BTK), is essential for the survival of nodal ABC-type DLBCL with wild-type *CARD11* and in addition, knockdown of proximal B-cell receptor units, i.e. *CD79B*, was selectively toxic to wild-type *CARD11* nodal ABC-type DLBCL, but not to other lymphomas.<sup>10</sup> Furthermore, in a phase I trial, the BTK-inhibitor ibrutinib was well-tolerated and generated a clinical (partial) response in 40% of refractory nodal ABC-type DLBCL, both in patients with tumors bearing *CD79* mutations or a combination of *CD79* and *MYD88* mutations. However, patients with only *MYD88* mutations were refractory to this treatment, reflecting the B-cell receptor signaling-independency of these *MYD88*-mutated tumors and warranting assessment of the mutations status of these NF- $\kappa$ B related signaling molecules.<sup>19</sup>

In conclusion, seven out of ten cases of PCLBCL-LT showed genetic alterations in the NF-κB pathway. For pathway-activating mutations in the *CD79B* ITAM, *MYD88* L265P mutations and *CARD11* coiled-coil domain mutations, the percentage of tumors affected corresponds to the percentages in nodal ABC-type DLBCL (Table 2). However, although downregulated mRNA expression of *TNFAIP3* in our samples was highly suggestive for a role of this tumor suppressor in NF-κB activation, the genetic substrate for low expression is not completely evident in PCLBCL-LT, and therefore differs from the well-defined mechanisms downregulating the function of TNFAIP3 in nodal ABC-type DLBCL. Together, these findings strongly suggest a role for constitutive activation of the NF-κB pathway in PCLBCL-LT, and provide the rationale to explore the possibility of using specific therapy targeted at components of the NF-κB pathway in this type of lymphoma.

Figure 2. Pathway overview and genetic aberrancies in primary cutaneous large B-cell lymphoma, leg type



The suggested relations between the different components of B-cell receptor signaling and MYD88 signaling are represented.<sup>14</sup> The molecules affected by genetic aberrancies in PCLBCL-LT are indicated in red and the percentage of the cases affected by these aberrancies are indicated. Molecules that can be therapeutically targeted for inhibition of the NF-κB pathway are represented in green.

4



## References

1. Vermeer MH, Geelen FA, van Haselen CW, et al. (1996) Primary cutaneous large B-cell lymphomas of the legs. A distinct type of cutaneous B-cell lymphoma with an intermediate prognosis. Dutch Cutaneous Lymphoma Working Group. *Arch Dermatol* 132: 1304-8.
2. Senff NJ, Noordijk EM, Kim YH, et al. (2008) European Organization for Research and Treatment of Cancer and International Society for Cutaneous Lymphoma consensus recommendations for the management of cutaneous B-cell lymphomas. *Blood* 112: 1600-9.
3. Davis RE, Brown KD, Siebenlist U, et al. (2001) Constitutive nuclear factor kappaB activity is required for survival of activated B cell-like diffuse large B cell lymphoma cells. *J Exp Med* 194: 1861-74.
4. Grumont RJ, Gerondakis S. (2000) Rel induces interferon regulatory factor 4 (IRF-4) expression in lymphocytes: modulation of interferon-regulated gene expression by rel/nuclear factor kappaB. *J Exp Med.* 191: 1281-92.
5. Hoefnagel JJ, Dijkman R, Basso K, et al. (2005) Distinct types of primary cutaneous large B-cell lymphoma identified by gene expression profiling. *Blood* 105: 3671-8.
6. Ngo VN, Davis RE, Lamy L, et al. (2006) A loss-of-function RNA interference screen for molecular targets in cancer. *Nature* 441: 106-10.
7. Compagno M, Lim WK, Grunn A, et al. (2009) Mutations of multiple genes cause deregulation of NF-kappaB in diffuse large B-cell lymphoma. *Nature* 459: 717-21.
8. Ngo VN, Young RM, Schmitz R, et al. (2011) Oncogenically active MYD88 mutations in human lymphoma. *Nature* 470: 115-9.
9. Honma K, Tsuzuki S, Nakagawa M, et al. (2009) TNFAIP3/A20 functions as a novel tumor suppressor gene in several subtypes of non-Hodgkin lymphomas. *Blood* 114: 2467-75.
10. Davis RE, Ngo VN, Lenz G, et al. (2010) Chronic active B-cell-receptor signalling in diffuse large B-cell lymphoma. *Nature* 463: 88-92.
11. Lenz G, Davis RE, Ngo VN, et al. (2008) Oncogenic CARD11 mutations in human diffuse large B cell lymphoma. *Science* 319: 1676-9.
12. Friedberg JW, Sharman J, Sweetenham J, et al. (2010) Inhibition of Syk with fostamatinib disodium has significant clinical activity in non-Hodgkin lymphoma and chronic lymphocytic leukemia. *Blood* 115: 2578-85.
13. Advani RH, Buggy JJ, Sharman JP, et al. (2013) Bruton tyrosine kinase inhibitor ibrutinib (PCI-32765) has significant activity in patients with relapsed/refractory B-cell malignancies. *J Clin Oncol* 31: 88-94.
14. Yang Y, Shaffer AL, III, Emre NC, et al. (2012) Exploiting synthetic lethality for the therapy of ABC diffuse large B cell lymphoma. *Cancer cell* 21: 723-37.
15. Naylor TL, Tang H, Ratsch BA, et al. (2011) Protein kinase C inhibitor sotrastaurin selectively inhibits the growth of CD79 mutant diffuse large B-cell lymphomas. *Cancer Res* 71: 2643-53.
16. Robertson MJ, Kahl BS, Vose JM, et al. (2007) Phase II study of enzastaurin, a protein kinase C beta inhibitor, in patients with relapsed or refractory diffuse large B-cell lymphoma. *J Clin Oncol* 25: 1741-6.
17. Fontan L, Yang C, Kabaleeswaran V, et al. (2012) MALT1 small molecule inhibitors specifically suppress ABC-DLBCL in vitro and in vivo. *Cancer cell* 22: 812-24.
18. Nagel D, Spranger S, Vincendeau M, et al. (2012) Pharmacologic inhibition of MALT1 protease by phenothiazines as a therapeutic approach for the treatment of aggressive ABC-DLBCL. *Cancer cell* 22: 825-37.
19. Wilson WH, Gerecitano JF, Goy A, et al. (2012) The Bruton's Tyrosine Kinase (BTK) Inhibitor, Ibrutinib (PCI-32765), Has Preferential Activity in the ABC Subtype of Relapsed/Refractory De Novo Diffuse Large B-Cell Lymphoma (DLBCL): Interim Results of a Multicenter, Open-Label, Phase 2 Study. *Blood (ASH Annual Meeting Abstracts)* 120: 4039.

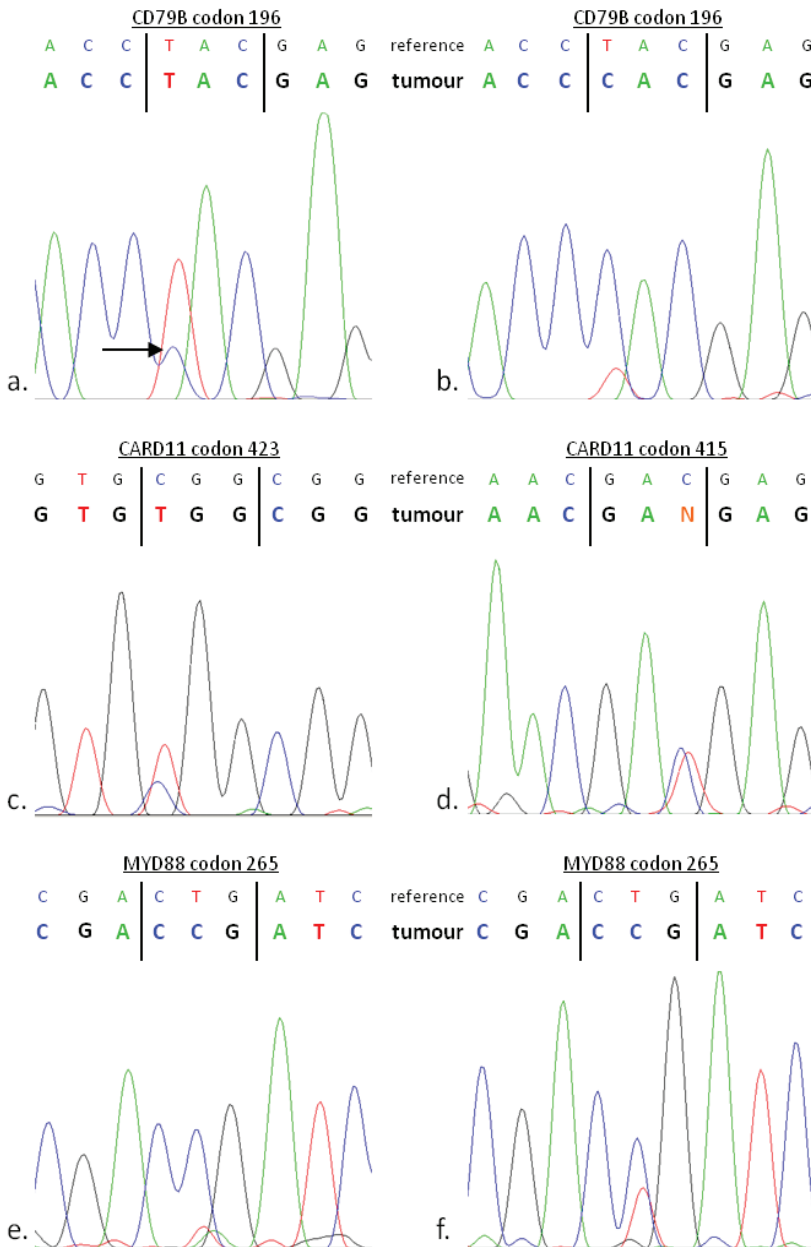
20. Willemze R, Jaffe ES, Burg G, et al. (2005) WHO-EORTC classification for cutaneous lymphomas. *Blood* 105: 3768-85.
21. Meijer CJLM, Vergier B, Duncan LM, et al. (2008) Primary cutaneous DLBCL, leg type. In: Swerdlow SH, Campo E, Harris NL, et al., eds. WHO classification of tumours of haematopoietic and lymphoid tissues. Lyon: IARC Press 242.
22. Booman M, Szuhai K, Rosenwald A, et al. (2008) Genomic alterations and gene expression in primary diffuse large B-cell lymphomas of immune-privileged sites: the importance of apoptosis and immunomodulatory pathways. *J Pathol* 216: 209-17.
23. Lenz G, Wright GW, Emre NC, et al. (2008) Molecular subtypes of diffuse large B-cell lymphoma arise by distinct genetic pathways. *Proc Natl Acad Sci USA* 105: 13520-5.
24. van Kester MS, Borg MK, Zoutman WH, et al. (2012) A meta-analysis of gene expression data identifies a molecular signature characteristic for tumor-stage mycosis fungoides. *J Invest Dermatol* 132: 2050-9.
25. Wertz IE, O'Rourke KM, Zhou H, et al. (2004) De-ubiquitination and ubiquitin ligase domains of A20 downregulate NF-κappaB signalling. *Nature* 430: 694-9.
26. Dijkman R, Tensen CP, Jordanova ES, et al. (2006) Array-based comparative genomic hybridization analysis reveals recurrent chromosomal alterations and prognostic parameters in primary cutaneous large B-cell lymphoma. *J Clin Oncol* 24: 296-305.
27. Tagawa H, Suguro M, Tsuzuki S, et al. (2005) Comparison of genome profiles for identification of distinct subgroups of diffuse large B-cell lymphoma. *Blood* 106: 1770-7.
28. Chu Y, Vahl JC, Kumar D, et al. (2011) B cells lacking the tumor suppressor TNFAIP3/A20 display impaired differentiation and hyperactivation and cause inflammation and autoimmunity in aged mice. *Blood* 117: 2227-36.
29. Dal Porto JM, Gauld SB, Merrell KT, et al. (2004) B cell antigen receptor signaling 101. *Mol Immunol* 41: 599-613.
30. Sauna ZE, Kimchi-Sarfaty C. (2011) Understanding the contribution of synonymous mutations to human disease. *Nature reviews Genetics* 12: 683-91.
31. Lamason RL, McCully RR, Lew SM, et al. (2010) Oncogenic CARD11 mutations induce hyperactive signaling by disrupting autoinhibition by the PKC-responsive inhibitory domain. *Biochemistry* 49: 8240-50.
32. Montesinos-Rongen M, Godlewska E, Brunn A, et al. (2011) Activating L265P mutations of the MYD88 gene are common in primary central nervous system lymphoma. *Acta Neuropathol* 122: 791-2.
33. Gonzalez-Aguilar A, Idbaih A, Boisselier B, et al. (2012) Recurrent mutations of MYD88 and TBL1XR1 in primary central nervous system lymphomas. *Clin Cancer Res* 18: 5203-11.
34. Pham-Ledard A, Cappellen D, Martinez F, et al. (2012) MYD88 somatic mutation is a genetic feature of primary cutaneous diffuse large B-cell lymphoma, leg type. *J Invest Dermatol* 132: 2118-20.
35. Sommer K, Guo B, Pomerantz JL, et al. (2005) Phosphorylation of the CARMA1 linker controls NF-κappaB activation. *Immunity* 23: 561-74.

Supplemental Table 1. Patient characteristics

	Sex	Age at diagnosis (years)	Skin site of primary tumor	Immunohistochemistry				Initial therapy	Disease recurrence	PFS (months)	Follow-up (months)	Current status	
				BCL2	BCL6	CD10	IRF4/ MUM1						B-cell receptor
1	m	84	legs + other	+	+	-	+	IgM IgD κ	RT	yes	1	24	D <sup>+</sup>
2	f	75	both legs	+	+	-	+	IgM λ	PCT + RT	yes	12	54	D <sup>+</sup>
3	f	79	leg	+	+	-	+	IgM κ	RT	no	20	21	A <sup>0</sup>
4	f	81	leg	+	-	-	+	IgM IgD	PCT + RT	yes	20	39	D <sup>+</sup>
5	m	81	leg	+	+	-	+	IgM IgD λ	none	no	0	2	D <sup>+</sup>
6	m	53	legs + other	+	+	-	+	IgM κ	PCT	yes	6	96	A <sup>+</sup>
7	m	68	leg	+	+	-	+	IgM IgD λ	PCT	yes	17	60	D <sup>+</sup>
8	f	83	leg	+	+	-	+	IgM IgD κ	PCT + RT	yes	34	38	D <sup>+</sup>
9	m	83	leg	+	+	-	+	IgM IgD κ	RT	no	49	50	A <sup>0</sup>
10	f	76	leg	+	-	+	+	IgM κ	RT	no	0	13	D <sup>+</sup>

m: male; f: female; PFS: progression-free survival; RT: radiotherapy; PCT: polychemotherapy; A<sup>+</sup>: alive with disease; A<sup>0</sup>: alive without disease; D<sup>+</sup>: death with disease.

Supplemental Figure 1. Sequencing results of *CD79B*, *MYD88*, and *CARD11*



DNA (a) and cDNA (b) sequences of *CD79B* exon 5 in tumor sample 8, concordant with a Y196H mutation. Although in DNA, the dominant sequence of codon 196 is equal to the reference sequence, a clear C-peak is visible under the T-peak (arrow), indicating a nucleotide substitution. In cDNA of the same tumor, the C-peak is dominant, suggesting a predominant expression of the mutated allele. cDNA sequence of *CARD11* exon 9 of tumor sample 5 showing a R423W mutation (c) and of tumor sample 6 with a silent mutation in codon 415 (d). DNA (e) and cDNA (f) sequences of *MYD88* exon 5 in tumor sample 4 showing a L265P mutation.

Supplemental Table 2. Primers for quantitative PCR

Gene		Sequence 5'- 3'	Product size
<i>TNFAIP3</i> (1) <sup>1</sup>	- forward	CTGGGACCATGGCACAACCTC	182 bp
	- reverse	CGGAAGGTTCCATGGGATTC	
<i>TNFAIP3</i> (2)	- forward	CCATGGCACAACCTCATCTCA	172 bp
	- reverse	GAAGGTTCCATGGGATTCTG	
<i>TMEM222</i>	- forward	CGCCTCTGAGGAGTACAAGC	92 bp
	- reverse	TGTAGCGCATCAGATTCAGG	
<i>ARF5</i>	- forward	TGCTGATGAACTCCAGAAGATGC	144 bp
	- reverse	CGGCTGCGTAAGTGCTGTAG	
<i>ZDHCC5</i>	- forward	TATCGGCCGGGTTACAGTAG	95 bp
	- reverse	GTTGGCTCCTTCAAGCTGTC	

1. Braun FCM, Grabarczyk P, Möbs M, et al. (2011) Tumor suppressor TNFAIP3 (A20) is frequently deleted in Sézary syndrome. *Leukemia* 25: 1494-1501.

Supplemental Table 3. Primers for mutational analysis DNA

Gene		Sequence 5'- 3'	Product size
<i>CD79B</i>	- forward	TCTTGCAGAATGCACCTCAC	159 bp
	- reverse	CCAACCACACCAGCAGATAG	
<i>MYD88</i> <sup>2</sup>	- forward	CTGGGGTTGAAGACTGGGCT	276 bp
	- reverse	TGGACAGGCAGACAGATAC	
<i>CARD11</i> <sup>3</sup>	exon 5 - forward	CAGTGCCTCGTGGGCAGAGT	502 bp
	- reverse	GTCACCCTGGCGGAGTAGCC	
exon 6	- forward	CTGGAGAAGGTTTCTTGGAGC	425 bp
	- reverse	ACACCCTGGCAGGTTTCATC	
exon 7	- forward	CCCAGGATACGCCCAAGCAA	593 bp
	- reverse	CCCAGGCCCTCATCTGGTTG	
exon 8	- forward	TCCCCTATGTTACCTGGTCTGTAGTG	573 bp
	- reverse	GCCTGTGACTTCCAAAAAAGCC	
exon 9	- forward	CCTCAGTGCCCTCATCTGTAAAATG	765 bp
	- reverse	CAAAGGACAAGGAGCCATTTCATTG	
exon 10	- forward	CCAGAAGCCTGGGAGGAGGA	564 bp
	- reverse	AGCGAGTCGCAGGATTCCA	

2. Pham-Ledard A, Cappellen D, Martinez F, et al. (2012) MYD88 somatic mutation is a genetic feature of primary cutaneous diffuse large B-cell lymphoma, leg type. *J Invest Dermatol* 132: 2118-20

3. Lenz G, Davis RE, Ngo VN, et al. (2008) Oncogenic CARD11 mutations in human diffuse large B-cell lymphoma. *Science* 319: 1676-9.

Supplemental Table 4. Primers for mutational analysis cDNA

Gene		Sequence 5'- 3'	Product size
<i>CD79B</i>	- forward	AGTCATGGGATTCAGCACCT	218 bp
	- reverse	GCAGCGTCACTATGTCCTCA	
<i>MYD88</i>	- forward	AGGAGATGATCCGGCAACT	297 bp
	- reverse	CGCAGACAGTGATGAACCTC	
<i>CARD11</i>	exon 9 - forward	AATGTACAAGCACCGCATGA	295 bp
	- reverse	GATGGTTACTGCGAGGTTCC	





**Genetic alterations in B-cell  
activation-related transcription factors in  
primary cutaneous large B-cell lymphoma,  
leg type**

*Submitted*

Lianne Koens<sup>1</sup>

Willem H. Zoutman<sup>2</sup>

Passorn Winkler<sup>3</sup>

Grzegorz K. Przybylski<sup>3,4</sup>

Piotr Grabarczyk<sup>3</sup>

Maarten H. Vermeer<sup>2</sup>

Rein Willemze<sup>2</sup>

Patty M. Jansen<sup>1</sup>

Christian A. Schmidt<sup>3</sup>

Cornelis P. Tensen<sup>2</sup>

Departments of <sup>1</sup>Pathology; and <sup>2</sup>Dermatology, Leiden University  
Medical Center, Leiden, The Netherlands;

<sup>3</sup>Clinic for Internal Medicine C , University Greifswald, Greifswald,  
Germany and <sup>4</sup>Institute of Human Genetics, Polish Academy of  
Sciences, Poznan, Poland





## Abstract

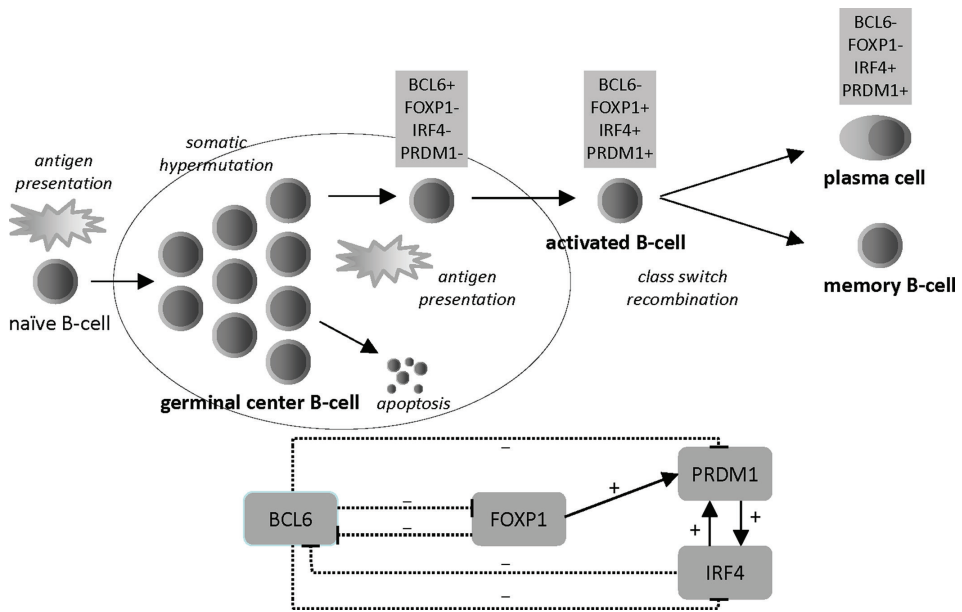
The postulated normal counterpart of primary cutaneous diffuse large B-cell lymphoma, leg type (PCLBCL-LT) is an antigen-activated post-germinal center B-cell. However, in contrast to post-germinal center B-cells, immunohistochemical studies have shown that PCLBCL-LT expresses *BCL6*, *FOXP1* and *IRF4*, and that *Blimp1* (encoded by *PRDM1*) is not detected. To find out if these abnormal findings could be explained by genetic alterations, as is occasionally the case in nodal activated B-cell type diffuse large B-cell lymphoma (ABC-DLBCL), we generated an overview of genetic aberrancies of *BCL6*, *FOXP1*, *PRDM1* and *IRF4* combined with immunohistochemistry in 10 well-defined cases of PCLBCL-LT. While immunohistochemistry showed positivity in 8 out of 10 cases for *BCL6* and in all cases for *FOXP1* and *IRF4*, no evidence of translocations or amplifications involving these genes by fine-tiling comparative genomic hybridization (FT-CGH) combined with ligation-mediated PCR (LM-PCR) was encountered, that could explain high protein levels. However, high protein levels of *FOXP1* are not only based on the detection of the full length protein, but most probably also comprise N-terminally truncated proteins. This is partly based on small deletions in the *FOXP1* gene and partly due to the presence of alternative isoforms 3 and 9. *PRDM1*, of which the protein *Blimp1* is consistently absent by immunohistochemistry, was heterozygously deleted according to FT-CGH analysis in 5 cases. No additional *PRDM1* mutations were encountered in the heterozygously deleted cases, and variations in mRNA levels were independent of the deletions. Together, these results show that in PCLBCL-LT genetic alterations in *BCL6*, *IRF4*, *FOXP1* and *PRDM1* are not involved in the alterations of protein levels of *IRF4*, *FOXP1* and/or *PRDM1* relative to its normal counterpart.

## Introduction

Primary cutaneous large B-cell lymphoma, leg type (PCLBCL-LT) is the most aggressive type of primary cutaneous B-cell lymphoma, with a 5 year overall survival of approximately 40%.<sup>1</sup> This lymphoma is regarded as an extranodal variant of nodal diffuse large B-cell lymphoma (DLBCL) with activated B-cell (ABC) genotype, as both lymphoma subtypes are thought to be derived from B-cells that are blocked in differentiation in the transitional stage between germinal center B-cell and plasma cell.<sup>2,3</sup> In nodal DLBCL, several mechanisms have been described that might (in part) be responsible for this differentiation arrest, for example translocations involving B-cell lymphoma 6 (*BCL6*)<sup>4,5</sup> and/or deletion and mutations of PR domain containing 1, with ZNF domain (*PRDM1*).<sup>4,6</sup> Other molecules driving B-cells towards plasma cell differentiation include interferon regulatory factor-4 (*IRF4*) and forkhead box protein 1 (*FOXP1*), and sporadic genetic alterations, such as translocations involving these genes, also occur in nodal DLBCL (see Figure 1).<sup>7,8</sup>

In normal B-cell development, *BCL6* is expressed in germinal center B-cells in high levels to sustain the germinal center reaction, amongst others by downregulation of *Blimp1* expression, the protein encoded by *PRDM1*.<sup>9</sup> After a successful germinal center reaction, *BCL6* is downregulated, leading to expression of *Blimp1*. This *Blimp1* expression is sufficient to allow B-cells to undergo plasma cell maturation, and also induces other transcription factors, such as *IRF4*, which are also part of the plasma cell program.<sup>10</sup> Furthermore, *FOXP1* expression is inversely correlated to *BCL6* expression, thereby occurring in a post germinal center stage, and *FOXP1* is also able to upregulate the expression of *Blimp1*.<sup>11</sup>

Figure 1. B-cell development and transcription factors



The normal germinal center reaction and antigen-dependent B-cell activation are depicted along with the immunohistochemical profile of the germinal center B-cell, activated B-cell and plasma cell concerning activation-related transcription factors.

Previous immunohistochemical studies of PCLBCL-LT by our group have shown that BCL6 is expressed in more than half of the cases, IRF4 and FOXP1 are virtually always expressed by the tumor cells, and that no substantial expression of Blimp1 is detected.<sup>12</sup> In the context of normal B-cell development, the expression of germinal center protein BCL6 together with post-germinal center activation proteins IRF4 and/or FOXP1 seems aberrant, and also, the absence of Blimp1 expression despite expression of IRF4 and/or FOXP1 is not what is expected (Figure 1). However, knowledge of potential underlying genetic mechanisms for the aberrant immunohistochemical expression of these transcription factors in PCLBCL-LT is limited.

We generated an overview of genetic aberrations of these transcription factors in 10 well-defined cases of PCLBCL-LT, in order to gain more insight into the pathogenesis of the presumed differentiation arrest in malignant B-cells.

## Materials and methods

### Sample collection

Frozen biopsy primary tumor material and formalin fixed and paraffin embedded (FFPE) tumor material of 10 PCLBCL-LT cases was available from the archive of the Leiden University Medical Center (Leiden, The Netherlands). All tissue samples were handled in a coded fashion, according to the Dutch National Ethical guidelines (Code for Proper Secondary Use of Human Tissue, Dutch Federation of Medical Scientific Societies). A diagnosis of PCLBCL-LT was made

according to criteria of the WHO-EORTC<sup>13</sup> and WHO classification,<sup>14</sup> and confirmed by a panel of hematopathologists and dermatologists, aided by several routinely performed immunohistochemical stainings. Cases were only included when frozen biopsy material contained a tumor cell percentage of at least 75%, as assessed by immunohistochemical stainings for CD20 and CD3. In all cases physical examination, total blood count, computed tomography scan, and bone marrow did not show extracutaneous disease at inclusion. Patient characteristics are summarized in Supplemental Table 4.

#### *DNA and RNA isolation and cDNA synthesis*

Genomic DNA was extracted from frozen biopsy specimens using the Genomic-tip 20/G method, according to the protocol supplied by the provider (Qiagen, Hilden, Germany). RNA was isolated from frozen biopsy specimens by the TRIzol method (Life Technologies, Carlsbad, CA, USA). 0.5 µg of total RNA was treated with RQ1 DNase I (Promega, Madison, WI) and reverse-transcribed by use of the iScript cDNA Synthesis kit (Bio-Rad, Veenendaal, The Netherlands).

#### *High-density fine-tiling DNA array*

A custom designed high-density fine-tiling oligonucleotide array with a resolution of 10 kB, oligonucleotide probes of 45-60 bp, and 15 bp median probe spacing was set up for the genomic regions containing *BCL6*, *FOXP1*, *PRDM1*, and *IRF4* and dual specificity protein phosphatase 22 (*DUSP22*) (for details see Supplemental Table 1), according to the human genome, built 19 (February 2009; Human Genome Browser, University of California, Santa Cruz, CA, USA). The array was prepared using Maskless Array Synthesizer Technology (NimbleGen Systems, Reykjavik, Iceland). The mean fluorescence signal intensity was normalized to reference DNA (healthy donor DNA from blood, Promega, Madison, USA) and analyzed using SignalMap software (NimbleGen Systems) in order to detect copy number alteration in the investigated chromosomal regions.

#### *Confirmation of deletions in the FOXP1 gene*

PCR amplification of tumor DNA flanking the regions of *FOXP1* that were deleted as was detected by FT-CGH was performed using forward and reverse primers (listed in Supplemental Table 2) on the C1000 Touch™ Thermal Cycler (Bio-Rad) using a touchdown PCR protocol as previously described.<sup>15</sup> The purified PCR products were subjected to Sanger sequencing both with forward and reverse primers on the ABI 3730 (Applied Biosystems, Foster City, CA). Mutation Surveyor software (SoftGenetic) was used for analysis of single nucleotide alterations.

#### *Mutational analysis of PRDM1*

Individual exons of *PRDM1* (1 to 7) were amplified in separate PCRs (primer pairs listed in Supplemental Table 2, applying the touch down protocol as described elsewhere<sup>15</sup>) using PCLBCL, LT tumor DNA as a template and purified PCR products were sequenced as described above.

### *Ligation-mediated PCR*

DNA losses in *FOXP1* and the *DUSP22* region were analyzed by ligation-mediated PCR (LM-PCR) as described in detail elsewhere.<sup>16</sup> Supplemental Table 3 lists the primers that were used and the different primers combinations are described in the Supplemental Materials and Methods.

### *PRDM1 and DUSP22 gene expression*

mRNA expression of both isoforms of *PRDM1*, i.e. *PRDM1α* en *PRDM1β* was analyzed by quantitative RT-PCR (qPCR) as well as expression of *DUSP22*. Primer efficiencies were 101, 108, and 88%, respectively. *TMEM222*, *ZDHCC5*, and *ARF5* were used as reference gene set.<sup>15</sup> The qPCR reactions were run on cDNA in triplicate with the use of iQ SYBR Green Super-Mix (Bio-Rad) on the CFX384™ Real-Time System (Bio-Rad). The output data were analyzed using Bio-Rad CFX Manager software applying the  $\Delta\Delta Cq$  method. Relative expression was normalized to the determined reference gene set. Cycle parameters for all transcripts analyzed were as follows: denaturing for 15 seconds at 95 °C, and annealing and extension for 20 seconds at 60 °C, for 40 cycles. Specificity of the PCR products was confirmed by melting curve analysis. Primer sequences are listed in Supplemental Table 2.

### *FOXP1 promoter methylation assay*

The methylation assay was performed as previously described.<sup>15</sup> The primers for the *FOXP1* promoter CpG island amplified a 293 bp genomic region near the transcription start site and covering the promoter CpG island of *FOXP1*. 14 CpGs were situated in this amplicon. The presence of methylated DNA in the samples was detected through a peak with a higher melting curve temperature (78,6 °C) as compared to unmethylated DNA (76,6 °C), using bisulfite converted unmethylated human semen DNA and methylated human DNA (Chemicon, Hampshire, UK) as references as described before.<sup>17</sup>

### *FOXP1 (alternative) transcript analysis*

For amplification of *FOXP1* tumor sample cDNA, different primer combinations were developed (see Supplemental Table 2) and PCR was performed as described above.

### *Immunohistochemistry*

Immunohistochemistry for BCL6, *FOXP1* and *IRF4* was performed as previously described.<sup>12</sup>

## **Results**

The B-cell activation-related transcription factors BCL6, *FOXP1*, *PRDM1*/Blimp1 and *IRF4* were investigated in PCLBCL, LT, and an overview of the identified aberrations is given in Table 1.

### *BCL6*

BCL6 immunohistochemistry was considered positive if 30% or more of the tumor cells showed nuclear staining.<sup>18</sup> Eight out of 10 cases were scored positive, and 6 of these cases

showed more than 75% positive tumor cell nuclei. FT-CGH showed no evidence of translocations or amplifications involving *BCL6* that could lead to autonomous upregulation of *BCL6* expression.

Table 1. Overview of transcription factor alterations

	<b>BCL6</b>		<b>FOXP1<sup>a</sup></b>		<b>PRDM1<sup>a</sup></b>			<b>IRF4 – DUSP22</b>	
	IHC <sup>b</sup>	FT-array <sup>c</sup>	FT-array <sup>c</sup>	Pathogenic isoforms	FT-array <sup>c</sup>	Mutation	PRDM1 $\alpha$ qPCR <sup>d</sup>	PRDM1 $\beta$ qPCR <sup>d</sup>	FT-array <sup>c</sup>
1	pos	+/+	+/+	isoform 3	+/+	no	0,01	0,31	+/- (loss between genes)
2	pos	+/+	+/+	no	+/+	N/A	0,03	1,00	+/+
3	pos	+/+	+/+	no	+/-	no	2,41	0,12	+/- (loss between genes)
4	neg	+/+	+/- (del ex 4, 5, 6, 7)	isoform 3	+/-	no	3,02	0,16	+/+
5	pos	+/+	+/- (del ex 5, 6, 7)	no	+/-	no	2,44	0,16	+/+
6	pos	+/+	+/+	no	+/+	no	N/A	N/A	+/+
7	pos	+/+	+/- (del ex 3)	no	+/+	ex 4 c.843 C>G (D607E)	3,07	0,22	ampl DUSP22
8	pos	+/+	+/+	isoform 3	+/+	no	0,64	0,07	+/+
9	pos	+/+	+/+	isoform 3	+/-	N/A	16,82	0,05	ampl DUSP22
10	neg	+/+	+/+	isoform 3, isoform 9	+/-	ex 7 c.2376 G>A (silent)	0,69	0,08	+/- (loss part of DUSP22)

a All 10 cases showed immunohistochemical positivity for both FOXP1 and IRF4; b pos = positive; neg = negative; c FT-array = high density DNA fine-tiling array; +/+ = no alteration; +/- = heterozygous DNA loss; ampl = amplification; del = deletion; ex = exon; d  $\Delta\Delta Cq$  relative to set of reference genes.

### FOXP1

FOXP1 immunohistochemistry showed strong nuclear expression in over 90% of tumor cells in all 10 cases. By FT-CGH, there was no evidence of amplification of the FOXP1 gene, as a potential explanation for (autonomous) upregulation of FOXP1. Instead, heterozygous DNA loss of part of the *FOXP1* gene was encountered in 3 out of 10 cases (see Figure 2). As these deletions might be part of a translocation/rearrangement, which could also potentially lead to upregulation of FOXP1, further exploration by LM-PCR was performed. However, no linkage of the regions flanking these DNA losses to other parts of the genome was detected. Therefore, most likely, the DNA loss represents a heterozygous deletion rather than a break involved in a translocation/rearrangement. The presence of these deletions was confirmed by PCR amplification and subsequent sequencing on tumor DNA of the three involved cases. All break points were situated in introns, thereby deleting complete exons. Case 4 showed heterozygous DNA loss comprising exon 4 to 7 (exon 4 and 5 non-coding, exon 6 and 7 coding). In case 5 there was DNA loss in exon 5 to 7, and between the rearranged fragments a DNA fragment was inserted containing 6 nucleotides of unknown origin and a 402 bp fragment of a repetitive sequence derived from the deleted region. In case 7, the DNA

loss was encountered in exon 3 (non-coding), with 2 homologous nucleotides inserted at the rearrangement site. To investigate whether the DNA strand with these deletions was actually transcribed in these tumors, RNA transcript analysis by PCR using primers located in exon 2 and exon 8, flanking the deleted regions, with sequencing of the product was performed. In two of the three cases showing a deletion in *FOXP1*, an RNA transcript with concordant deletions was encountered, next to normal length transcripts. The promoter methylation assay showed no evidence of hypermethylation of the promoter island of *FOXP1* that could explain the absence of a shorter transcript in the remaining case without a concomitant aberrant transcript. Exploring additional alternative transcripts of *FOXP1*, previously reported alternative N-truncated protein coding transcripts with presumed oncogenic potential (isoform 3 and 9)<sup>19</sup> were detected in 5 cases and 1 case, respectively.

### *PRDM1*

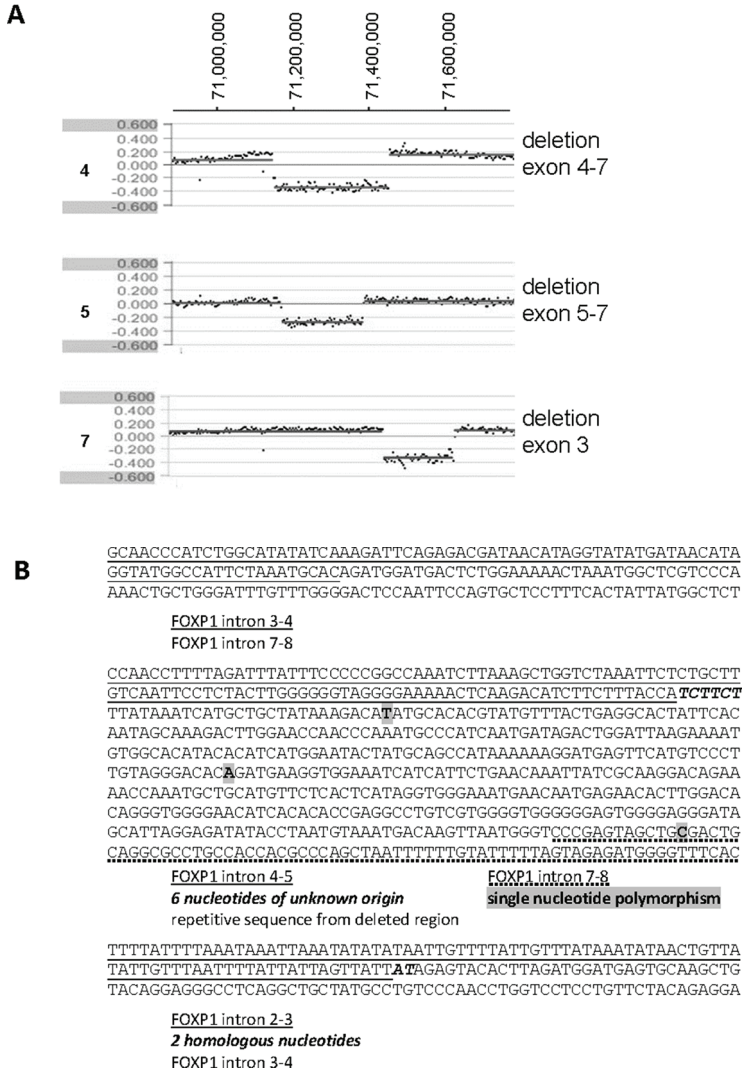
Blimp1 immunohistochemistry was not performed, as previous studies by our group already showed complete absence of nuclear staining for this protein in all cases of PCLBCL-LT.<sup>12</sup> The complete DNA region of *PRDM1* covered by the FT-CGH experiment, showed heterozygous DNA loss in 5 out of 10 cases, but no homozygous loss was detected that would be explanatory for the absence of Blimp1 protein. In order to search for other genetic alterations explaining altered or diminished gene transcription, PCR amplification and subsequent sequencing of all exons of *PRDM1* was performed. Only one missense mutation was detected, concerning a c.843 C>G (D607E) mutation in exon 4 in case 7. However, as this case had two alleles of the *PRDM1* gene present by FT-CGH, and the mutation was heterozygous, no evidence for absence of the Blimp1 protein by genetic inactivation was detected. Of note, one additional mutation was found in case 10 (exon 7, c.2376 G>A), this however concerned a silent mutation. Next, we explored whether the absence of the Blimp1 protein was reflected by RNA levels and whether RNA levels were lower in cases with heterozygous deletions or mutations in *PRDM1*. qPCR for *PRDM1α*, the full-length transcript of *PRDM1*, detected this transcript in all cases, and showed substantially varying amounts of mRNA, irrespective of heterozygous DNA loss or missense mutation. As the *PRDM1* gene has an alternative transcript lacking the PR domain, *PRDM1β*, which has a possible oncogenic potential,<sup>20</sup> we also explored this transcript by qPCR. Again, amounts varied and were not related to other aberrations in the gene. Except for case 1 and 2, *PRDM1β* levels were lower than levels of *PRDM1α* and very low relative to the expression of the reference genes (see Table 1).

### *IRF4 – DUSP22*

*IRF4* immunohistochemistry was strongly positive in all ten cases. The *IRF4* gene showed no gains by FT-CGH as a sign of (autonomous) upregulation of the gene, and losses as part of a translocation were also not encountered in the *IRF4* gene. In the region just upstream of *IRF4*, heterozygous DNA loss or DNA gain was observed in part in the region harboring the *DUSP22* locus. In anaplastic large cell lymphoma, a translocation between *DUSP22* and *FRAH7* on chromosome 7 was recently described.<sup>21</sup> However, in our cases LM-PCR of the region flanking the deletions did not show linkage of this DNA region to another DNA region, and therefore there was no evidence that these deletions were involved in a translocation/rearrangement. Furthermore, by performing qPCR analysis, the cases with deletion and/or amplification of *DUSP22* did not show differences in mRNA expression levels compared to the cases without

these genetic alterations. Thereby, the biological significance of these genetic alterations in PCLBCL-LT remains unknown.

Figure 2. High-density DNA fine-tiling array chromosome 3



(A) The FOXP1 gene locus on chromosome 3 (71,003,865 – 71,633,140) is depicted. The X-axis represents the chromosomal position of the probes, while the y-axis represents the log<sub>2</sub>-ratio of the read numbers per probe relative to control DNA. DNA losses between -0.200 and -0.400 are considered heterozygous losses. (B) Sequences of the break points in FOXP1 as assessed by PCR on tumor DNA are represented. While in case 4, there was a direct link between intron 3-4 and intron 7-8, case 5 and 7 showed insertions between the break points detected by FT-CGH analysis. In case 5, 6 nucleotides of unknown origin and a 402 base pair repetitive sequence from the deleted region were inserted. In case 7, 2 homologous nucleotides were inserted.

5



## Discussion

This study investigated genomic alterations in B-cell activation-related transcription factors in PCLBCL-LT. With 8 out of 10 cases showing high levels of the germinal center protein BCL6 by immunohistochemistry, it is remarkable that the same cases also have high protein levels of FOXP1 and IRF4, which are normally downregulated by BCL6, and show absence of Blimp1 protein, which is upregulated by FOXP1 and IRF4 in a physiological situation (see Figure 1). We could not find evidence that BCL6, FOXP1 and/or IRF4 have an autonomous way of protein upregulation, as we did not encounter translocations or amplifications involving these genes. Moreover, the absence of Blimp1 protein by immunohistochemistry in PCLBCL-LT could not be explained by genetic silencing through homozygous deletion of the gene, or heterozygous deletion with concomitant missense or nonsense mutations. These alterations actually have been described in ABC-DLBCL, the nodal counterpart of PCLBCL-LT. Especially genetic inactivation of PRDM1 is frequently detected in ABC-DLBCL, occurring in approximately one-third of cases.<sup>4,6</sup> Translocations involving *IRF4* have only sporadically been described in nodal ABC-DLBCL<sup>7</sup> and translocations involving *FOXP1* are also infrequent, but might preferentially be detected in extranodal DLBCL.<sup>8</sup>

Blimp1 immunohistochemistry was previously reported to be consistently negative in PCLBCL-LT<sup>12</sup> using the purified recombinant GST fusion protein encoding N-terminal amino acids 1-347 of human BLIMP1 antibody (clone BUR162<sup>12</sup>), covering exons 2 to 5. The proteins of both *PRDM1α*, the full-length transcript (containing exon 1-7), and *PRDM1β*, the alternative transcript (containing exon 1β and exon 4-7),<sup>20</sup> should be detected by this polyclonal antibody. Unexpectedly the lack of detectable protein was not reflected by absence or very low levels of both transcripts. Blimp1 downregulation might therefore be an epigenetic phenomenon. For example, microRNA let-7 might play a role in nodal ABC-type DLBCL by negatively regulating Blimp1 expression at a posttranscriptional level.<sup>22</sup> For *IRF4*, our results are concordant with previous FISH studies in PCLBCL-LT, in which this type of lymphoma has been reported to have immunohistochemical (over)expression of IRF4 without gene rearrangements.<sup>23</sup> Alternatively, as IRF4 is a target gene of the nuclear factor (NF)-κB signaling pathway,<sup>24</sup> upregulation of IRF4 might be related to constitutive activation of the NF-κB pathway. Indeed in 70% of PCLBCL-LT, genetic aberrations in NF-κB-activating genes were encountered that might lead to aberrant pathway activation.<sup>15</sup> No FOXP1 translocations have previously been reported in PCLBCL-LT,<sup>25</sup> which is in line with our results. However, amplification of FOXP1 as detected by fluorescent in situ hybridization was detected in 82% of PCLBCL-LT,<sup>25</sup> while this was not present in any case of our cohort using the very sensitive FT-CGH method. No genetic mechanism underlying consistent upregulation of FOXP1 has been detected, but our study revealed that high protein levels of FOXP1 reflect more than merely the presence of the full-length isoform of FOXP1. As the commonly used JC12 antibody binds in the C-terminal region of the protein, various N-truncated proteins will also be detected by this antibody. Next to the full-length transcript of *FOXP1*, in some of our cases we encountered *FOXP1* isoforms 3 and 9. Furthermore, we detected not previously described N-truncated isoforms, based on small DNA deletions in the *FOXP1* gene. *FOXP1* isoform 3 and 9 were suggested to have oncogenic potential in nodal ABC-DLBCL,<sup>19</sup> which might be due to the related increased expression of NF-κB associated genes, as was reported for nodal follicular lymphomas.<sup>26</sup> FOXP1 has furthermore been implicated in class switch recombination (CSR). PCLBCL-LT characteristically shows intracytoplasmic expression of IgM, in part combined with IgD, which might imply a defect in CSR.<sup>27</sup> Although the exact mechanism behind the absence of CSR is not completely understood, in nodal ABC-DLBCL and primary central nervous system DLBCL it has been suggested

to be caused by mutations in the switch regions of the constant chain.<sup>28,29</sup> In a recent report, constitutional expression of FOXP1 led to impairment of switching from IgM to IgG1. It can be speculated that FOXP1 might therefore also play a factor in the absence of CSR in PCLBCL-LT, leading to a differentiation arrest in the post-germinal center state.

In summary, high protein levels of transcription factors BCL6, IRF4 and FOXP1 in PCLBCL-LT do not seem to be related to autonomous upregulation due to amplification or translocations involving the genes. However, the high protein levels of FOXP1 represent proteins from a variety of *FOXP1* transcripts, some not previously described, and others with a presumed oncogenic potential. Although protein levels of Blimp1 are undetectable by immunohistochemistry, mRNA levels of *PRDM1* (both *PRDM1a* and *PRDM1b*) varied substantially between the cases, and seemed to be unrelated to heterozygous deletions and/or mutations encountered in the gene.

## References

1. Senff NJ, Noordijk EM, Kim YH, et al. (2008) European Organization for Research and Treatment of Cancer and International Society for Cutaneous Lymphoma consensus recommendations for the management of cutaneous B-cell lymphomas. *Blood* 112: 1600-9.
2. Alizadeh AA, Eisen MB, Davis RE, et al. (2000) Distinct types of diffuse large B-cell lymphoma identified by gene expression profiling. *Nature* 403: 503-11.
3. Hoefnagel JJ, Dijkman R, Basso K, et al. (2005) Distinct types of primary cutaneous large B-cell lymphoma identified by gene expression profiling. *Blood* 105: 3671-8.
4. Mandelbaum J, Bhagat G, Tang H, et al. (2010) BLIMP1 is a tumor suppressor gene frequently disrupted in activated B cell-like diffuse large B cell lymphoma. *Cancer Cell* 18: 568-79.
5. Ye BH, Chaganti S, Chang CC, et al. (1995) Chromosomal translocations cause deregulated BCL6 expression by promoter substitution in B cell lymphoma. *EMBO J* 14: 6209-17.
6. Pasqualucci L, Compagno M, Houldsworth J, et al. (2006) Inactivation of the PRDM1/BLIMP1 gene in diffuse large B cell lymphoma. *J Exp Med* 203: 311-7.
7. Salaverria I, Philipp C, Oschlies I, et al. (2011) Translocations activating IRF4 identify a subtype of germinal center-derived B-cell lymphoma affecting predominantly children and young adults. *Blood* 118: 139-47.
8. Goatly A, Bacon CM, Nakamura S, et al. (2008) FOXP1 abnormalities in lymphoma: translocation breakpoint mapping reveals insights into deregulated transcriptional control. *Mod Pathol* 21: 902-11.
9. Shaffer AL, Yu X, He Y, et al. (2000) BCL-6 represses genes that function in lymphocyte differentiation, inflammation, and cell cycle control. *Immunity* 13: 199-212.
10. Sciammas R, Davis MM. (2004) Modular nature of Blimp-1 in the regulation of gene expression during B cell maturation. *J Immunol* 172: 5427-40.
11. Sagardoy A, Martinez-Ferrandis JI, Roa S, et al. (2013) Downregulation of FOXP1 is required during germinal center B-cell function. *Blood* 121: 4311-20.
12. Hoefnagel JJ, Mulder MM, Dreef E, et al. (2006) Expression of B-cell transcription factors in primary cutaneous B-cell lymphoma. *Mod Pathol* 19: 1270-6.
13. Willemze R, Jaffe ES, Burg G, et al. (2005) WHO-EORTC classification for cutaneous lymphomas. *Blood* 105: 3768-85.
14. Meijer CJLM, Vergier B, Duncan LM, et al. (2008) Primary cutaneous DLBCL, leg type. In: Swerdlow SH, Campo E, Harris NL, et al., eds. WHO classification of tumours of haematopoietic and lymphoid tissues. Lyon: IARC Press 242.
15. Koens L, Zoutman WH, Ngarmleertsirichai P, et al. (2014) Nuclear Factor-kappaB Pathway-Activating Gene Aberrancies in Primary Cutaneous Large B-Cell Lymphoma, Leg Type. *J Invest Dermatol* 134: 290-2.
16. Przybylski GK, Dik WA, Wanzeck J, et al. (2005) Disruption of the BCL11B gene through inv(14)(q11.2q32.31) results in the expression of BCL11B-TRDC fusion transcripts and is associated with the absence of wild-type BCL11B transcripts in T-ALL. *Leukemia* 19: 201-8.
17. van Kester MS, Borg MK, Zoutman WH, et al. (2012) A meta-analysis of gene expression data identifies a molecular signature characteristic for tumor-stage mycosis fungoides. *J Invest Dermatol* 132: 2050-9.
18. Hans CP, Weisenburger DD, Greiner TC, et al. (2004) Confirmation of the molecular classification of diffuse large B-cell lymphoma by immunohistochemistry using a tissue microarray. *Blood* 103: 275-82.
19. Brown PJ, Ashe SL, Leich E, et al. (2008) Potentially oncogenic B-cell activation-induced smaller isoforms of FOXP1 are highly expressed in the activated B cell-like subtype of DLBCL. *Blood* 111: 2816-24.

20. Gyory I, Fejer G, Ghosh N, et al. (2003) Identification of a functionally impaired positive regulatory domain 1 binding factor 1 transcription repressor in myeloma cell lines. *J Immunol* 170: 3125-33.
21. Feldman AL, Dogan A, Smith DI, et al. (2011) Discovery of recurrent t(6;7)(p25.3;q32.3) translocations in ALK-negative anaplastic large cell lymphomas by massively parallel genomic sequencing. *Blood* 117: 915-9.
22. Nie K, Zhang T, Allawi H, et al. (2010) Epigenetic down-regulation of the tumor suppressor gene PRDM1/Blimp-1 in diffuse large B cell lymphomas: a potential role of the microRNA let-7. *Am J Pathol* 177: 1470-9.
23. Pham-Ledard A, Prochazkova-Carlotti M, Vergier B, et al. (2010) IRF4 expression without IRF4 rearrangement is a general feature of primary cutaneous diffuse large B-cell lymphoma, leg type. *J Invest Dermatol* 130: 1470-2.
24. Davis RE, Brown KD, Siebenlist U, et al. (2001) Constitutive nuclear factor kappaB activity is required for survival of activated B cell-like diffuse large B cell lymphoma cells. *J Exp Med* 194: 1861-74.
25. Espinet B, Garcia-Herrera A, Gallardo F, et al. (2011) FOXP1 molecular cytogenetics and protein expression analyses in primary cutaneous large B cell lymphoma, leg-type. *Histol Histopathol* 26: 213-21.
26. Green MR, Gandhi MK, Courtney MJ, et al. (2009) Relative abundance of full-length and truncated FOXP1 isoforms is associated with differential NFkappaB activity in Follicular Lymphoma. *Leukemia Res* 33: 1699-1702.
27. Koens L, Vermeer MH, Willemze R, et al. (2010) IgM expression on paraffin sections distinguishes primary cutaneous large B-cell lymphoma, leg type from primary cutaneous follicle center lymphoma. *Am J Surg Pathol* 34: 1043-8.
28. Lenz G, Nagel I, Siebert R, et al. (2007) Aberrant immunoglobulin class switch recombination and switch translocations in activated B cell-like diffuse large B cell lymphoma. *J Exp Med* 204: 633-43.
29. Montesinos-Rongen M, Schmitz R, Courts C, et al. (2005) Absence of immunoglobulin class switch in primary lymphomas of the central nervous system. *Am J Pathol* 166: 1773-9.

## Supplemental Materials and Methods

Primer combinations used in each DNA sample to characterize *FOXP1* deletions  
For details of the primers see Supplemental Table 3.

Sample 4: deleted sequence (303,819 bp involving exon 4-7); dna range=chr3:71140032-71443850.

### LM-PCR

upstream            1<sup>st</sup> PCR    3:71,139,678f + AP1  
                          2<sup>nd</sup> PCR    3:71,139,722f + AP2  
  
downstream        1<sup>st</sup> PCR    3:71,444,688r + AP1  
                          2<sup>nd</sup> PCR    3:71,444,606r + AP2

### confirmation PCR

3:71,139,678f + 3:71,444,688r        (1192 bp)

Sample 5: deleted sequence (217,427 bp involving exon 5-7); dna range=chr3:71,159,133-71,376,559; inserted sequence (402 bp involving intron 4-5); dna range=chr3:71,373,433-71,373,834

### LM-PCR

upstream            1<sup>st</sup> PCR    3:71,158,005f + AP1  
                          2<sup>nd</sup> PCR    3:71,158,509f + AP2  
  
downstream        1<sup>st</sup> PCR    3:71,377,299r + AP1  
                          2<sup>nd</sup> PCR    3:71,377,262r + AP2

### confirmation PCR

3:71,158,005f + 3:71,377,299r        (2169 bp)

Sample 7: deleted sequence (189,514 bp involving exon 3); dna range=chr3:71427920-71617433

### LM-PCR

upstream            1<sup>st</sup> PCR    3:71,427,220f + AP1  
                          2<sup>nd</sup> PCR    3:71,427,491f + AP2  
  
downstream        1<sup>st</sup> PCR    3:71,618,367r + AP1  
                          2<sup>nd</sup> PCR    3:71,618,274r + AP2

### confirmation PCR

3:71,427,220f + 3:71,618,367r        (1632 bp)

Supplemental Table 1. Coverage high-density DNA fine-tiling array

	<b>Position</b>	<b>Array coverage</b>
<i>FOXP1</i>	chr3: 71,004,737-71,633,140	chr3: 70,300-72,300
<i>BCL6</i>	chr3: 187,439,165-187,463,475	chr3: 186,400-188,400
<i>IRF4 – DUSP22</i>	chr6: 391,752-411,442	chr6: 0-2000
<i>PRDM1</i>	chr6: 106,534,195-106,557,814	chr6: 104,800-107,800

chr = chromosome.

Supplemental Table 2. Primer sets for polymerase chain reactions

Gene	Forward primer (5' – 3')	Reverse primer (5' – 3')	Product
<i>FOXP1</i>			
- ex 4-7 DNA	TATAATCCATGCTCCCTTCCCAAC	GATGAGGTACCCAGGTAAGGCTTCTC	1192 bp
- ex 5-7 DNA	GAAGCAGGGTGTATCTTCAACAG	GCCAAATCTTCTGCCTCCTTTAATGT	2169 bp
- ex 3 DNA	GAAAAGGGAATCAATACAGGCCAAGA	CCTTCATACCCCTATTTCTGCCATTA	1632 bp
- ex 16-21 cDNA	AACGAGAAGTTAGACCACCA	GAGGGCTCTCTTTTGAGG	540 bp
- ex 2-8 cDNA (1)	CTACTCCCTCCCGGACTC	AGCACTTGTCTGGAGGAT	682 bp
- ex 2-8 cDNA (2)	TACTCCCTCCCGGACTC	CTGGAGGATCTGCTGCATTT	672 bp
- ex 6-10 cDNA isoform 1/3	GTCGGGGGAGCAACCACCTTACTAG	AAGGCCTTGGCGCTGCAAAAGACAGGA	isoform 1: 556 bp isoform 3: 328 bp
- ex 7c-11 cDNA isoform 8/9	GTAGCTAACTCAACTGTCAGAACTGC	AGGAGACACATGTCGTGGTCAGATCC	isoform 8: 271 bp isoform 9: 535 bp
- CpG island MS-MCA	ATTTGTTGTGAGTTTYGTTTTGGTTT	CCTTCCCCAAAATCTCACAAAATTAC	293 bp
<i>PRDM1</i>			
- ex 1 DNA	AGCCGAGTGGCTAAGGAAAT	ACTGCGACATTAGCCCAAAA	416 bp
- ex 2 DNA	CTCTCAGAAAGGAGCCACAGG	GGTCCCAATCTTCTTGTC	355 bp
- ex 3 DNA	TCAAAGTAATGTTTCCCTGTGTTTT	CCCAGCTTTTTAGCTCCATT	221 bp
- ex 4 DNA	GGGAGCTTTGGGTCTGACTT	GGCAGAAACCGACATTAATGCG	359 bp
- ex 5 DNA (1)	TGTGTAATGCGCCCTTTTTTC	GTTGTTGATGCCATTCATGC	674 bp
- ex 5 DNA (2)	ACAACGCTCACTACCCCAAG	CCCTTGGACTGCTCTCTCTC	586 bp
- ex 6 DNA	GAGCCAGCTTGAGAGCAGAG	ATGGGAGGTTGACTCACAGA	239 bp
- ex 7 DNA	CCTGCTCTCTCTCCCTTA	TCCTACAGGCCCTTGACTC	669 bp
- <i>PRDM1α</i> cDNA RT-PCR	TTTGCTTGAAAAACGTGTG	ATTTTCATGGTCCCTTTGGT	106 bp
- <i>PRDM1β</i> cDNA RT-PCR	CCCGAACATGAAAAAGACGAT	TTCTCTTCATTAAAAGCCGTCAA	91 bp
<i>DUSP22</i>			
- cDNA RT-PCR	TAGTGCCAGGCCTATGTTGG	TTTCTTTGAAATGCTTGTGCAGG	92 bp

Supplemental Table 3. List of *FOXP1* Primers (5' -3') for LM-PCR and PCR

Primer	Sequence (5' - 3')	Location
Adaptor-specific		
- AP1	GTAATACGACTCACTATAGGGC	
- AP2	ACTATAGGGCACGCGTGGT	
Forward gene-specific		
- 3:71,427,220f	GAAAAGGGAATCAATACAGGCCAAGA	intron 3-4
- 3:71,427,491f	CTGTTATCCACGGGTTGTGCTTTC	intron 3-4
- 3:71,139,678f	TATAATCCATGCTTCCCTCCCAAC	intron 7-8
- 3:71,139,722f	TGAGCATACTCCCTGATCTTCTTTC	intron 7-8
- 3:71,158,005f	GAAGGCAGGGTGTGTATCTTCAACAG	intron 7-8
- 3:71,158,509f	CCAAACATAAAGCAGGGAAGTGTGAG	intron 7-8
Reverse gene-specific		
- 3:71,618,274r	TGGAGCATGTATTAGGGATGAAGTGA	intron 2-3
- 3:71,618,367r	CCTTCATACCCCTATTCTGCCATTA	intron 2-3
- 3:71,444,606r	AGCTTGGAAGAGAAGCATTCCAGACT	intron 3-4
- 3:71,444,688r	GATGAGGTACCCAGGTAAGGCTTCTC	intron 3-4
- 3:71,377,262r	ACACCCAGTCTTTTCAGCTTATCACG	intron 4-5
- 3:71,377,299r	GCCAAATCTTCTGCCTCTTAAATGT	intron 4-5

Supplemental Table 4. Patient characteristics

	Sex	Age (years)	Skin site of primary tumor	Initial therapy	Disease recurrence	PFS (months)	FU (months)	Current status
1	male	84	legs + other	RT	yes	1	24	D <sup>+</sup>
2	female	75	both legs	PCT + RT	yes	12	54	D <sup>+</sup>
3	female	79	leg	RT	no	20	21	A <sup>0</sup>
4	female	81	leg	PCT + RT	yes	20	39	D <sup>+</sup>
5	male	81	leg	none	no	0	2	D <sup>+</sup>
6	male	53	legs + other	PCT	yes	6	96	A <sup>+</sup>
7	male	68	leg	PCT	yes	17	60	D <sup>+</sup>
8	female	83	leg	PCT + RT	yes	34	38	D <sup>+</sup>
9	male	83	leg	RT	no	49	50	A <sup>0</sup>
10	female	76	leg	RT	no	0	13	D <sup>+</sup>

PFS = progression free survival; FU = follow-up; RT = radiotherapy; PCT = polychemotherapy; D<sup>+</sup> = died of disease; A<sup>0</sup> = alive without disease.







**Methotrexate-associated B-cell  
lymphoproliferative disorders presenting  
in the skin: a clinicopathologic and  
immunophenotypical study of ten cases**

*The American Journal of Surgical Pathology* 2014;  
38(7): 999-1006

Lianne Koens<sup>1</sup>

Nancy J. Senff<sup>2,3</sup>

Maarten H. Vermeer<sup>2</sup>

Rein Willemze<sup>2</sup>

Patty M. Jansen<sup>1</sup>

Departments of <sup>1</sup>Pathology and <sup>2</sup>Dermatology, Leiden University  
Medical Center, Leiden, The Netherlands

<sup>3</sup>Department of Dermatology, Saint Lucas Andreas Hospital,  
Amsterdam, The Netherlands



## Abstract

*Methotrexate (MTX)-associated B-cell lymphoproliferative disorders (B-LPD) may first present in the skin, but their clinicopathologic features are still ill defined. Differentiation from primary cutaneous follicle center lymphoma (PCFCL) and primary cutaneous diffuse large B-cell lymphoma, leg type (PCLBCL-LT) is important, as MTX-associated B-LPD may show spontaneous regression after withdrawal of MTX therapy. In the present study, the clinicopathologic and phenotypical features of 10 patients with MTX-associated B-LPD first presenting in the skin, including 5 EBV<sup>+</sup> and 5 EBV<sup>-</sup> cases, were investigated. Six patients had skin-limited disease. Clinically, abrogation of MTX therapy resulted in a complete response in 4 cases and a partial response in another 2. The 5-year disease-specific survival was 90%. MTX-associated B-LPD differed from PCFCL by the presence of ulcerating and/or generalized skin lesions, an infiltrate composed of centroblasts/immunoblasts rather than large centrocytes, reduced staining for CD79a, and expression of BCL2, IRF4, and FOXP1 in most cases. EBV<sup>+</sup> MTX-associated B-LPD differed from PCLBCL-LT by the presence ulcerative skin lesions, marked tumor cell polymorphism, reduced staining for CD79a, and expression of CD30 and EBV. EBV cases showed morphologic and immunophenotypical similarities to PCLBCL-LT, but differed by presentation with generalized skin lesions in 4 of 5 cases. The results of this study, showing a relatively good clinical outcome and spontaneous disease regression after only withdrawal of MTX in a considerable proportion of patients, underscores the importance of a careful wait-and-see policy before considering more aggressive therapies in patients with MTX-associated B-LPD of the skin.*

## Introduction

In recent years, the incidence and awareness of immunosuppression-related malignancies including non-Hodgkin lymphomas (NHLs) has increased. The immunosuppressive state leading to these NHLs might be caused by primary immune disorders, human immunodeficiency virus infections, or might be iatrogenic by the use of immunosuppressive agents.<sup>1</sup> The increased chronic use of immunosuppressive drugs for autoimmune diseases is indeed associated with higher incidence of NHL, especially of B-cell origin.<sup>2</sup> Although the immunosuppressive drug methotrexate (MTX) was first reported to be effective in patients with rheumatoid arthritis and psoriasis in 1951,<sup>3</sup> MTX-associated B-cell lymphoproliferative disorders (B-LPD) were not described until 1985.<sup>4</sup> Since that time, many reports of MTX-associated NHL have been published, particularly in patients with rheumatoid arthritis. Most of these lymphomas were B-cell NHL, mainly diffuse large B-cell lymphomas (DLBCL), both Epstein Barr virus (EBV) related and unrelated.<sup>2</sup> Of interest, there are several reports of spontaneous regression of these lymphomas after withdrawal of MTX, underlining the potential pathogenetic role of MTX in these lymphomas.<sup>5</sup>

Reports of MTX-associated B-LPD presenting in the skin and in particular those presenting with only skin lesions are limited.<sup>6-10</sup> MTX-associated B-LPD presenting in the skin should be differentiated from primary cutaneous follicle center lymphoma (PCFCL) with a diffuse growth pattern, from primary cutaneous large B-cell lymphoma, leg type (PCLBCL-LT), and from secondary cutaneous manifestation of a primary nodal DLBCL or high grade follicular lymphoma. The differential diagnosis furthermore comprises EBV<sup>+</sup> DLBCL of the elderly and lymphomatoid granulomatosis. PCFCL characteristically presents with localized skin lesions on the trunk or on the face, most commonly the scalp, are highly responsive to local radiotherapy, and have an excellent prognosis.<sup>11,12</sup> PCLBCL-LT characteristically present with

skin tumors on the (lower) legs in elderly females, run a much more aggressive course than PCFCL, and should be treated primarily with systemic chemotherapy in combination with rituximab (R-CHOP).<sup>11,12</sup> R-CHOP is also the first choice of treatment in patients with nodal DLBCL or high-grade follicular lymphoma secondarily involving the skin.<sup>12-14</sup> In contrast, in MTX-associated B-LPD the effect of cessation of MTX should first be awaited, before more aggressive therapies are considered. Differentiation between these different entities is therefore extremely important but may be very difficult, particularly if relevant clinical data are not provided.

In the present study we reviewed the clinical, histologic, and immunophenotypic data of 10 patients with an MTX-associated B-LPD first presenting in the skin. The aim of this study was to find out if these MTX-associated B-LPDs show characteristic clinicopathologic features that allow their recognition, even in the absence of adequate clinical data, and may be used in the differentiation from other DLBCL presenting in the skin.

**Table 1.** Immunohistochemistry details

<b>Antibody</b>	<b>Clone</b>	<b>Company</b>	<b>AR</b>	<b>Dilution</b>	<b>Chromogen</b>
CD20	L26	DAKO, Glostrup, Denmark	EDTA	1:400	DAB
CD79a	JCB117	DAKO	EDTA	1:50	DAB
CD3	F7.2.38	DAKO	EDTA	1:100	DAB
BCL2	124	DAKO	EDTA	1:25	DAB
BCL6	PG-B6p	DAKO	EDTA	1:40	DAB
CD10	56C6	DAKO	EDTA	1:40	DAB
CD35	BERMACD	DAKO	citrate	1:10	DAB
IRF4/MUM1	MUM1p	DAKO	EDTA	1:200	DAB
FOXP1	JC12	kind gift of dr. A.H. Banham*	citrate	1:400	DAB
MYC	Y69	Abcam, Cambridge, UK	EDTA	1:100	DAB
heavy chains	NA	DAKO	citrate	1:4000- 1:8000	DAB+
light chains	NA	DAKO	citrate	1:16000	DAB+
CD30	BerH2	DAKO	citrate	1:100	DAB
CD15	Carb-3	DAKO	EDTA	1:400	DAB
LMP1	CS1-4	DAKO	EDTA	1:40	DAB

\* Nuffield Department of Clinical Laboratory Sciences, John Radcliffe Hospital, Oxford, UK.

AR: antigen retrieval; DAB: 3,3'-diaminobenzidine; DAB+: 3,3'-diaminobenzidine with enhancer; EDTA: ethylenediaminetetraacetic acid; NA: not applicable.

## Materials and Methods

Formalin fixed and paraffin embedded skin biopsies of 10 patients with an MTX-associated B-LPD were collected from the archive of the Dutch Cutaneous Lymphomas Working Group. In all patients adequate staging procedures had been performed, which included complete physical examination, total blood count, bone marrow biopsy, and computed tomography scans. The diagnosis had been confirmed by a panel of dermatologists and hematopathologists during one of the quarterly meetings of the Working Group. Details of the immunohistochemical staining procedures are presented in Table 1. Immunohistochemical staining was considered positive if  $\geq 30\%$  of the tumor cells showed staining with the specific antibody

for BCL2, BCL6, CD10, IRF4/MUM1, and FOXP1<sup>15</sup> or  $\geq 40\%$  for MYC.<sup>16</sup> CD30 was either scored positive or negative depending on whether all tumor cells showed or did not show staining for this marker. In situ hybridization for EBV-encoded RNA expression was assessed by hybridization on slides using a fluorescein-conjugated EBER PNA probe (Y5200, Dako, Glostrup, Denmark) and scored positive in the case of any nuclear staining in atypical large lymphoid cells. DNA was extracted from formalin-fixed and paraffin-embedded sections using standard protocols, and clonal rearrangements of the IGH and IGK locus were detected by polymerase chain reaction using Identiclon IGH and IGK gene clonality assays (InVivoScribe Technology, Carlsbad, CA).<sup>17</sup> The potential rearrangements were interpreted in conjunction with a polyclonal, monoclonal and blank control.

After the interpretation of MYC immunohistochemistry in the above-described cases, comparison of these results with cases of PCFCL and PCLBCL-LT seemed warranted. As the MYC immunohistochemistry in these lymphomas has not been performed before, we selected 6 cases of PCFCL and 10 cases of PCLBCL-LT from the archive of the Dutch Cutaneous Lymphomas Working Group and performed MYC immunohistochemistry as described in Table 1. All tissue samples were handled in a coded fashion, according to the Dutch National Ethical guidelines (Code for Proper Secondary Use of Human Tissue, Dutch Federation of Medical Scientific Societies).

## Results

### *Clinical characteristics*

The clinical patient characteristics, categorized as EBV<sup>+</sup> or EBV<sup>-</sup> as assessed by RNA in situ hybridization, are represented in Figure 1 and Table 2. The study group included 6 females and 4 males. The median age of presentation was 76 years (range, 57 to 88 y), and the median time of MTX treatment was 4 years (range, 1 to 8 y). Five patients had generalized skin lesions at presentation, 3 patients presented with multiple skin lesions on 1 leg, whereas 2 patients had presented with a solitary lesion. Ulceration was observed in 3 patients, all of them being EBV<sup>+</sup>. Staging procedures revealed extracutaneous localizations in 4 of 10 patients, whereas the remaining 6 patients had skin-limited disease. In all 10 patients MTX treatment was discontinued, which resulted in complete resolution of the cutaneous and nodal localizations in 4 of them (cases 4, 5, 6 and 8). In 2 other patients radiation therapy of residual skin lesions (cases 9 and 10) also resulted in a complete response. Initial treatment with systemic polychemotherapy (CHOP or R-CHOP) resulted in a complete response in 3 of 4 patients (cases 1, 2 and 7), whereas 1 patient (case 3) died of cardiac failure during R-CHOP treatment. During follow-up, 1 patient (case 10), developed extensive nodal involvement, which was successfully treated with R-CHOP. After a median follow-up of 24 months (range, 6 to 86 mo) 7 patients are in complete remission, only 1 died of lymphoma, whereas 2 patients died of unrelated disease. Five year disease-specific survival was 90%.

### *Histology*

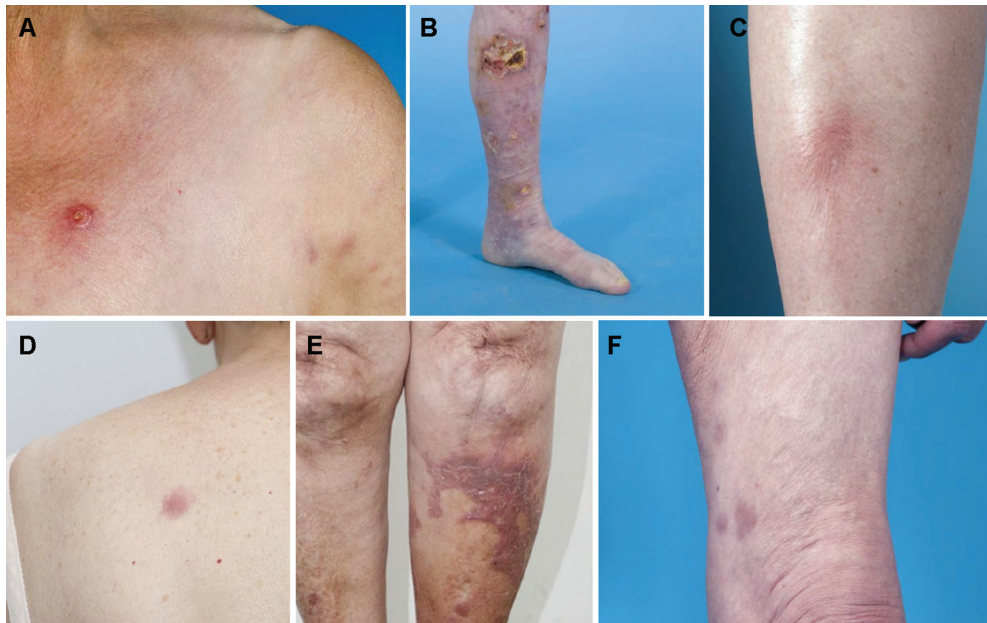
A complete overview of tumor characteristics is given in Table 3, and the histology of representative EBV<sup>+</sup> and EBV<sup>-</sup> cases is depicted in Figures 2 and 3, respectively. Most cases showed a diffuse (n = 7) infiltrate of large B cells, whereas 2 cases showed a perivascular infiltrate and 1 case a partly follicular infiltrate. The amount of admixed T cells ranged from 5% to 50%. Tumor cell morphology was very variable between the different cases. Most of the EBV<sup>+</sup> cases

showed a predominance of centroblasts and immunoblasts of varying size and were admixed with some polymorphic tumor cells with complex nuclear configuration, sometimes with a Reed-Sternberg-like appearance (Fig. 2B). EBV cases showed a more monomorphic infiltrate of either centroblasts or immunoblasts (Fig. 3B), or a combination of both, generally without tumor cells with complex nuclear configuration. Although cases 1 and 10 showed some admixture of large centrocytes, these centrocytes were never the predominant cell type of the malignant infiltrate. Mitotic figures were easily detected in all cases. Case 7 showed abundant apoptosis throughout the whole tumor.

### *Immunohistochemistry*

Immunohistochemistry showed considerable differences between the 5 EBV<sup>-</sup> and the 5 EBV<sup>+</sup> cases (Table 3, Figs. 2, 3). Whereas B-cell lineage markers were strongly expressed in all EBV<sup>-</sup> tumors, 4 of 5 EBV<sup>+</sup> tumors showed reduced expression of CD79a, combined with complete loss of expression of CD20 in case 2. For the cases with loss of 1 or both of these markers, B-cell lineage specificity was further confirmed by positive immunohistochemistry for PAX5, OCT2, and BOB1 (data not shown). Furthermore, all cases showed clonal rearrangements of the B-cell receptor, except for case 6, which showed polyclonal B-cell receptor rearrangements along with intracytoplasmic expression of IgM and  $\lambda$ .

**Figure 1.** Clinical manifestation of MTX-associated B-LPD in the skin



Case 1 presented with generalized plaques and small tumors, one of which on the chest showed focal ulceration (A). In case 2, extensive lesions on the lower left leg with marked ulceration were encountered (B). Case 4 presented with 2 deep seated nodules on the right leg clinically resembling erythema nodosum (C). Case 7 showed small nonulcerating nodules on the trunk (D) and extensive plaques on the left lower leg (E). In case 8, multiple small plaques were encountered on both arms and legs (F).

Table 2. Patient clinical characteristics

Sex	Age	MTX indication	Duration of MTX treatment (y)	Skin lesions	Other lesions	Treatment	Outcome	Recurrence	Status
EBV-positive*									
1	F	rheumatoid arthritis	4	generalized plaques and tumors, focal ulceration	lymph nodes, bone marrow, spleen	MTX stop, R-CHOP	CR	no	A-86
2	F	dermatomyositis	1.5	extensive ulcerating lesions on left lower leg	lymph nodes	MTX stop, CHOP	CR	no	D-16
3	M	dermatomyositis	unknown	ulcerating lesions on left lower leg	no	MTX stop, modified R-CHOP	NR	no	D-6
4	F	psoriatic arthritis	2	two nodules on right leg simulating erythema nodosum	lymph nodes	MTX stop	CR	no	A-46
5	M	rheumatoid arthritis	unknown	solitary plaque on head	no	MTX stop	CR	no	A-22
EBV-negative*									
6	F	rheumatoid arthritis	5	solitary tumor on right upper arm	no	MTX stop	CR	no	A-46
7	F	rheumatoid arthritis	7	extensive plaques on left lower leg; nodules on trunk	pleura	MTX stop, R-CHOP	PD	yes	D+15
8	M	rheumatoid arthritis	1	multiple plaques on arms and legs	no	MTX stop	CR	no	A-23
9	F	Morbus Still	unknown	plaques on chest and face	no	MTX stop, RT	CR	no	A-34
10	M	rheumatoid arthritis	8	generalized plaques	no	MTX stop, RT	CR	yes	A-57

\* EBV-status established by EBV in situ hybridization (EBER); A-: alive without disease; CR: complete remission; D-: died of causes unrelated to the lymphoma; D+: died of lymphoma; NR: no response; PD: progressive disease; PR: partial remission; R-CHOP: rituximab, cyclophosphamide, doxorubicin, vincristine, prednisone (polychemotherapy); RT: radiotherapy; y: years.



In the EBV group, all patients showed very strong nuclear expression of FOXP1 and MYC in the tumor cells, while FOXP1 and MYC were expressed by only 2 and 1 of 5 EBV<sup>+</sup> cases, respectively. In contrast, IRF4 and CD30 were strongly expressed in all 5 EBV<sup>+</sup> cases, but in 3 and 1 of 5 cases, respectively, in the EBV group. LMP1 was expressed in 4 of 5 EBV<sup>+</sup> cases but in none of the EBV<sup>-</sup> cases. CD15 was never substantially coexpressed in CD30<sup>+</sup> tumors, apart from a sporadic (larger) tumor cell in some cases. BCL2 and BCL6 were expressed in 8 and 7 of 10 cases, respectively, and were not differentially expressed in the EBV<sup>+</sup> and EBV<sup>-</sup> group. Of the 8 BCL2<sup>+</sup> cases, 7 showed positivity in > 75% of the tumor cells, whereas 1 case (case 4) showed positivity of this marker in approximately 30% of the tumor cells. The amount of expression of BCL6 was more variable, ranging from 30% to 100% of tumor cell positivity. Only 1 case (case 10) showed remnants of follicular dendritic networks in a CD35 stain, whereas all other cases were completely negative for CD35.

#### *MYC immunohistochemistry in PCFCL and PCLBCL-LT*

The 6 cases of PCFCL all showed only scattered nuclear tumor cell staining and were therefore interpreted as negative. The tumor cells of the 10 cases of PCLBCL-LT, however, showed virtually all strongly nuclear staining, and all cases were considered positive.

## **Discussion**

In the present study, we evaluated the clinicopathologic and immunophenotypical characteristics of 10 patients with MTX-associated B-LPD first presenting in the skin. Recognition of these lymphomas is important, as abrogation of MTX therapy may result in spontaneous remission and should therefore be considered before more aggressive therapies are used. In absence of adequate clinical data, these lymphomas might for example be misinterpreted as PCFCL, PCLBCL-LT, or skin localizations of a nodal DLBCL, leading to potential overtreatment with radiotherapy and/or chemotherapy. The main goal of the present study was to find out whether MTX therapy-associated B-LPDs presenting in the skin show clinical, histomorphologic and/or immunophenotypical characteristics that are different from those found in PCFCL and PCLBCL-LT and might be helpful in recognizing these MTX-associated B-LPDs, even if crucial clinical information is lacking. Follow-up data of the 10 patients included in this study indicate that these MTX-associated B-LPD have a relatively good prognosis, especially when compared to PCLBCL-LT. After a median follow-up of 24 months, 7 of 10 patients are still alive without disease, including the 4 patients who were withdrawn from MTX therapy without any other additional therapy given. Only 1 patient eventually died of lymphoma despite treatment with polychemotherapy. Previous studies suggested that spontaneous regression after cessation of MTX is preferentially detected in EBV<sup>+</sup> DLBCL.<sup>18,19</sup> However, in our series of MTX-associated B-LPD first presenting in the skin, the cases showing spontaneous regression were equally divided over the EBV<sup>+</sup> and EBV<sup>-</sup> group.

Differentiation between these MTX-associated B-LPDs and PCFCLs is generally not difficult. PCFCL normally presents with localized, nonulcerating skin lesions on the trunk or face, in particular the scalp, and uncommonly with lesions on the legs or with generalized skin lesions.<sup>11</sup> In contrast, most MTX-associated B-LPD in this study presented with generalized skin lesions, which often involved the legs and showed ulceration in 3 of them.

Histologically, PCFCLs show a predominance of large centrocytes with variable numbers

of admixed centroblasts, and have a BCL6<sup>+</sup>, BCL2<sup>-</sup>, IRF4<sup>-</sup>, FOXP1<sup>-</sup> phenotype and do not express intracytoplasmic immunoglobulins.<sup>20,21</sup> Although most cases of PCFCL have a diffuse growth pattern, remnants of follicular dendritic cell networks are often found using appropriate markers. None of the MTX-associated B-LPDs showed a predominance of centrocytes, and most cases strongly expressed BCL2 (8 of 10 cases), IRF4 (8 of 10 cases), FOXP1 (7 of 10 cases), and monotypic cytoplasmic immunoglobulin heavy and/or light chains (5 of 10 cases). Remnants of FDC networks were only found in 1 of 10 cases (case 10). In addition, the tumor cells did not express BCL2 and IRF4 in this case. However, the clinical presentation (generalized plaques), tumor cell morphology (a predominance of centroblasts with only few admixed centrocytes), and strong expression of FOXP1, MYC and CD30 argue against a diagnosis of PCFCL.

In nodal DLBCLs immunohistochemical expression of MYC is associated with an inferior survival.<sup>22</sup> To the best of our knowledge reports on MYC expression in CBCL have not been published. For the purpose of this study we therefore performed MYC expression analysis in 10 well-defined cases of PCLBCL-LT and 6 cases of PCFCL. Strong nuclear expression in virtually all tumor cells was found in all PCLBCL-LT, whereas PCFCL contained only few scattered positive cells (Table 4). It is noteworthy that immunohistochemical double expression of BCL2 and MYC has been associated with an aggressive clinical course and overall inferior prognosis in nodal DLBCL,<sup>23</sup> while in our cohort this association was not found.

There were also major differences between EBV<sup>+</sup> MTX-associated B-LPD and PCLBCL-LT. Clinically, 3 of 5 cases showed (extensive) ulceration, which is uncommon in PCLBCL-LT. Histologically, the tumor cells in these EBV<sup>+</sup> lymphomas often showed marked polymorphism and often contained Reed Sternberg-like large tumor cells with complex nuclear configurations, whereas PCLBCL-LTs generally show a more monomorphic infiltrate of centroblasts or immunoblasts. In contrast to PCLBCL-LT, EBV<sup>+</sup> MTX-associated B-LPD strongly expressed CD30, whereas FOXP1 and MYC were expressed by only 2 and 1 of 5 cases, respectively. The consistent expression of CD30 is seen in most EBV<sup>+</sup> lymphomas due to the induction of CD30 in B-cells by EBV.<sup>24</sup> In addition, weak or absent expression CD79a in 4 of the cases, combined with loss of expression of CD20 in 1 case, has not been reported in PCLBCL-LT. Reduced or absent expression of CD20 was also described in 31% of EBV<sup>+</sup> mucocutaneous ulcers, an EBV-associated mucocutaneous large B-cell proliferation, usually related to an immunosuppressive state,<sup>25</sup> which suggests a possible relation between EBV infection and B-cell marker loss. Some of the features of EBV<sup>+</sup> MTX-associated B-LPDs, including spontaneous regression and loss of expression of CD20, show overlap with EBV<sup>+</sup> mucocutaneous ulcers. However, none of our cases exactly matched the criteria of EBV<sup>+</sup> mucocutaneous ulcers, as these characteristically present with solitary sharply circumscribed ulcers.<sup>25</sup> Differentiation of lymphomatoid granulomatosis from EBV<sup>+</sup> MTX-associated B-LPD is based on the clinical presentation, for example, skin lesions combined with (bilateral) pulmonary nodules as well as the histopathological growth pattern, showing angioinvasion and angiodestruction.<sup>26</sup> Distinction from EBV<sup>+</sup> DLBCL of the elderly might be more challenging, especially as our patients are generally older and have received MTX treatment for several years, and therefore a combination of both age-related and MTX-related immunodeficiency might contribute to lymphomagenesis.

Figure 2. EBV<sup>+</sup> MTX-associated B-LPD in the skin

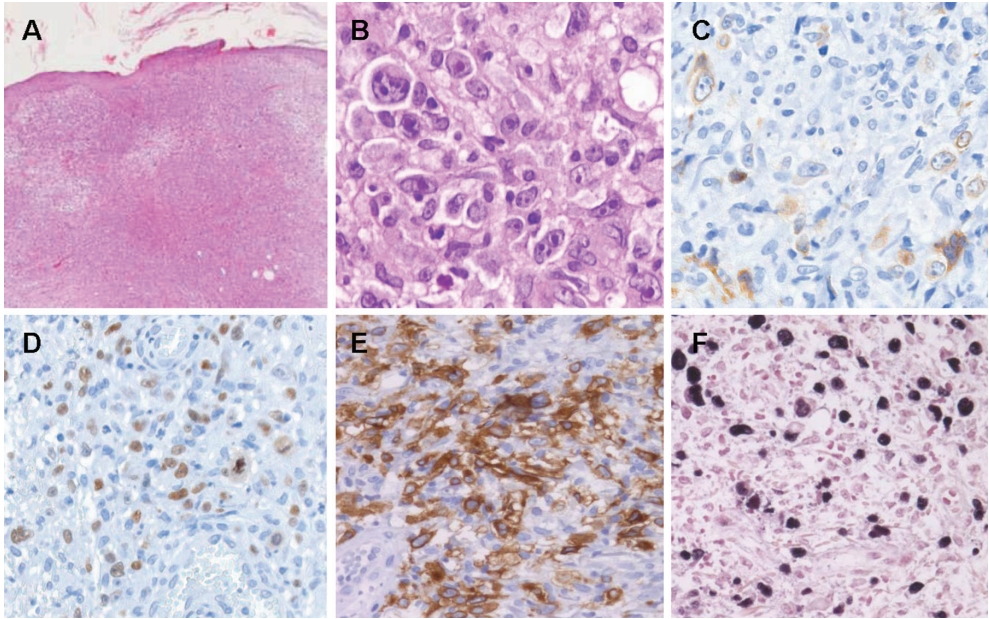
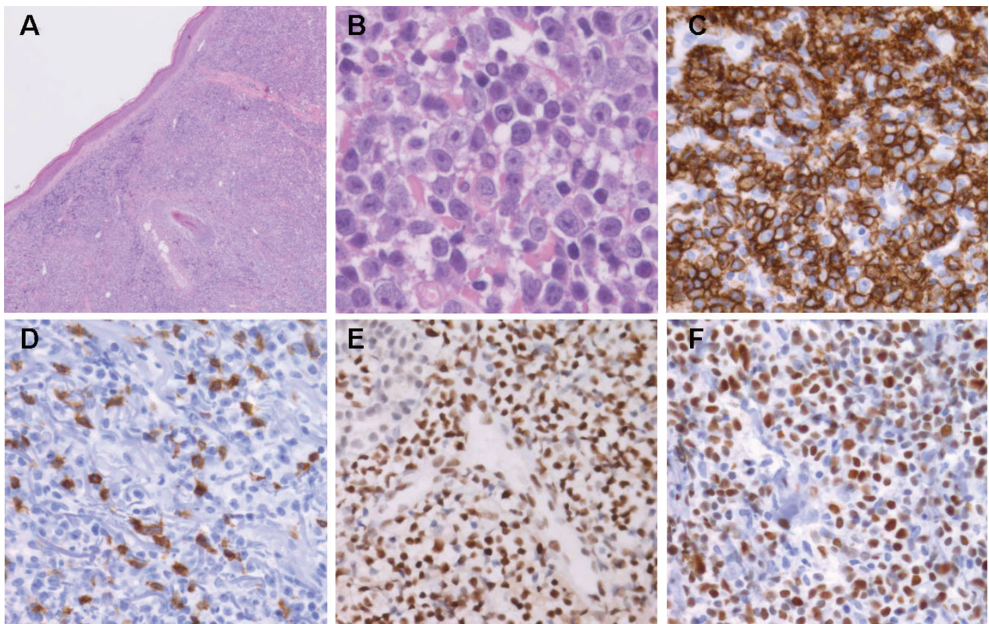


Figure 3. EBV<sup>-</sup> MTX-associated B-LPD in the skin



6

\* Legend to Figure 2 (previous page): Representative slides from case 2. In overview, the tumor showed a diffuse growth pattern (A). The tumor cell morphology was highly variable with some admixed very large and multi-lobated tumor cells (B). The tumor cells did not show immunohistochemical positivity for B-cell marker CD20 and showed weak expression of CD79a (C), although the cells were positive for B-cell lineage markers PAX5 (D), OCT2, and BOB1, and showed clonal B-cell rearrangements. CD30 showed strong membranous positivity (E) and EBER showed positivity in scattered large tumor cells.

\* Legend to Figure 3 (previous page): Representative slides from case 8. In overview, the tumor showed a diffuse growth pattern (A). The tumor cells had a predominantly immunoblastic morphology with a large central nucleolus and round nuclear contour (B). The tumor cells showed strong immunohistochemical expression of B-cell marker CD20 (C). The amount of admixed T-lymphocytes in a CD3 stain was low (D). FOXP1 (E) and MYC (F) showed diffuse and very strong nuclear staining in almost all tumor cells.

Histologic differentiation between EBV<sup>-</sup> MTX-associated B-LPD and PCLBCL-LT is much more difficult. Both conditions show a rather monotonous proliferation of centroblasts and/or immunoblasts and a very similar phenotype including expression of MYC (Table 4). However, > 85% of patients with PCLBCL-LT present with skin tumors confined to 1 or both legs.<sup>11</sup> Presentation with generalized skin lesions is uncommon in this group and should raise suspicion that the patient has another type of DLBCL, that is, an MTX-associated or otherwise immunodeficiency-associated B-LPD or a secondary cutaneous DLBCL.

In conclusion, in a patient presenting with skin tumors with the histologic features of a DLBCL, the presence of ulcerating and/or generalized skin lesions, marked tumor cell polymorphism, and reduced staining for CD79a, diagnosis of MTX- or immunodeficiency-associated B-LPD should be considered. In such cases EBV and CD30 expression should be performed, if not investigated already routinely. The relatively good clinical outcome and spontaneous disease regression after only withdrawal of MTX in a considerable proportion of patients warrants for a period of careful wait-and-see policy before considering more aggressive therapies in MTX-associated B-LPD of the skin.

Table 3. Tumor characteristics

Predominant cell type	T-cell admixture	Immunohistochemistry											B-cell clonality		
		CD20	CD79a	BCL2	BCL6	CD10	IRF4	FOXP1	MYC	CD30	cytoplasmic Ig				
EBV-positive*															
1	CB/IB	+	+/-	+	-	-	+	-	-	+	-	-	+	igG λ	monoclonal
2	polymorphic IB	-	+/-^	-	+	-	+	+	-	-	-	-	+	0	monoclonal
3	CB/IB	+	+	+	+	-	+	+	+	+	+	+	+	igM κ	monoclonal
4	polymorphic CB/IB	+	+/-	+	+	-	+	-	-	-	-	-	+	0	monoclonal
5	polymorphic CB/IB	+	+^	+	-	-	+	-	-	-	-	-	+	0	monoclonal
EBV-negative*															
6	polymorphic CB	+	+	+	+	+	+	+	+	+	+	+	-	igM λ	polyclonal
7	CB	+	+	+	+	-	+	+	+	+	+	+	-	0	monoclonal
8	IB	+	+	+	-	+	-	-	+	+	+	-	-	igM IgD κ	monoclonal
9	IB	+	+	+	+	-	+	+	+	+	+	+	-	igM IgD	monoclonal
10	CB/IB	+	+	-	+	-	-	-	+	+	+	+	+	0	monoclonal

\* EBV-status established by EBV in situ hybridization (EBER).

^ Partly positive and partly negative.

-: negative expression; +/-: weak expression; +: positive expression by immunohistochemistry; CB: centroblastic; IB: immunoblastic; ig: immunoglobulin.

## References

1. Swerdlow SH, Campo E, Harris NL, et al. (2008) WHO Classification of Tumours Haematopoietic and Lymphoid Tissues. Geneva, Switzerland: WHO PRESS.
2. Tran H, Nourse J, Hall S, et al. (2008) Immunodeficiency-associated lymphomas. *Blood reviews*. 22: 261-81.
3. Gubner R, August S, Ginsberg V. (1951) Therapeutic suppression of tissue reactivity. II. Effect of aminopterin in rheumatoid arthritis and psoriasis. *Am J Med Sciences* 221: 176-82.
4. Weinstein A, Marlowe S, Korn J, et al. (1985) Low-dose methotrexate treatment of rheumatoid arthritis. Long-term observations. *Am J Med* 79: 331-7.
5. Rizzi R, Curci P, Delia M, et al. (2009) Spontaneous remission of "methotrexate-associated lymphoproliferative disorders" after discontinuation of immunosuppressive treatment for autoimmune disease. Review of the literature. *Med Oncol* 26:1-9.
6. Verma S, Frambach GE, Seilstad KH, et al. (2005) Epstein-Barr virus-associated B-cell lymphoma in the setting of iatrogenic immune dysregulation presenting initially in the skin. *J Cutan Pathol* 32: 474-83.
7. Pfistershammer K, Petzelbauer P, Stingl G, et al. (2010) Methotrexate-induced primary cutaneous diffuse large B-cell lymphoma with an 'angiocentric' histological morphology. *Clin Exp Dermatol* 35: 59-62.
8. Tournadre A, D'Incan M, Dubost JJ, et al. (2001) Cutaneous lymphoma associated with Epstein-Barr virus infection in 2 patients treated with methotrexate. *Mayo Clin Proc Mayo Clin* 76: 845-8.
9. Chai C, White WL, Shea CR, et al. (1999) Epstein Barr virus-associated lymphoproliferative-disorders primarily involving the skin. *J Cutan Pathol* 26: 242-7.
10. Rausch T, Cairoli A, Benhattar J, et al. (2013) EBV+ cutaneous B-cell lymphoproliferation of the leg in an elderly patient with mycosis fungoides and methotrexate treatment. *APMIS* 121: 79-84.
11. Senff NJ, Hoefnagel JJ, Jansen PM, et al. (2007) Reclassification of 300 primary cutaneous B-Cell lymphomas according to the new WHO-EORTC classification for cutaneous lymphomas: comparison with previous classifications and identification of prognostic markers. *J Clin Oncol* 25: 1581-7.
12. Senff NJ, Noordijk EM, Kim YH, et al. (2008) European Organization for Research and Treatment of Cancer and International Society for Cutaneous Lymphoma consensus recommendations for the management of cutaneous B-cell lymphomas. *Blood* 112: 1600-9.
13. Tilly H, Dreyling M, Group EGW. (2009) Diffuse large B-cell non-Hodgkin's lymphoma: ESMO clinical recommendations for diagnosis, treatment and follow-up. *Ann Oncol* 20 Suppl 4: 110-2.
14. Dreyling M, Group EGW. (2009) Newly diagnosed and relapsed follicular lymphoma: ESMO clinical recommendations for diagnosis, treatment and follow-up. *Ann Oncol* 20 Suppl 4: 119-20.
15. Meyer PN, Fu K, Greiner TC, et al. (2011) Immunohistochemical methods for predicting cell of origin and survival in patients with diffuse large B-cell lymphoma treated with rituximab. *J Clin Oncol* 29: 200-7.
16. Horn H, Ziepert M, Becher C, et al. (2013) MYC status in concert with BCL2 and BCL6 expression predicts outcome in diffuse large B-cell lymphoma. *Blood* 121: 2253-63.
17. van Dongen JJ, Langerak AW, Bruggemann M, et al. (2003) Design and standardization of PCR primers and protocols for detection of clonal immunoglobulin and T-cell receptor gene recombinations in suspect lymphoproliferations: report of the BIOMED-2 Concerted Action BMH4-CT98-3936. *Leukemia* 17: 2257-317.
18. Hoshida Y, Xu JX, Fujita S, et al. (2007) Lymphoproliferative disorders in rheumatoid arthritis: clinicopathological analysis of 76 cases in relation to methotrexate medication. *J Rheumatol* 34: 322-31.
19. Feldman AL, Dogan A, Smith DI, et al. (2011) Discovery of recurrent t(6;7)(p25.3;q32.3) translocations in ALK-negative anaplastic large cell lymphomas by massively parallel genomic sequencing. *Blood* 117: 915-9.

20. Hoefnagel JJ, Mulder MM, Dreef E, et al. (2006) Expression of B-cell transcription factors in primary cutaneous B-cell lymphoma. *Mod Pathol* 19: 1270-6.
21. Hoefnagel JJ, Vermeer MH, Jansen PM, et al. (2003) Bcl-2, Bcl-6 and CD10 expression in cutaneous B-cell lymphoma: further support for a follicle centre cell origin and differential diagnostic significance. *Br J Dermatol* 149: 1183-91.
22. Valera A, Lopez-Guillermo A, Cardesa-Salzmann T, et al. (2013) MYC protein expression and genetic alterations have prognostic impact in patients with diffuse large B-cell lymphoma treated with immunochemotherapy. *Haematologica* 98: 1554-62.
23. Hu S, Xu-Monette ZY, Tzankov A, et al. (2013) MYC/BCL2 protein coexpression contributes to the inferior survival of activated B-cell subtype of diffuse large B-cell lymphoma and demonstrates high-risk gene expression signatures: a report from The International DLBCL Rituximab-CHOP Consortium Program. *Blood* 121: 4021-31.
24. Gregory CD, Edwards CF, Milner A, et al. (1988) Isolation of a normal B cell subset with a Burkitt-like phenotype and transformation in vitro with Epstein-Barr virus. *Int J Cancer* 42: 213-20.
25. Dojcinov SD, Venkataraman G, Raffeld M, et al. (2010) EBV positive mucocutaneous ulcer--a study of 26 cases associated with various sources of immunosuppression. *Am J Surg Pathol* 34: 405-17.
26. Jaffe ES, Wilson WH. (1997) Lymphomatoid granulomatosis: pathogenesis, pathology and clinical implications. *Cancer Surveys* 30: 233-48.







# 7

## Summary and discussion



In the WHO-EORTC classification, B-cell lymphomas primarily presenting in the skin are categorized as primary cutaneous marginal zone B-cell lymphoma (PCMZBL), primary cutaneous follicle center lymphoma (PCFCL) or primary cutaneous large B-cell lymphoma, leg type (PCLBCL-LT).<sup>1</sup> The three subtypes have their own clinicopathologic characteristics, but differentiation between PCFCL and PCLBCL-LT can sometimes be challenging. These two lymphoma subtypes generally show clinical differences in presentation, i.e. localized skin lesions on the head, in particular the scalp, or trunk for PCFCL, and skin lesions on one or both legs for PCLBCL-LT, but the distinction between the two entities is primarily based on specific tumor cell morphology, i.e. large cells with cleaved nuclei (centrocytes) in PCFCL and large cells with round nuclei (centroblasts and immunoblasts) in PCLBCL-LT.<sup>1,2</sup> However this distinction based on tumor cell morphology can become challenging when cases of PCFCL have a diffuse growth pattern and lack the follicular infiltrate that is distinct from the growth pattern of PCLBCL-LT. Accurately separating these two types of lymphoma has large implications for the patient, as PCFCL are treated with local radiotherapy (5-year overall survival (OS) 95%), but patients with PCLBCL-LT are preferentially treated with polychemotherapy, and still have an unfavorable clinical outcome (5-year OS survival 50%).<sup>3</sup>

Recent guidelines indicate that patients with PCLBCL-LT should be treated with R-CHOP, cyclophosphamide, doxorubicin, vincristine, and prednisone combined with monoclonal antibody rituximab, directed at CD20 at the surface membrane of B-lymphocytes.<sup>4</sup> However, due to the relatively high age at first presentation and concomitant comorbidities, not all patients are eligible for this type of chemotherapy. Furthermore, a proportion of patients receiving polychemotherapy still show an aggressive clinical course after initial response, leading to a challenge in further treatment strategies. Patients might therefore benefit from therapies that are less toxic and target more specifically the lymphoma cells, to reduce morbidity and increase survival. Molecular and/or genetic characterization of these tumors is thus warranted and might reveal better insight into the pathogenesis of the disease. These insights might eventually yield potential targets for therapy directed specifically at these targets.

A rare type of diffuse large B-cell lymphoma (DLBCL) presenting in the skin is methotrexate (MTX)-associated B-cell lymphoproliferative disorder (B-LPD). This lymphoma belongs to the group of 'iatrogenic immunodeficiency-associated lymphoproliferative disorders'<sup>5</sup> and develops in patients with autoimmune disorders (mainly rheumatoid arthritis) receiving chronic low-dose treatment with MTX. The clinicopathologic features of MTX-associated B-LPD first presenting in the skin are still ill-defined, as there are only sporadic reports in literature.<sup>6-10</sup> Differentiation from PCFCL and PCLBCL-LT is nonetheless important, as these lymphomas require a different therapeutic approach. It seems warranted to stop MTX treatment and follow a careful wait-and-see policy to evaluate potential remission before considering more aggressive therapies, as regression of MTX-associated lymphomas after abrogation of MTX treatment has been reported.<sup>11</sup>

The studies presented in this thesis investigated clinicopathologic and genetic aspects of PCFCL and PCLBCL-LT. The main aims of this thesis were (1) to define additional diagnostic markers that could aid in the differential diagnosis of PCFCL with a diffuse growth pattern from PCLBCL-LT, (2) to investigate molecular and genetic alterations in PCLBCL-LT underlying the pathogenesis of this type of lymphoma, and (3) to better define the group of MTX-associated B-LPD presenting in the skin, in order to find clinicopathologic and/or immunophenotypic characteristics that would allow rapid recognition of these lymphomas. In this final chapter, these issues will be discussed based on the data and observations described in the preceding chapters and in recent literature.

## Differentiation between PCFCL and PCLBCL-LT

### *IgM immunohistochemistry*

Gene expression profiling studies in PCFCL and PCLBCL-LT have demonstrated different gene expression profiles for both lymphoma subtypes, including higher expression of immunoglobulin mu heavy chain enhancer and constant region (*IGHM*) transcripts in PCLBCL-LT as compared to PCFCL.<sup>12</sup> In **chapter 2**, we explored whether these differences were also reflected at protein levels, and performed B-cell heavy and light chain characterization for 53 patients with PCFCL and 40 patients with PCLBCL-LT by immunohistochemistry on formalin-fixed and paraffin-embedded (FFPE) tumor biopsy specimens. All 40 cases of PCLBCL-LT consistently showed cytoplasmic staining for IgM, in 18 of them with coexpression of IgD. In contrast, only 5 of the PCFCL cases showed cytoplasmic staining for IgM and/or IgD. Not only PCLBCL-LT presenting on the leg, but also those cases presenting on the trunk or head, showed strong expression of IgM, implying that for lesions on these locations IgM expression might be used as an additional marker in differentiating between PCFCL and PCLBCL-LT in clinical pathology practice. However, the three PCFCLs that presented on the leg(s) also expressed IgM. Therefore, IgM expression does not seem to discriminate between both lymphoma subtypes when presenting on the leg. Recent studies confirmed our findings, demonstrating expression of IgM in 10 out of 10 cases of PCLBCL-LT and only 3 out of 30 cases of PCFCL.<sup>13</sup>

### *MicroRNA profiling*

MicroRNAs can regulate gene expression of their target genes by being able to inhibit translational initiation by blocking ribosomes and they can also directly target mRNA at the 3 prime untranslated region leading to degradation of the molecule.<sup>14</sup> Higher expression of a certain microRNA might therefore silence a tumor suppressor gene, while loss of expression might cause oncogenes to be upregulated. Through these mechanisms, microRNAs are thought to contribute in oncogenesis (reviewed in <sup>15</sup>). In **chapter 3** we investigated microRNA profiles by performing high-throughput sequencing analysis on frozen tumor biopsies from 6 cases of PCFCL and 13 cases of PCLBCL-LT. Analogous to previous gene expression profiling studies,<sup>12</sup> we tried to cluster PCFCL and PCLBCL-LT based on their microRNome. In contrast to gene expression profiling, cluster analysis of the complete microRNA profile did not discriminate the lymphoma subtypes. As gene expression profiles of PCFCL and PCLBCL-LT were concordant with a germinal center B-cell (GCB) and activated B-cell (ABC), respectively, we tried to cluster the two cutaneous lymphoma subtypes by three different microRNA profiles of these two B-cell subtypes from literature.<sup>16-18</sup> These microRNA profiles were reported to be able to separate nodal ABC-type from GCB-type DLBCL, but we were not able to separate our two groups by one of these methods. Still, the extensive profiling method yielded 16 individual mature microRNAs that were differentially expressed between PCFCL and PCLBCL-LT. Single microRNA quantitative PCR (qPCR) was conducted for 11 of these 16 microRNAs on FFPE tumor biopsies of 20 additional cases (10 cases of PCFCL and 10 cases of PCLBCL-LT), confirming higher expression of miR-9-5p, miR-31-5p, miR-129-2-3p and miR-214-3p in PCFCL as compared to PCLBCL-LT. This technique can easily be performed on routine biopsy specimens. Especially the detection of miR-129-3p by RT-qPCR on FFPE tumor biopsies might be helpful in clinical settings, as this microRNA was not expressed in a detectable amount in PCLBCL-LT, but showed substantial expression in about half of the cases of PCFCL. This microRNA therefore seems a rather specific, yet not highly sensitive, marker for PCFCL. Remarkably, this miR-129-2-3p was also specifically expressed in substantial amounts in GCB-type nodal DLBCL as compared to ABC-type DLBCL in our RT-qPCR control group of 20 nodal DLBCLs, and therefore

seems a true germinal center-related microRNA.

## Pathogenesis of primary cutaneous diffuse large B-cell lymphoma, leg type

### *Class switch recombination*

In **chapter 2** we demonstrated consistent immunohistochemical cytoplasmic expression of IgM in 40 cases of PCLBCL-LT, with co-expression of IgD in about half of them. As genotyping showed that PCLBCL-LT have the profile of a post-germinal center, activated B-cell,<sup>12</sup> it is expected that class switch recombination (CSR) from IgM (and IgD) to IgG or IgA has occurred. Given this presumed germinal center experience, the absence of CSR in PCLBCL-LT is surprising and might indicate a defect in the CSR mechanism. Although deficiency of the RNA-editing enzyme activation-induced cytidine deaminase (AID) is associated with impairment of CSR,<sup>19</sup> relatively high levels of AID have been demonstrated in PCLBCL-LT,<sup>20</sup> so the absence of CSR cannot be explained by shortage of AID. The expression of IgM is not exclusive for PCLBCL-LT. Over 50% of nodal DLBCL also show immunohistochemical expression of IgM in the tumor cells,<sup>21,22</sup> and high levels of IgM RNA are more frequently encountered in ABC-type DLBCL than in GCB-type DLBCL.<sup>23</sup> IgM expression therefore seems ABC-type related, and is indeed also encountered in primary central nervous system (CNS) DLBCL, and primary testicular DLBCL, two types of extranodal DLBCL that are also of ABC-type.<sup>24,25</sup> In nodal ABC-type DLBCL as well as in primary CNS DLBCL it was suggested that CSR was impaired due to the high frequency of mutations in the switch regions of the constant chain, comprising both intra-S $\mu$  and intra-S $\gamma$  deletion/recombination events,<sup>26,27</sup> but data concerning these switch regions are not available for PCLBCL-LT. Noteworthy, it was recently described that transcription factor forkhead box protein 1 (FOXP1) might also play a role in (blocking) CSR, as constitutional expression of FOXP1 led to impairment of switching from IgM to IgG1.<sup>28</sup> Indeed in PCLBCL-LT, immunohistochemical FOXP1 expression is consistently high, as was shown in **chapter 5**, although the exact underlying mechanism for this high expression is not yet understood.

### *Nuclear factor-kappa B*

Aberrant constitutive activation of the nuclear factor-kappa B (NF- $\kappa$ B) signal transduction pathway has been implicated in tumor cell survival of nodal ABC-type DLBCL and other types of B-cell lymphomas. Studies on the molecular background of NF- $\kappa$ B pathway activation have demonstrated that mutations in multiple genes can cause deregulation of NF- $\kappa$ B signaling in nodal ABC-type DLBCL.<sup>29</sup> The genes most frequently affected by genetic aberrations are tumor necrosis factor, alpha-induced 3 (*TNFAIP3*, *A20*), cluster of differentiation 79B (*CD79B*), caspase recruitment domain-containing protein 11 (*CARD11*), and myeloid differentiation primary response gene 88 (*MYD88*), which all can contribute to constitutive activation of the NF- $\kappa$ B pathway, and in two-third of cases of nodal ABC-type DLBCL, one or more of these genes are affected.<sup>30</sup> In **chapter 4**, we investigated NF- $\kappa$ B activating genetic aberrancies in 10 cases of PCLBCL-LT. Tumor suppressor gene *TNFAIP3* was heterozygously deleted in 4 cases. No additional promoter hypermethylation was detected that would lead to epigenetic silencing of the non-deleted allele. A *CD79B* Y196 mutation was found in 2 cases in both DNA and cDNA. The coiled-coil domain of *CARD11* contained a D415E and a R423W mutation in 1 sample. At genomic level, the oncogenic *MYD88* L265P mutation was found in 4 cases, 3 of which showed the same mutation at transcriptional level. Combined, 7 out of 10 cases of PCLBCL-LT showed genetic alterations in genes that regulate NF- $\kappa$ B activation. Although estimation of the real proportion of alterations is difficult in this relatively small study co-

hort, for pathway activating mutations in *CD79B*, *MYD88*, and *CARD11* the percentages of tumors affected strikingly resemble those present in nodal ABC-DLBCL.<sup>30</sup> However, the homozygous deletion and/or epigenetic silencing of *TNFAIP3*, as is encountered in 23% of cases of nodal ABC-DLBCL,<sup>30</sup> was not detected in our cases of PCLBCL-LT. The data on the deletion of (part of) chromosome 6q, on which *TNFAIP3* is located, are in line with previous studies in PCLBCL-LT using conventional array comparative genomic hybridization<sup>31</sup> or fluorescent in situ hybridization.<sup>32</sup> Furthermore, other studies detected *MYD88* L265P mutations in 69% of PCLBCL-LT cases.<sup>32,33</sup>

Several molecules in the NF- $\kappa$ B pathway have already been selectively targeted in B-cell NHL *in vitro* and *in vivo* to explore potential new treatments strategies. For example, sotrastaurin can interfere with NF- $\kappa$ B pathway activation, by inhibition of PKC- $\beta$ , which is required for *CARD11*-dependent activation of the NF- $\kappa$ B pathway.<sup>34</sup> Sotrastaurin was shown to be selectively toxic for *CD79*-mutant DLBCL in a mouse xenograft model<sup>35</sup> as compared to unmutated DLBCL, but only in presence of wild-type *CARD11*. An RNA interference screen revealed that a BCR signaling component, Bruton's tyrosine kinase (BTK), is essential for the survival of nodal ABC-type DLBCL with wild-type *CARD11* and in addition, knockdown of proximal B-cell receptor units, i.e. *CD79B*, was selectively toxic to wild-type *CARD11* nodal ABC-type DLBCL, but not to other lymphomas.<sup>36</sup> Furthermore, in a phase I trial, the BTK-inhibitor ibrutinib was well-tolerated and generated a clinical (partial) response in 40% of refractory nodal ABC-type DLBCL, both in patients with tumors bearing *CD79* mutations or a combination of *CD79* and *MYD88* mutations. However, patients with only *MYD88* mutations were refractory to this treatment, reflecting the B-cell receptor signaling-independency of these *MYD88*-mutated tumors.<sup>37</sup> The potency of ibrutinib in treating nodal ABC-DLBCL has recently been further explored, in a high throughput combinatorial screening study, yielding drugs that could cooperate with ibrutinib in killing ABC-DLBCL cells *in vitro*.<sup>38</sup> Together, these results imply the relevance of somatic mutations in *CD79B*, *CARD11* and *MYD88* in developing new treatments for nodal ABC-DLBCL, and potentially for the treatment of PCLBCL-LT. Especially the impact of ibrutinib in the treatment of (several types of) B-cell lymphomas seems promising in treating PCLBCL-LT patients who are not eligible for aggressive treatment or who quickly relapse after receiving polychemotherapy.<sup>39</sup> Therefore, particularly investigating the mutational status of *MYD88* in PCLBCL-LT might become of clinical relevance, as these patients will potentially not benefit from treatment with ibrutinib.

As 70% of PCLBCL-LT shows genetic aberrancies in NF- $\kappa$ B pathway-related genes, our data also emphasize the relevance of NF- $\kappa$ B signaling in this type of lymphoma. In nodal ABC-DLBCL, NF- $\kappa$ B signaling has been recognized as a key feature.<sup>40</sup> The lack of genetic aberrancies in the remaining 30% of our cases studied does not necessarily imply physiological NF- $\kappa$ B signaling in these cases, as activating mutations in pathway components are not the only pathophysiologic mechanism underlying constitutive signaling of this pathway. For example, hedgehog signaling is deregulated in DLBCL.<sup>41</sup> The dysregulation might partly be due to copy number gains involving smoothed (SMO), which is a signal transducer subunit of the hedgehog pathway.<sup>42</sup> Aberrant hedgehog signaling has been linked to NF- $\kappa$ B pathway activation in DLBCL through SMO, which is able to recruit G-protein subunits that lead to NF- $\kappa$ B pathway activation through PKC- $\beta$  – *CARD11* signaling.<sup>43</sup> Furthermore, several microRNAs have been implicated in NF- $\kappa$ B pathway activation. MiR-155 is able to downregulate I $\kappa$ B kinases, which will lead to enhanced NF- $\kappa$ B signaling.<sup>44</sup> MiR-21 blocks translation of phosphatase and tensin homolog (*PTEN*), which is a tumor suppressor inhibiting the activation of NF- $\kappa$ B by AKT signaling. Both microRNAs are frequently reported to be upregulated in nodal ABC-DLBCL as

compared to GCB-DLBCL, concordant with NF- $\kappa$ B being a feature of ABC-DLBCL. However, in our cohort explored in **chapter 3**, we did not encounter differences in expression levels of miR-155 and miR-21 between PCLBCL-LT and PCFCL. This might imply that these microRNAs do not contribute in aberrant NF- $\kappa$ B signaling in PCLBCL-LT, or that aberrant signaling is also a feature of PCFCL. This unclarity warrants for further investigation into this topic.

### *Transcription factors*

In physiologic circumstances, B-cell lymphoma 6 (BCL6) is expressed in germinal center B-cells and downregulates Blimp1 expression, the protein encoded by of PR domain containing 1, with ZNF domain (*PRDM1*).<sup>45</sup> After a successful germinal center reaction, BCL6 is downregulated, leading to expression of Blimp1. This Blimp1 expression is sufficient to allow B-cells to undergo plasma cell maturation, and also induces other transcription factors, such as interferon regulatory factor-4 (IRF4), which are also part of the plasma cell program.<sup>46</sup> Furthermore, FOXP1 expression is inversely correlated to BCL6 expression, thereby occurring in a post germinal center stage, and FOXP1 is also able to upregulate the expression of Blimp1.<sup>28</sup> Noteworthy, the immunohistochemical profile of PCLBCL-LT concerning these transcription factors is inconsistent with the profile of activated B-cells, its presumed cell of origin, as BCL6 is expressed in more than half of the cases, IRF4 and FOXP1 are virtually always expressed by the tumor cells, and no substantial expression of Blimp1 is detected.<sup>47</sup> The activated B-cell, as normal counterpart of PCLBCL-LT, is arrested in differentiation in a transitional stage between germinal center B-cell and plasma cell.<sup>12</sup> In nodal DLBCL, several mechanisms have been described that might (in part) be responsible for this differentiation arrest, for example translocations involving *BCL6*,<sup>48,49</sup> deletion and mutations *PRDM1*.<sup>48,50</sup> Other molecules driving B-cells towards plasma cell differentiation include IRF4 and FOXP1, and sporadic genetic alterations, such as translocations involving these genes, also occur in nodal DLBCL.<sup>51,52</sup> In **chapter 5**, we investigated genetic and immunohistochemical alterations of these B-cell activation-related transcription factors in ten cases of PCLBCL-LT. We could not find evidence that *BCL6*, *FOXP1* and/or *IRF4* have an autonomous way of protein upregulation, as we did not encounter translocations or amplifications involving these genes. Moreover, the absence of Blimp1 protein by immunohistochemistry in PCLBCL-LT could not be explained by genetic silencing through homozygous deletion of the gene, or heterozygous deletion with concomitant missense or nonsense mutations. These alterations actually have been described in ABC-DLBCL, the nodal counterpart of PCLBCL-LT. Especially genetic inactivation of *PRDM1* is frequently detected in ABC-DLBCL, occurring in approximately one-third of cases.<sup>48,50</sup> Translocations involving *IRF4* have only sporadically been described in nodal ABC-DLBCL<sup>51</sup> and translocations involving *FOXP1* are also infrequent, but might preferentially be detected in extranodal DLBCL.<sup>52</sup>

### *MYC*

In the study described in **chapter 6**, in which we compared MTX-B-LPD presenting in the skin with PCFCL and PCLBCL-LT, we demonstrated that PCLBCL-LT were consistently positive for MYC immunohistochemistry, and more than 75% of the tumor cells showed nuclear staining in the 10 cases investigated. In nodal DLBCL, high percentages of MYC-positive tumor cells have been linked to *MYC* rearrangement, gain and/or amplification (53, 54). However, in PCLBCL-LT, data concerning translocations involving the *MYC* gene vary, from occurrence in sporadic cases<sup>55</sup> to approximately one-third of cases.<sup>56</sup> Reports of gains or amplification of the *MYC* gene have to our knowledge not been reported and were not found in the same cohort of 10 patients PCLBCL-LT, for which immunohistochemistry was reported, by using fine



tiling comparative genomic hybridization (FT-CGH) analysis (Koens et al, unpublished data). Above that, in this cohort, FT-CGH analysis did also not reveal evidence of translocations involving the *MYC* gene. *MYC* protein levels are therefore most likely upregulated by other mechanisms. *MYC* is under physiologic circumstances repressed by B-cell transcription factor Blimp-1 in post-germinal center B-cells.<sup>57</sup> This protein is however absent in PCLBCL-LT<sup>47</sup> and this absence might therefore contribute to high levels of *MYC* protein.

### **Methotrexate-associated B-cell lymphoproliferative disorder presenting in the skin**

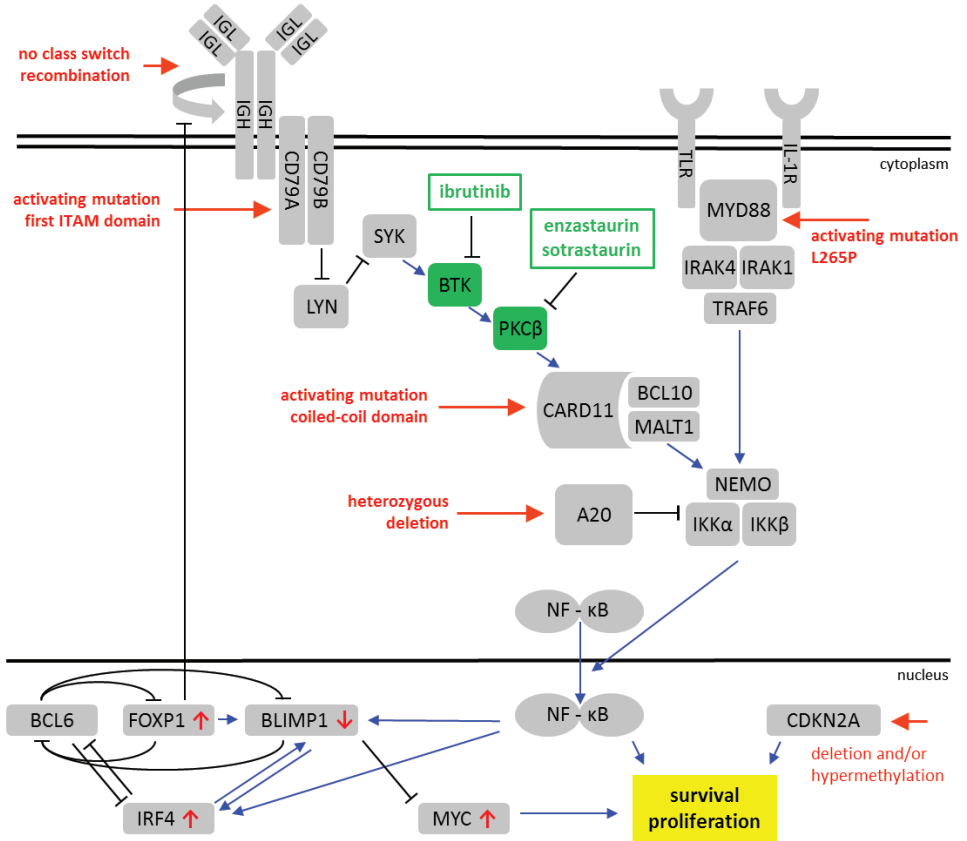
In **chapter 6** the clinicopathologic and phenotypical features of 10 patients with MTX-associated B-LPD first presenting in the skin were studied, including 5 Epstein Barr virus (EBV)-positive and 5 EBV-negative cases. 6 patients had skin-limited disease. Clinically, abrogation of MTX therapy resulted in a complete response in four cases and a partial response in another two. The 5-year disease-specific survival was 90%. MTX-associated B-LPD differed from PCFCL by the presence of ulcerating and/or generalized skin lesions, an infiltrate composed of centroblasts/immunoblasts rather than large centrocytes, reduced staining for CD79a, expression of BCL2, IRF4, FOXP1 in most cases, and monotypic intracytoplasmic immunoglobulin expression in half of the cases. EBV-positive MTX-associated B-LPD differed from PCLBCL-LT by the presence of ulcerating skin lesions, marked tumor cell polymorphism, reduced staining for CD79a, and expression of CD30 and EBV. EBV-negative cases showed morphological and immunophenotypical similarities to PCLBCL-LT, but differed by presentation with generalized skin lesions in 4 of 5 cases. The good clinical outcome and spontaneous disease regression that occurred after withdrawal of MTX in a considerable proportion of patients, underscores the importance of a careful wait-and-see policy before considering more aggressive therapies in patients with MTX-associated B-LPD of the skin.

### **Concluding remarks and perspectives**

Through the different studies described in this thesis more knowledge is gained about the clinicopathologic (and genetic) aspects of PCFCL, PCLBCL-LT and MTX-associated B-LPD presenting in the skin. The results aid in better definition of these separate entities, and thereby generate leads for diagnosing these lymphomas in clinical practice. The differences in microRNA profile further support the notion that PCFCL and PCLBCL-LT are different molecular entities with different biological behavior. An up-to-date overview of clinicopathologic, immunophenotypical and molecular genetic features of PCFCL and PCLBCL-LT is given in Table 1. For PCLBCL-LT therapeutical improvement is much needed and delineation of molecular or genetic events in the development and/or progression of this type of lymphoma might yield potential leads for targeted therapy. Currently known potential genetic events and involved molecular pathways in PCLBCL-LT are depicted in Figure 1. In the light of potential treatments, the studies described in this thesis provide evidence that components of the NF- $\kappa$ B pathway might be interesting therapeutical targets. As targeted therapy based on specific molecular characteristics is extensively explored in nodal DLBCL,<sup>58</sup> it will be important to further investigate these specific molecular features in PCLBCL-LT, to find out whether these therapies might also be beneficial for patients with this type of lymphoma. The observed differences between MTX-associated B-LPD presenting in the skin and PCFCL and PCLBCL-LT might give clinicians clues for diagnosing this rare entity. However, it is still unknown which cases will spontaneously resolve after abrogation of MTX therapy and which will show progressive disease and therefore require more aggressive treatment. More studies on the

molecular and genetic background of MTX-associated B-LPD presenting in the skin are therefore required to better understand its biological behavior.

Figure 1. Molecular and genetic pathways and aberrations in PCLBCL-LT



The (previously) demonstrated aberrations are depicted in red of which the ones represented in bold were demonstrated in the studies described in this thesis. The green boxes represent a selection of therapeutical targets that are under current investigation in nodal DLBCL.

**Table 1.** Main clinicopathologic, immunophenotypic and molecular genetic features of PCFCL and PCLBCL-LT

	<b>PCFCL</b>	<b>PCLBCL-LT</b>
Clinical features		
- lesions	solitary or multiple tumors	solitary or multiple tumors
- site of primary presentation	head and/or trunk	one or both leg(s)
- cutaneous relapse	30%	69%
- nodal/visceral dissemination	10%	47%
- 5 year OS/DSS	87% / 95%	37% / 50%
- first choice treatment	local radiotherapy	R-CHOP
Histopathology		
- infiltrate	diffuse or (partly) follicular	diffuse
- B-cell morphology	centrocytes (cleaved)	centroblasts/immunoblasts
		round)
- T-cell admixture	abundant	sparse
Immunohistochemistry		
- B-cells		
* B-cell lineage markers	CD20+, CD79a+, PAX5+	CD20+, CD79a+, PAX5+
* germinal center markers	BCL2-, BCL6+, CD10-	BCL2+, BCL6+/-, CD10-
* activation markers	IRF4/MUM1-, FOXP1-	IRF4/MUM1+, FOXP1+
* <b>B-cell receptor</b>	<b>heavy/light chains- (intracytoplasmic)</b>	<b>IgM+, IgD+/-, monotypic light chain+ (intracytoplasmic)</b>
* <b>cell cycle regulator marker</b>	<b>MYC-</b>	<b>MYC+</b>
- background	CD21/CD35: (remnants of) follicular dendritic networks	CD21/CD35: no (remnants of) follicular dendritic networks
Molecular genetics		
- copy number alteration	amplification 2p16.1 region, deletion 14q11.2-q12	deletion 6q arm, deletion 9p21.3 region
- gene expression profiling	high expression SPINK2	high expression <i>IGHM</i> , <i>PIM1</i> , <i>PIM2</i> , <i>IRF4</i> and <i>OCT2</i>
- <b>microRNA profiling</b>	<b>miR-129-2-3p present in 50%</b>	<b>no miR-129-2-3p present</b>
- <b>NF-κB pathway mutations</b>	<b>not available</b>	<b>MYD88 mutations 40%, CD79B mutations 20%, CARD11 mutations 10%</b>

The characteristics represented in bold are results of the studies described in this thesis.

## References

1. Willemze R, Jaffe ES, Burg G, et al. (2005) WHO-EORTC classification for cutaneous lymphomas. *Blood* 105: 3768-85.
2. Swerdlow SH, Campo E, Harris NL, et al. (2008) World Health Organisation Classification of Tumours of Haematopoietic and Lymphoid Tissues. In: Harris NL, ed. *Mature B-cell neoplasms*: IARC Press, Lyon: 179-267.
3. Senff NJ, Hoefnagel JJ, Jansen PM, et al. (2007) Reclassification of 300 primary cutaneous B-Cell lymphomas according to the new WHO-EORTC classification for cutaneous lymphomas: comparison with previous classifications and identification of prognostic markers. *J Clin Oncol* 25: 1581-7.
4. Senff NJ, Noordijk EM, Kim YH, et al. (2008) European Organization for Research and Treatment of Cancer and International Society for Cutaneous Lymphoma consensus recommendations for the management of cutaneous B-cell lymphomas. *Blood* 112: 1600-9.
5. Swerdlow SH, Campo E, Harris NL, et al. (2008) World Health Organisation Classification of Tumours of Haematopoietic and Lymphoid Tissues. In: Gaulard P, Swerdlow SH, Harris NL, et al., eds. *Other iatrogenic immunodeficiency-associated lymphoproliferative disorders*: IARC Press, Lyon: 350-1.
6. Verma S, Frambach GE, Seilstad KH, et al. (2005) Epstein-Barr virus-associated B-cell lymphoma in the setting of iatrogenic immune dysregulation presenting initially in the skin. *J Cutan Pathol* 32: 474-83.
7. Pfistershammer K, Petzelbauer P, Stingl G, et al. (2001) Methotrexate-induced primary cutaneous diffuse large B-cell lymphoma with an 'angiocentric' histological morphology. *Clin Exp Dermatol* 35: 59-62.
8. Tournadre A, D'Incan M, Dubost JJ, et al. (2001) Cutaneous lymphoma associated with Epstein-Barr virus infection in 2 patients treated with methotrexate. *Mayo Clin Proc Mayo Clinic* 76: 845-8.
9. Chai C, White WL, Shea CR, et al. (1999) Epstein Barr virus-associated lymphoproliferative-disorders primarily involving the skin. *J Cutan Pathol* 26: 242-7.
10. Rausch T, Cairolì A, Benhattar J, et al. (2013) EBV+ cutaneous B-cell lymphoproliferation of the leg in an elderly patient with mycosis fungoides and methotrexate treatment. *APMIS* 121: 79-84.
11. Rizzi R, Curci P, Delia M, et al. (2009) Spontaneous remission of "methotrexate-associated lymphoproliferative disorders" after discontinuation of immunosuppressive treatment for autoimmune disease. Review of the literature. *Medi Oncol* 26: 1-9.
12. Hoefnagel JJ, Dijkman R, Basso K, et al. (2005) Distinct types of primary cutaneous large B-cell lymphoma identified by gene expression profiling. *Blood* 105: 3671-8.
13. Demirkesen C, Tuzuner N, Esen T, et al. (2011) The expression of IgM is helpful in the differentiation of primary cutaneous diffuse large B cell lymphoma and follicle center lymphoma. *Leukemia Res* 35: 1269-72.
14. Bartel DP. (2004) MicroRNAs: genomics, biogenesis, mechanism, and function. *Cell* 116: 281-97.
15. Calin GA, Croce CM. (2006) MicroRNA signatures in human cancers. *Nature Rev Cancer* 6: 857-66.
16. Montes-Moreno S, Martínez N, Sánchez-Espiridión B, et al. (2011) miRNA expression in diffuse large B-cell lymphoma treated with chemoimmunotherapy. *Blood* 118: 1034-40.
17. Culpin RE, Proctor SJ, Angus B, et al. (2010) A 9 series microRNA signature differentiates between germinal centre and activated B-cell-like diffuse large B-cell lymphoma cell lines. *Int J Oncol* 37: 367-76.
18. Lawrie CH, Chi J, Taylor S, et al. (2009) Expression of microRNAs in diffuse large B cell lymphoma is associated with immunophenotype, survival and transformation from follicular lymphoma. *J Cell Mol Med* 13: 1248-60.
19. Muramatsu M, Kinoshita K, Fagarasan S, et al. (2000) Class switch recombination and hypermutation require activation-induced cytidine deaminase (AID), a potential RNA editing enzyme. *Cell* 102: 553-63.

20. Dijkman R, Tensen CP, Buettner M, et al. (2006) Primary cutaneous follicle center lymphoma and primary cutaneous large B-cell lymphoma, leg type, are both targeted by aberrant somatic hypermutation but demonstrate differential expression of AID. *Blood* 107: 4926-9.
21. Miyazaki K, Yamaguchi M, Suguro M, et al. (2008) Gene expression profiling of diffuse large B-cell lymphoma supervised by CD21 expression. *Br J Haematol* 142: 562-70.
22. Ogawa S, Yamaguchi M, Oka K, et al. (2004) CD21S antigen expression in tumour cells of diffuse large B-cell lymphomas is an independent prognostic factor indicating better overall survival. *Br J Haematol* 125: 180-6.
23. Wright G, Tan B, Rosenwald A, et al. (2003) A gene expression-based method to diagnose clinically distinct subgroups of diffuse large B cell lymphoma. *Proc Natl Acad Sci USA* 100: 9991-6.
24. Booman M, Douwes J, Glas AM, et al. (2006) Primary testicular diffuse large B-cell lymphomas have activated B-cell-like subtype characteristics. *J Pathol* 210: 163-71.
25. Camilleri-Broet S, Criniere E, Broet P, et al. (2006) A uniform activated B-cell-like immunophenotype might explain the poor prognosis of primary central nervous system lymphomas: analysis of 83 cases. *Blood* 107: 190-6.
26. Lenz G, Nagel I, Siebert R, et al. (2007) Aberrant immunoglobulin class switch recombination and switch translocations in activated B cell-like diffuse large B cell lymphoma. *J Exp Med* 204: 633-43.
27. Montesinos-Rongen M, Schmitz R, Courts C, et al. (2005) Absence of immunoglobulin class switch in primary lymphomas of the central nervous system. *Am J Pathol* 166: 1773-9.
28. Sagardoy A, Martinez-Ferrandis JI, Roa S, et al. (2013) Downregulation of FOXP1 is required during germinal center B-cell function. *Blood* 121: 4311-20.
29. Compagno M, Lim WK, Grunn A, et al. (2009) Mutations of multiple genes cause deregulation of NF-kappaB in diffuse large B-cell lymphoma. *Nature* 459: 717-21.
30. Ngo VN, Young RM, Schmitz R, et al. (2011) Oncogenically active MYD88 mutations in human lymphoma. *Nature* 470: 115-9.
31. Dijkman R, Tensen CP, Jordanova ES, et al. (2006) Array-based comparative genomic hybridization analysis reveals recurrent chromosomal alterations and prognostic parameters in primary cutaneous large B-cell lymphoma. *J Clin Oncol* 24: 296-305.
32. Pham-Ledard A, Prochazkova-Carlotti M, Andrique L, et al. (2014) Multiple genetic alterations in primary cutaneous large B-cell lymphoma, leg type support a common lymphomagenesis with activated B-cell-like diffuse large B-cell lymphoma. *Mod Pathol* 27: 402-11.
33. Pham-Ledard A, Cappellen D, Martinez F, et al. (2012) MYD88 somatic mutation is a genetic feature of primary cutaneous diffuse large B-cell lymphoma, leg type. *J Invest Dermatol* 132: 2118-20.
34. Sommer K, Guo B, Pomerantz JL, et al. (2005) Phosphorylation of the CARMA1 linker controls NF-kappaB activation. *Immunity* 23: 561-74.
35. Naylor TL, Tang H, Ratsch BA, et al. (2011) Protein kinase C inhibitor sotrastaurin selectively inhibits the growth of CD79 mutant diffuse large B-cell lymphomas. *Cancer Res* 71: 2643-53.
36. Davis RE, Ngo VN, Lenz G, et al. (2010) Chronic active B-cell-receptor signalling in diffuse large B-cell lymphoma. *Nature* 463: 88-92.
37. Wilson WH, Gerecitano JF, Goy A, et al. (2012) The Bruton's Tyrosine Kinase (BTK) Inhibitor, Ibrutinib (PCI-32765), Has Preferential Activity in the ABC Subtype of Relapsed/Refractory De Novo Diffuse Large B-Cell Lymphoma (DLBCL): Interim Results of a Multicenter, Open-Label, Phase 2 Study. *Blood (ASH Annual Meeting Abstracts)* 120: 4039.
38. Mathews Griner LA, Guha R, Shinn P, et al. (2014) High-throughput combinatorial screening identifies drugs that cooperate with ibrutinib to kill activated B-cell-like diffuse large B-cell lymphoma cells. *Proc Natl Acad Sci USA* 111: 2349-54.

39. Gyory I, Fejer G, Ghosh N, et al. (2003) Identification of a functionally impaired positive regulatory domain I binding factor 1 transcription repressor in myeloma cell lines. *J Immunol* 170: 3125-33.
40. Davis RE, Brown KD, Siebenlist U, et al. (2001) Constitutive nuclear factor kappaB activity is required for survival of activated B cell-like diffuse large B cell lymphoma cells. *J Exp Med* 194: 1861-74.
41. Singh RR, Kim JE, Davuluri Y, et al. (2010) Hedgehog signaling pathway is activated in diffuse large B-cell lymphoma and contributes to tumor cell survival and proliferation. *Leukemia* 24: 1025-36.
42. Ramirez E, Singh RR, Kunkalla K, et al. (2012) Defining causative factors contributing in the activation of hedgehog signaling in diffuse large B-cell lymphoma. *Leukemia Res* 36: 1267-73.
43. Qu C, Liu Y, Kunkalla K, et al. (2013) Trimeric G protein-CARMA1 axis links smoothed, the hedgehog receptor transducer, to NF-kappaB activation in diffuse large B-cell lymphoma. *Blood* 121: 4718-28.
44. Ma X, Becker Buscaglia LE, Barker JR, et al. (2011) MicroRNAs in NF-kappaB signaling. *J Mol Cell Biol* 3: 159-66.
45. Shaffer AL, Yu X, He Y, et al. (2000) BCL-6 represses genes that function in lymphocyte differentiation, inflammation, and cell cycle control. *Immunity* 13: 199-212.
46. Sciammas R, Davis MM. (2004) Modular nature of Blimp-1 in the regulation of gene expression during B cell maturation. *J Immunol* 172: 5427-40.
47. Hoefnagel JJ, Mulder MM, Dreef E, et al. (2006) Expression of B-cell transcription factors in primary cutaneous B-cell lymphoma. *Mod Pathol* 19: 1270-76.
48. Mandelbaum J, Bhagat G, Tang H, et al. (2010) BLIMP1 is a tumor suppressor gene frequently disrupted in activated B cell-like diffuse large B cell lymphoma. *Cancer cell* 18: 568-79.
49. Ye BH, Chaganti S, Chang CC, et al. (1995) Chromosomal translocations cause deregulated BCL6 expression by promoter substitution in B cell lymphoma. *EMBO J* 14: 6209-17.
50. Pasqualucci L, Compagno M, Houldsworth J, et al. (2006) Inactivation of the PRDM1/BLIMP1 gene in diffuse large B cell lymphoma. *J Exp Med* 203: 311-7.
51. Salaverria I, Philipp C, Oschlies I, et al. (2011) Translocations activating IRF4 identify a subtype of germinal center-derived B-cell lymphoma affecting predominantly children and young adults. *Blood* 118: 139-47.
52. Goatly A, Bacon CM, Nakamura S, et al. (2008) FOXP1 abnormalities in lymphoma: translocation breakpoint mapping reveals insights into deregulated transcriptional control. *Mod Pathol* 21: 902-11.
53. Green TM, Nielsen O, de Stricker K, et al. (2012) High levels of nuclear MYC protein predict the presence of MYC rearrangement in diffuse large B-cell lymphoma. *Am J Surg Pathol* 36: 612-9.
54. Valera A, Lopez-Guillermo A, Cardesa-Salzmann T, et al. (2013) MYC protein expression and genetic alterations have prognostic impact in patients with diffuse large B-cell lymphoma treated with immunochemotherapy. *Haematologica* 98: 1554-62.
55. Wiesner T, Streubel B, Huber D, et al. (2005) Genetic aberrations in primary cutaneous large B-cell lymphoma: a fluorescence in situ hybridization study of 25 cases. *Am J Surg Pathol* 29: 666-73.
56. Hallermann C, Kaune KM, Gesk S, et al. (2004) Molecular cytogenetic analysis of chromosomal breakpoints in the IGH, MYC, BCL6, and MALT1 gene loci in primary cutaneous B-cell lymphomas. *J Invest Dermatol* 123: 213-9.
57. Lin Y, Wong K, Calame K. (1997) Repression of c-myc transcription by Blimp-1, an inducer of terminal B cell differentiation. *Science* 276: 596-9.
58. Barton S, Hawkes EA, Wotherspoon A, et al. (2012) Are we ready to stratify treatment for diffuse large B-cell lymphoma using molecular hallmarks? *The Oncologist* 17: 1562-73.



## Nederlandse samenvatting

Primair cutane lymfomen zijn maligne non-Hodgkinlymfomen (NHL) die zich primair in de huid presenteren zonder ziektemanifestaties buiten de huid op het tijdstip dat de diagnose gesteld wordt. Primair cutane lymfomen dienen onderscheiden te worden van nodale NHL die zich secundair in de huid manifesteren, aangezien het NHL zijn met een specifiek biologisch gedrag en een specifieke prognose. Om deze reden worden ze vaak ook anders behandeld dan hun nodale tegenhangers. De verschillende typen primair cutane lymfomen worden ook als specifieke entiteiten beschreven in de recentste classificatiesystemen voor lymforeticulaire maligniteiten, zoals de World Health Organization (WHO)-European Organization for Treatment of Cancer (EORTC)-classificatie en de WHO-classificatie (2008).

Terwijl nodale NHL voornamelijk van B-celorigine zijn, behoren de primair cutane B-cellymfomen (CBCL) tot de minderheid (20-25%) van alle primair cutane lymfomen. In de WHO-EORTC-classificatie wordt de groep van CBCL ingedeeld in primair cutane marginale zone B-cellymfomen (PCMZBL), primair cutane follikelcentrumlymfomen (PCFCL) en primair cutane diffuus grootcellige B-cellymfomen – beentype (PCLBCL-LT). PCMZBL toont histologisch een gemengd infiltraat waarin onder andere kleine maligne B-cellen worden aangetroffen, die morfologisch variëren van marginalezonecellen tot lymfoplasmacytoïde cellen en plasmacellen. De plasmacellen tonen karakteristiek immunohistochemisch monotypische intracytoplasmatische expressie van immunoglobulines. PCMZBL is een indolent type NHL met een ziektespecifieke 5-jaarsoverleving van vrijwel 100%. PCFCL toont histologisch hoofdzakelijk middelgrote tot grote centrocyten (morfologisch gekliefde cellen), bijgemengd met een variabel aantal centroblasten. Het groeipatroon van dit infiltraat is folliculair, folliculair en diffuus of, zoals in de meeste gevallen, diffuus. Het histologische groeipatroon is niet gerelateerd aan de prognose. De patiënten presenteren zich klinisch met gelokaliseerde huidtumoren, die zich voornamelijk op het (behaarde) hoofd of de romp bevinden. De tumoren reageren zeer goed op lokale radiotherapie en de ziekte heeft een zeer gunstige prognose (5-jaarsoverleving 95%). PCLBCL-LT toont histologisch een diffuus groeiend infiltraat, dat is opgebouwd uit centroblasten en/of immunoblasten (morfologisch ronde cellen) met over het algemeen weinig bijgemengde, reactieve T-cellen. Patiënten met PCLBCL-LT presenteren zich klinisch met huidtumoren op één of beide benen en hebben veelal een agressief ziektebeloop (5-jaarsoverleving 50%). De voorkeursbehandeling bestaat derhalve uit meerdere cycli agressieve immunochemotherapie.

### Onderscheid tussen PCFCL en PCLBCL-LT

Het clinicopathologische onderscheid tussen PCFCL met een diffuus groeipatroon en PCLBCL-LT kan soms erg lastig zijn. Deze differentiatie is echter van groot belang, gezien de verschillen in klinisch beloop en voorkeursbehandeling.

#### *IgM immunohistochemie*

Bij een eerdere verrichte genexpressiestudie werd veel hogere expressie van immuunglobuline zware keten mu (*IgM*) gevonden in PCLBCL-LT vergeleken met PCFCL. Om uit te vinden of dit verschil zich ook manifesteert op eiwitniveau werden in **hoofdstuk 2** immunohistochemische kleuringen voor zware en lichte ketens verricht op paraffinemateriaal van 53



tumorbipten van patiënten met PCFCL en 40 van patiënten met PCLBCL-LT. Alle 40 PCLBCL-LT-bioten toonden intracytoplasmatische expressie van IgM in de tumorcellen, waarbij er bij 18 van deze bioten co-expressie was van IgD. Dit betrof zowel PCLBCL-LT met tumoren op de benen als met tumoren op andere plaatsen. Daarentegen werd intracytoplasmatische expressie van IgM slechts in 5 van de 53 PCFCL-bioten gezien. De 3 patiënten met PCFCL die zich presenteerden met tumoren op de benen waren alle 3 positief voor IgM (en IgD). Dit betekent dat intracytoplasmatische expressie van IgM (en IgD) vooral goed kan differentiëren tussen PCFCL en PCLBCL-LT met tumoren die zich op het tijdstip van de diagnose niet op de benen bevinden. Aangezien het simpel uit te voeren immuunhistochemische kleuringen betreft die op paraffinebioten kunnen worden verricht, kunnen deze kleuringen in de dagelijkse klinische praktijk bijdragen aan het maken van het onderscheid tussen PCFCL en PCLBCL-LT.

### *MicroRNA-profilering*

MicroRNA's kunnen de genexpressie van hun doelgenen reguleren. Dit kan onder andere middels het inhiberen van de translationele initiatie van het doelgen door het blokkeren van ribosomen. MicroRNA's kunnen ook direct binden aan het reeds gevormde messenger RNA van het doelgen, wat leidt tot directe degradatie van dit molecuul. Als een bepaald microRNA in hoge mate tot expressie komt, zou dit derhalve kunnen leiden tot het onderdrukken van expressie van een tumorsupressorgen, terwijl verlies van expressie van een bepaald microRNA zou kunnen zorgen voor hogere expressie van oncogenen. Middels deze mechanismen zouden microRNA's bij kunnen dragen aan de oncogenese van tumoren.

In **hoofdstuk 3** werd het complete microRNA-profiel bepaald op vriesmateriaal van huidtumoren van 6 patiënten met PCFCL en 13 patiënten met PCLBCL-LT met behulp van high-throughput sequencing. Overeenkomstig de clusteranalyses van eerdere genexpressiestudies werd geprobeerd de casus PCFCL en PCLBCL-LT te clusteren op basis van de gegeneerde microRNA-profielen. In tegenstelling tot de genexpressiestudies kon deze clusteranalyse echter geen evident onderscheid maken tussen PCFCL en PCLBCL-LT. Aangezien eerder op basis van genexpressieprofielen was aangetoond dat PCFCL en PCLBCL-LT gelijkenissen vertonen met respectievelijk kiemcentrum-B-cellen (GCB) en geactiveerde B-cellen (ABC), werd vervolgens geprobeerd clusteranalyse te verrichten op basis van 3 geselecteerde microRNA-profielen, waarvan in de literatuur beschreven is dat deze onderscheid kunnen maken tussen nodale diffuus grootcellige B-cellymfomen (DLBCL) van het GCB- en het ABC-type. Ook middels clusteranalyse volgens deze profielen was het echter niet mogelijk de PCFCL en PCLBCL-LT evident te onderscheiden. Er werd echter wel van 16 individuele microRNA's aangetoond dat deze differentieel tot expressie kwamen tussen PCFCL en PCLBCL-LT. Van 11 van deze 16 individuele microRNA's werd een kwantitatieve PCR (qPCR)-analyse verricht op in formaline gefixeerd en in paraffine ingebed (FFPE) tumorweefsel van 20 additionele patiënten (10 PCFCL en 10 PCLBCL-LT). Hiermee werd de hogere expressie van miR-9-5p, miR-31-5p, miR-129-2-3p en miR-214-3p in PCFCL in vergelijking met PCLBCL-LT bevestigd. Deze techniek kan gemakkelijk worden verricht op routinematig verwerkte biopsiespecimens. Vooral het detecteren van miR-129-3p door middel van qPCR op FFPE tumorweefsel zou mogelijk in de kliniek van aanvullende waarde kunnen zijn, aangezien dit microRNA in geen enkel PCLBCL-LT-biopt gedetecteerd werd, maar wel in ongeveer de helft van de PCFCL-bioten. Alhoewel de sensitiviteit niet erg hoog is, lijkt dit microRNA derhalve wel een zeer specifieke marker voor PCFCL. Het is bovendien opvallend dat microRNA-129-2-3p in de controlegroep van 20 nodale DLBCL ook duidelijk hoger tot expressie kwam in de GCB-bioten dan in de

ABC-biopten. Mogelijkerwijs betreft het dus een kiemcentrumgerelateerde microRNA.

### **Pathogenese van PCLBCL-LT**

Alhoewel een deel van de PCLBCL-LT-patiënten langdurige remissie toont na behandeling met agressieve immunochemotherapie, treden bij een deel van de patiënten ook snelle recidieven op met hierop volgende progressieve ziekte. Omdat een groot deel van de patiënten oudere mensen betreft die vaak comorbiditeit tonen, zal ook niet elke patiënt agressieve chemotherapie lichamelijk kunnen verdragen. Zowel het vaak niet afdoende zijn van de huidige chemotherapeutische behandeling, als het klinisch niet in aanmerking komen voor chemotherapie, dwingt tot het zoeken naar additionele behandelingsopties voor PCLBCL-LT. Het zou vooral voordelig zijn strategieën te vinden die minder toxisch zijn en die direct gericht zijn op alleen de maligne cellen. Hiervoor is het van belang een beter inzicht te krijgen in de pathogenese van PCLBCL-LT, omdat dit potentiële aangrijpingspunten voor therapie op kan leveren.

#### *Class-switchrecombinatie*

In **hoofdstuk 2** werd consistente immuunhistochemische expressie van IgM aangetoond in 40 PCLBCL-LT-biopten, waarbij de helft co-expressie van IgD toonde. Aangezien genexpressiestudies hebben aangetoond dat PCLBCL-LT het profiel heeft van een post-kiemcentrum, geactiveerde B-cel, zou echter verwacht worden dat de maligne B-cellen van dit lymfoom class-switchrecombinatie (CSR) van IgM (en IgD) naar IgG of IgA zouden hebben ondergaan. De afwezigheid van CSR in PCLBCL-LT zou derhalve kunnen wijzen op een defect in het CSR-mechanisme. Eerder is deficiëntie van activatie-geïnduceerde cytidine deaminase (AID) gelinkt aan onvolkomen CSR. Van PCLBCL-LT is echter bekend dat het AID relatief hoog tot expressie brengt, dus een tekort aan AID is in dit type lymfoom geen verklaring voor de afwezigheid van CSR. De expressie van IgM wordt niet exclusief gezien in PCLBCL-LT, maar onder andere ook in andere DLBCL, zowel nodaal als extranodaal. Het betreft dan voornamelijk DLBCL die ook van het ABC-type zijn, zoals nodale ABC-DLBCL, primaire centraal zenuwstelsel DLBCL en primair testiculaire DLBCL. Bij nodale ABC-DLBCL en primaire centraal zenuwstelsel DLBCL is eerder gesuggereerd dat CSR in deze lymfomen afwezig zou zijn door mutaties in de switch-regio van het immuunglobuline-zwareketengen. Data over deze regio in PCLBCL-LT zijn echter niet beschikbaar.

#### *Nuclear factor-kappa B*

Aberrante constitutieve activatie van de nuclear factor kappa B (NF- $\kappa$ B) signaaltransductieroute is betrokken bij tumorceloverleving van onder andere nodale ABC-DLBCL. Op moleculair niveau is van afwijkingen in meerdere genen aangetoond dat deze kunnen bijdragen aan de aberrante activatie in dit type lymfoom. In tweederde van de gevallen betreft dit afwijkingen in tumor necrosis factor-alpha induced-protein 3 (*TNFAIP3*), cluster of differentiation 79B (*CD79B*), caspase recruitment domain-containing protein 11 (*CARD11*) en/of myeloid differentiation primary response gene 88 (*MYD88*). In **hoofdstuk 4** onderzochten we een selectie van NF- $\kappa$ B-activerende genafwijkingen in 10 PCLBCL-LT-biopten. Er werd een heterozygote deletie van tumorsupressorgen *TNFAIP3* aangetoond in 4 biopten. Er werd geen additionele hypermethylering van de promoterregio van dit gen aangetoond die zou kunnen leiden tot epigenetische downregulatie van het niet-gedeleteerde allel. Een *CD79B* Y196-mutatie werd

in 2 casus aangetoond in zowel DNA als cDNA. Eén tumor toonde zowel een D415E- als een R423W-mutatie in *CARD11*. In het DNA van 4 tumoren werd een L265P-mutatie aangetroffen in *MYD88*, waarbij 3 van deze tumoren dezelfde mutatie in het cDNA toonden. In totaal werden in 7 van de 10 PCLBCL-LT-biopten afwijkingen aangetroffen in de onderzochte genen die NF- $\kappa$ B-activatie reguleren. Alhoewel het een kleine groep betreft, komen de percentages genetische afwijkingen in *CD79B*, *CARD11* en *MYD88* opvallend overeen met die in nodale ABC-DLBCL. Daarentegen tonen nodale ABC-DLBCL in ongeveer een kwart van de gevallen homozygote deletie en/of epigenetische downregulatie van *TNFAIP3*, waarvoor in PCLBCL-LT geen aanwijzingen werden gevonden.

Het selectief inhiberen van meerdere moleculen van de NF- $\kappa$ B-siginaaltransductieroute wordt reeds onderzocht als mogelijke therapie voor B-cel NHL. Zo kan sotrastaurin met activatie van de NF- $\kappa$ B-siginaaltransductieroute interfereren door inhibitie van PKC- $\beta$ , een molecuul dat vereist is voor *CARD11*-afhankelijke NF- $\kappa$ B-activatie en in een muis xenograftmodel was sotrastaurin alleen effectief in *CD79B*-gemuteerde DLBCL. Middels RNA-interferentiescreening werd aangetoond dat Brutons tyrosine kinase (BTK), een component van B-celreceptor-signalering, essentieel is voor tumorceloverleving in nodale ABC-DLBCL als er sprake is van wildtype *CARD11*. Bovendien was het uitschakelen van proximale onderdelen van de B-celreceptor, zoals *CD79B*, selectief toxisch in nodale ABC-DLBCL, maar niet in andere lymfomen. In een fase I-onderzoek werd de BTK-inhibitor ibrutinib goed getolereerd en genereerde dit medicijn een klinische (partiële) respons in 40% van de refractaire nodale ABC-DLBCL. Deze (partiële) respons werd zowel in patiënten met tumoren met *CD79*-mutaties als in tumoren met *CD79*- en *MYD88*-mutaties gezien. Als er alleen *MYD88*-mutaties in de tumoren werden aangetroffen, toonden deze patiënten echter geen klinische respons op ibrutinib. De potentie van ibrutinib in de behandeling van nodale ABC-DLBCL werd recent verder onderzocht in een high throughput- combinatiestudie, waarin medicijnen werden ontdekt die zouden kunnen samenwerken met ibrutinib om ABC-DLBCL-cellen *in vitro* te doden. Samengevat laten deze resultaten de relevantie van somatische mutaties in *CD79B*, *CARD11* en *MYD88* zien bij het ontwikkelen van nieuwe medicijnen tegen nodale ABC-DLBCL en mogelijk ook voor de behandeling van PCLBCL-LT. Met name de impact van behandeling met ibrutinib op (verschillende soorten) B-cellymfomen lijkt beloftevol voor de behandeling van patiënten met PCLBCL-LT die niet in aanmerking komen voor agressieve behandeling of die een snel recidief tonen na behandeling met conventionele chemotherapie. Met name onderzoek naar de mutatiestatus van *MYD88* in patiënten met PCLBCL-LT zou klinisch belangrijk kunnen worden, omdat deze patiënten mogelijk geen baat zouden hebben bij behandeling met ibrutinib.

Aangezien 70% van de tumoren genetische afwijkingen tonen in NF- $\kappa$ B-siginaaltransductieroutegerelateerde genen, benadrukken onze data ook de relevantie van NF- $\kappa$ B-signalering in PCLBCL-LT. In nodale ABC-DLBCL wordt NF- $\kappa$ B-signalering als essentiële eigenschap beschouwd. Dat 30% van onze casus geen genetische afwijkingen in deze genen toont, betekent niet zonder meer dat er geen afwijkende NF- $\kappa$ B-signalering is in deze casus. Er is namelijk een beperkt aantal onderdelen van de route bestudeerd, de canonical en niet de non-canonical route is onderzocht en ten derde zijn de verschillende activerende mutaties in componenten van de siginaaltransductieroute niet de enige pathofysiologische mechanismen die ten grondslag kunnen liggen aan constitutieve activatie van deze route. Hedgehogsignalering is bijvoorbeeld ontregeld in DLBCL. Deze ontregeling is waarschijnlijk gedeeltelijk veroorzaakt door gain/amplificatie van *smoothed (SMO)*. SMO is een transductiesubunit van hedgehogsignalering. In DLBCL is ontregelde hedgehogsignalering gelinkt aan de NF- $\kappa$ B-siginaaltransductieroute via SMO, aangezien SMO in staat is G-eiwitsubunits te recrutereren die tot

NF- $\kappa$ B-activatie leiden middels PKC- $\beta$  – CARD11-signalering. Tot slot zijn waarschijnlijk ook meerdere microRNA's betrokken in NF- $\kappa$ B-activatie. MiR-155 kan I $\kappa$ B-kinases downreguleren, wat vervolgens leidt tot verhoogde NF- $\kappa$ B-activatie. MiR-21 kan translatie van phosphatase and tensin homolog (*PTEN*) blokkeren. *PTEN* is een tumorsuppressor die normaalgesproken NF- $\kappa$ B-activatie inhibeert door middel van AKT-signalering. Van beide microRNA's wordt relatief frequent gerapporteerd dat ze hoger tot expressie komen in nodale ABC-DLBCL dan in GCB-DLBCL, overeenkomstig het feit dat NF- $\kappa$ B-signalering een essentiële eigenschap is van ABC-DLBCL. Wij troffen in ons cohort dat is onderzocht in **hoofdstuk 3** echter geen significante verschillen in expressie van miR-155 en/of miR-21 aan tussen PCLBCL-LT en PCFCL. Dit zou kunnen betekenen dat deze microRNA's niet bijdragen aan afwijkende NF- $\kappa$ B-signalering in PCLBCL-LT of dat afwijkende signalering ook een kenmerk zou kunnen zijn van PCFCL. Aangezien dit niet duidelijk is, is meer onderzoek op dit gebied gewenst.

### *Transcriptiefactoren*

Onder fysiologische omstandigheden wordt B-cell lymphoma 6 (*BCL6*) tot expressie gebracht in kiemcentrum-B-cellen en onderdrukt dit eiwit expressie van Blimp1, het eiwit dat gecodeerd wordt door PR domain containing 1, with zinc finger domain (*PRDM1*). Na een succesvolle kiemcentrumreactie vermindert de expressie van *BCL6*, wat leidt tot expressie van Blimp1. Deze expressie van Blimp1 is in principe voldoende om B-cellen plasmaceldifferentiatie te laten ondergaan en induceert ook de expressie van andere transcriptiefactoren die betrokken zijn bij het plasmacelprogramma, zoals interferon regulatory factor-4 (*IRF4*). Daarnaast is de expressie van forkhead box P1 (*FOXP1*) omgekeerd evenredig met de expressie van *BCL6* en komt *FOXP1*-expressie dus voor in B-cellen na de kiemcentrumreactie. Ook *FOXP1* kan de expressie van Blimp1 induceren. Het immuunhistochemische profiel van PCLBCL-LT betreffende deze transcriptiefactoren is echter niet consistent met het profiel van de geactiveerde B-cellen, de veronderstelde normale tegenhanger van dit lymfoom. *BCL6* komt namelijk in meer dan de helft van de casus tot expressie, *IRF4* en *FOXP1* worden vrijwel altijd gedetecteerd in de tumorcellen en van Blimp1 is nooit substantiële expressie in tumorcellen aangetoond.

De geactiveerde B-cel, als veronderstelde normale tegenhanger van PCLBCL-LT, toont een differentiatiestop in de transitionele fase tussen kiemcentrum-B-cel en plasmacel. Er zijn in nodale DLBCL meerdere mechanismen beschreven die (gedeeltelijk) verantwoordelijk kunnen zijn voor deze stop, zoals bijvoorbeeld translocaties met betrokkenheid van *BCL6* en deleties van en mutaties in *PRDM1*. *IRF4* en *FOXP1* zijn andere transcriptiefactoren die B-cellen richting plasmaceldifferentiatie kunnen drijven. Sporadische genetische afwijkingen met betrokkenheid van deze genen, zoals translocaties, kunnen ook voorkomen in nodale DLBCL. In **hoofdstuk 5** onderzochten we genetische en immuunhistochemische afwijkingen van deze B-celactivatiegerelateerde transcriptiefactoren in 10 PCLBCL-LT-biopten. Er werden geen aanwijzingen gevonden dat *BCL6*, *FOXP1* en/of *IRF4* een autonome manier van verhoogde expressie toonden, aangezien geen translocaties of amplificaties in de genen werden aangetroffen. Daarnaast kon de afwezigheid van het eiwit Blimp1 door middel van immuunhistochemie niet verklaard worden door genetische inactivatie, dat wil zeggen door homozygote deletie van *PRDM1* of door heterozygote deletie met bijkomende relevante mutatie in het niet-gedeleteerde allel. Deze genetische inactivatie van *PRDM1* is wel beschreven in ABC-DLBCL, de nodale tegenhanger van PCLBCL-LT, waarbij het in ongeveer eenderde van de gevallen voorkomt. Translocaties die *IRF4* betreffen zijn slechts sporadisch gerapporteerd in nodale ABC-DLBCL en ook *FOXP1* is in deze lymfomen niet vaak betrokken in een translocatie,

alhoewel deze mogelijk vaker voorkomen in extranodale DLBCL.

## MYC

In de studie die is beschreven in **hoofdstuk 6**, waarin we methotrexaat (MTX)-geassocieerde B-cellymfoproliferatieve aandoeningen (B-LPD) die zich in de huid manifesteren vergeleken met PCFCL en PCLBCL-LT, toonden we aan dat in alle 10 onderzochte PCLBCL-LT in meer dan 75% van de tumorcellen het MYC-eiwit tot expressie werd gebracht. In nodale DLBCL zijn hoge percentages MYC-positieve tumorcellen geassocieerd met *MYC*-herschikking, -gain en/of-amplificatie. In PCLBCL-LT variëren de data over translocaties met betrokkenheid van *MYC* nogal, van sporadisch tot eenderde van de gevallen. Publicaties over gain of amplificatie van *MYC* in PCLBCL-LT zijn er echter niet en wij troffen dit ook middels DNA array niet aan in de tumoren van ons cohort van 10 patiënten, waarop tevens de immunohistochemische kleuring was verricht. Bovendien werden middels deze methode in de tumoren ook geen aanwijzingen gevonden voor translocaties met betrokkenheid van *MYC*. Het MYC-eiwit komt derhalve waarschijnlijk middels andere mechanismen verhoogd tot expressie in PCLBCL-LT. Onder fysiologische omstandigheden wordt de expressie van MYC in geactiveerde B-cellen onderdrukt door B-celtranscriptiefactor Blimp1. Dit eiwit lijkt echter afwezig in PCLBCL-LT en mogelijk draagt deze afwezigheid bij aan de hoge expressie van het MYC-eiwit in dit lymfoom.

## Methotrexaatgeassocieerde B-cellymfoproliferatieve aandoeningen van de huid

In **hoofdstuk 6** werden de clinicopathologische en fenotypische kenmerken van 10 patiënten met MTX-geassocieerde B-LPD van de huid in kaart gebracht, waaronder 5 Epstein-Barrvirus (EBV)-positieve en 5 EBV-negatieve gevallen. Bij 6 patiënten was de aandoening beperkt tot de huid. Klinisch leidde het stoppen met de MTX-behandeling tot complete remissie bij 4 patiënten en tot partiële remissie in 2 andere patiënten. De 5-jaars ziektespecifieke overleving was 90%. Het verschil tussen MTX-geassocieerde B-LPD en PCFCL lag met name in de aanwezigheid van ulcererende en/of gegeneraliseerde huidlaesies, een infiltraat dat meer bestaat uit centroblasten/immunoblasten dan uit grote centrocyten, verminderde immunohistochemische aankleuring voor CD79a, expressie van BCL2, IRF4 en FOXP1 in de meeste MTX-geassocieerde B-LPD-gevallen en monotypische aankleuring voor intracytoplasmatische immuunglobulines in de helft van deze gevallen. EBV-positieve MTX-geassocieerde B-LPD verschilden van PCLBCL-LT wat betreft ulcererende huidlaesies, uitgesproken tumorcelpolymorfisme, verminderde immunohistochemische aankleuring voor CD79a en expressie van CD30 en EBV. EBV-negatieve gevallen toonden morfologisch en immunohistochemisch duidelijke overeenkomsten met PCLBCL-LT, maar verschilden met name in klinische presentatie, waarbij 4 van de 5 gevallen zich presenteerden met gegeneraliseerde huidlaesies. Het relatief gunstige klinische beloop en de spontane ziektereversie na slechts het stoppen van de behandeling met MTX in een aanzienlijk deel van deze patiënten benadrukt het belang van een zorgvuldig 'wait-and-see'-beleid alvorens een meer agressieve behandeling te overwegen.

## Concluderende opmerkingen

Door de verschillende studies die in dit proefschrift zijn beschreven is er meer inzicht verkregen in de clinicopathologische (en genetische) aspecten van PCFCL, PCLBCL-LT en MTX-geassocieerde B-LPD van de huid. De resultaten zijn behulpzaam in het beter definiëren van

deze aparte entiteiten en leveren daarmee aanknopingspunten voor het diagnosticeren van deze lymfomen in de klinische praktijk. De verschillen in microRNA-profielen tussen PCFCL en PCLBCL-LT ondersteunen nogmaals de opvatting dat PCFCL en PCLBCL-LT verschillende moleculaire entiteiten zijn met een verschillend biologisch gedrag. Op het moment is verbetering van de behandeling van PCLBCL-LT dringend gewenst. Het in detail in kaart brengen van moleculaire en/of genetische afwijkingen in de ontwikkeling en/of progressie van dit lymfoom zou potentiële aanknopingspunten voor doelgerichte behandeling kunnen opleveren. In het licht hiervan heeft de studie beschreven in **hoofdstuk 4** van dit proefschrift aangetoond dat componenten van de NF- $\kappa$ B-siginaaltransductieroute interessante therapeutische aangrijpingspunten zouden kunnen zijn. Doelgerichte behandeling op basis van specifieke moleculaire kenmerken wordt uitgebreid onderzocht in nodale DLBCL en daarom is het van belang om dezelfde moleculaire karakteristieken ook in PCLBCL-LT te onderzoeken. Op die manier kan vastgesteld worden of deze therapieën ook toegepast kunnen worden bij de behandeling van patiënten met PCLBCL-LT.

De geobserveerde verschillen tussen MTX-geassocieerde B-LPD van de huid en PCFCL en PCLBCL-LT zouden klinici goede aanknopingspunten kunnen geven om deze zeldzame aandoening te kunnen diagnosticeren. Het is echter nog onbekend welke patiënten spontane remissie zullen tonen na het stoppen van de behandeling met MTX en welke een progressief ziektebeloop zullen tonen en daarom agressievere behandeling behoeven. Verder onderzoek naar de moleculaire en genetische achtergrond van MTX-geassocieerde B-LPD in de huid is derhalve nodig om het biologische gedrag van deze ziekte beter te begrijpen.



## Curriculum vitae

Lianne Koens werd geboren op 29 juli 1982 te Delft. Zij groeide op in Pijnacker en doorliep haar middelbare school aan het Stanislascollege te Delft. Na het behalen van het eindexamen gymnasium in 2000, begon zij in datzelfde jaar met de studie Biomedische Wetenschappen aan de Rijksuniversiteit Leiden. Dit jaar werd afgerond met een propedeuse en in 2001 volgde de overstap naar de studie Geneeskunde aan dezelfde universiteit. Aan het eind van haar co-schappen volgde zij gedurende 10 weken een keuzecoschap Hematopathologie in het Leids Universitair Medisch Centrum. In 2007 werd het artsexamen behaald. Vanaf oktober 2007 was zij werkzaam als AIOSKO (arts in opleiding tot specialist en klinisch onderzoeker) op de afdeling Pathologie van het Leids Universitair Medisch Centrum met in eerste instantie prof. dr. G.J. Fleuren en later prof. dr. V.T.H.B.M. Smit als opleider. In 2009 werd officieel aangevangen met een promotieonderzoek naar primair cutane grootcellige B-cellymfomen onder begeleiding van prof. dr. R. Willemze (afdeling Dermatologie, Leids Universitair Medisch Centrum). Als verdiepingsstage in de opleiding tot patholoog bezocht zij in 2014 drie maanden de afdeling Hematopathologie van het UCLA Medical Center in Los Angeles onder begeleiding van dr. S. Song. Per 1 oktober 2014 is zij als patholoog werkzaam in het Academisch Medisch Centrum te Amsterdam.





## List of publications

Cutaneous gamma/delta T-cell lymphoma during treatment with etanercept for rheumatoid arthritis.

Koens L, Senff NJ, Vermeer MH, Ronday HK, Willemze R, Jansen PM.  
*Acta Dermato Venereologica* 2009; 89(6): 653-654.

IgM expression on paraffin sections distinguishes primary cutaneous large B-cell lymphoma, leg type from primary cutaneous follicle center lymphoma.

Koens L, Vermeer MH, Willemze R, Jansen PM.  
*The American Journal of Surgical Pathology* 2010; 34(7): 1043-1048.

MicroRNA profiling of primary cutaneous large B-cell lymphomas.

Koens L, Qin Y, Leung WY, Hageman L, Corver WE, Jansen PM, Willemze R, Vermeer MH, Tensen CP.  
(Abstract) *Journal of Hematopathology* 2012; 5: 256-257.

Impact of the microenvironment on the prognosis of primary bone diffuse large B-cell lymphoma.

Szepesi A, Rajnai H, Tímár B, Heyning FH, Koens L, Csomor J, Matolcsy A.  
(Abstract) *Journal of Hematopathology* 2012; 5: 267.

Nuclear factor- $\kappa$ B activation in primary lymphoma of bone.

Koens L, Heyning FH, Szepesi A, Matolcsy A, Hogendoorn PC, Jansen PM.  
*Virchows Archiv: an International Journal of Pathology* 2013; 462(3): 349-354.

MicroRNA Profiling of Primary Cutaneous Large B-Cell Lymphomas.

Koens L, Qin Y, Leung WY, Corver WE, Jansen PM, Willemze R, Vermeer MH, Tensen CP.  
*Public Library of Science ONE* 2013; 8(12): e82471.

The density of CD8+ T-cell infiltration and expression of BCL2 predicts outcome of primary diffuse large B-cell lymphoma of bone.

Rajnai H, Heyning FH, Koens L, Sebestyén A, Andrikovics H, Hogendoorn PC, Matolcsy A, Szepesi A.  
*Virchows Archiv: an International Journal of Pathology* 2014; 464(2): 229-239.

Programmed death-1 expression in cutaneous B-cell lymphoma.

Cetinozman F, Koens L, Jansen PM, Willemze R.  
*Journal of Cutaneous Pathology* 2014; 41(1): 14-21.

Nuclear Factor- $\kappa$ B pathway-activating gene aberrancies in primary cutaneous large B-cell lymphoma, leg type.

Koens L, Zoutman WH, Ngarmmlertsirichai P, Przybylski GK, Vermeer MH, Willemze R, Jansen PM, Schmidt CA, Tensen CP.

*Journal of Investigative Dermatology* 2014; 134(1): 290-292.

Methotrexate-associated B-cell lymphoproliferative disorders presenting in the skin: a clinicopathologic and immunophenotypical study of ten cases.

Koens L, Senff NJ, Vermeer MH, Willemze R, Jansen PM.

*The American Journal of Surgical Pathology* 2014; 38(7): 999-1006.

Genetic alterations in B-cell activation-related transcription factors in primary cutaneous large B-cell lymphoma, leg type.

Koens L, Zoutman WH, Winkler P, Przybylski GK, Vermeer MH, Willemze R, Jansen PM, Schmidt CA, Tensen CP.

*Submitted.*

Acute eosinophilic pneumonia.

Brackel CLH, Ropers FG, Vermaas-Fricot SFN, Koens L, Willems LNA, Rijkers-Mutsaerts ERVM.

*Submitted.*





## Nawoord

Er zijn meerdere mensen die ik graag apart wil noemen:

Rein Willemze

Patty Jansen

Kees Tensen

Maarten Vermeer

Medewerkers onderzoekslaboratorium Huidziekten  
(met name Qin, Wim, Coby en Leslie)

Leden Landelijke Werkgroep Cutane Lymfomen

Professor Schmidt, Grzegorz Przybylski, Piotr Grabarczyk en Passorn Winkler

Enno Dreef

Wai Leung

Henk Buermans

Wim Corver en Jan Oosting

Stéphanie Boonk en Fatoş Çetinözman

Franziska Pfau en Lois Hageman

Medeonderzoekers kamer P3-35

Pathologen en AIOS LUMC

Medewerkers afdeling pathologie LUMC

Paranimfen Marloes en Suzanne

Dinomar Daal

Liesbeth, Eveline, Katja en Marinke

Dacia, Rosanne, Jennifer, Esther en Esther

Dorottya, Marjan, Femke en Ellen

Toos, Wendy en Martijn

Bedankt voor de prettige begeleiding, samenwerking en/of ondersteuning in de periode dat dit proefschrift tot stand is gekomen!







